AWARD NUMBER: W81XWH-15-1-0473

TITLE: Does the Loss of Stromal Caveolin-1 Remodel the Tumor Microenvironment by Activating Src-Mediated PEAK1 and PI3K Pathways?

PRINCIPAL INVESTIGATOR: MARIANA REIS SOBREIRO PhD

CONTRACTING ORGANIZATION: Cedars-Sinai Medical Center
Los Angeles, CA 90048

REPORT DATE: November 2017

TYPE OF REPORT: Final

PREPARED FOR: U.S. Army Medical Research and Materiel Command
Fort Detrick, Maryland 21702-5012

REPORT DOCUMENTATION PAGE

Form Approved
OMB No. 0704-0188

1. REPORT DATE	2. REPORT TYPE	3. DATES COVERED
November 2017	Final	1 Sep 2015 - 31 Aug 2017

4. TITLE AND SUBTITLE

Does the Loss of Stromal Caveolin-1 Remodel the Tumor Microenvironment by Activating Src-Mediated PEAK1 and PI3K Pathways?

5a. CONTRACT NUMBER

5b. GRANT NUMBER
W81XWH-15-1-0473

5c. PROGRAM ELEMENT NUMBER

6. AUTHOR(S)

Mariana Reis Sobreiro, Wei Yang, Dolores Di Vizio Michael R Freeman.

E-Mail:Mariana.Sobreiro@cshs.org

5d. PROJECT NUMBER

5e. TASK NUMBER

5f. WORK UNIT NUMBER

7. PERFORMING ORGANIZATION NAME(S) AND ADDRESS(ES)

CEDARS-SINAI MEDICAL CENTER
8700 BEVERLY BLVD
LOS ANGELES CA 90048-1804

8. PERFORMING ORGANIZATION REPORT NUMBER

9. SPONSORING / MONITORING AGENCY NAME(S) AND ADDRESS(ES)

U.S. Army Medical Research and Materiel Command
Fort Detrick, Maryland 21702-5012

10. SPONSOR/MONITOR'S ACRONYM(S)

11. SPONSOR/MONITOR'S REPORT NUMBER(S)

12. DISTRIBUTION / AVAILABILITY STATEMENT

Approved for Public Release; Distribution Unlimited

13. SUPPLEMENTARY NOTES

14. ABSTRACT

This study describes a new mechanism of intercellular communication originating from extracellular vesicles (EVs). We demonstrate that in the context of prostate cancer, EV populations isolated from human patients harbor AKT1 and that AKT1 kinase activity is sustained in these particles, nominating them as active signaling platforms. Consistently, active AKT1 in circulating EVs from the plasma of metastatic prostate cancer patients is detected predominantly in large, tumor-derived EVs, termed large oncosomes (LO). LO internalization induces reprogramming of human normal prostate fibroblasts, as reflected by high levels of α-SMA, IL6, and MMP9. In turn, LO reprogrammed normal prostate fibroblasts stimulate endothelial tube formation in vitro.

15. SUBJECT TERMS
PI3K, Prostate Cancer, Extracellular Vesicles

16. SECURITY CLASSIFICATION OF:			17. LIMITATION OF ABSTRACT	18. NUMBER OF PAGES	19a. NAME OF RESPONSIBLE PERSON
a. REPORT	b. ABSTRACT	c. THIS PAGE			USAMRMC
U	U	U	UU	55	19b. TELEPHONE NUMBER *(include area code)*

Table of Contents

Page

1. INTRODUCTION

It has gradually become clear that the tumor stromal environment, also called the tumor microenvironment (TME), plays a crucial role in the initiation, progression and metastasis of cancer; hence, targeting the TME has emerged as a novel therapeutic strategy for cancer treatment (1). The TME consists of a compendium of cells (e.g., fibroblasts/myofibroblasts, vascular cells, immune cells, and etc.) along with the extracellular matrix (ECM) and extracellular molecules (2). Though many classic extracellular signaling molecules (e.g., hormones, peptide growth factors, and cytokines) are water-soluble, increasing evidence has shown that a variety of extracellular molecules are confined in extracellular vesicles (EVs), such as exosomes and microvesicles, and that EV-mediated intercellular communication plays an important role in cancer progression (3).

This project tested the hypothesis that the **loss of Cav1 in prostate stroma promotes prostate cancer (PCa) progression and metastasis by activating the Src-mediated PEAK1 and PI3K pathways (Aim 1) and by regulating the release of certain extracellular proteins (Aim 2).** To this end we purified EVs derived from cancer cells with the PI3K pathway constitutively active in order to study its interaction with cells from the tumor microenvironment. We first addressed whether stromal cells, vascular endothelial cells, cancer associated fibroblasts and tumor cells could take up tumor-derived EVs. To infer whether EVs have the potential to reprogram cells from the tumor microenvironment we performed a transcription factor array analysis in stromal cells after EV uptake. During the second year of the funding period we tested whether stromal cells promote cancer metastasis *in vivo*.

Specific Aim 1. Determine whether Cav1 loss activates the Src/PEAK1 and Src/PI3K pathways, whose cooperation enhances the dynamics of invadopodia-like protrusions and thus ECM degradation and EV secretion.

Specific Aim 2. Determine whether Cav1 loss regulates the release of certain extracellular proteins, in water-soluble or EV-confined form, that are important for PCa progression

2.KEYWORDS

PI3K**,** Prostate Cancer**,** Extracellular Vesicles

3. ACCOMPLISHMENTS

What were the major goals of the project?

Training Goal 1: Training and educational development in prostate cancer research

Milestone: Presentation of project data at a national meeting
Target months: 24
Percentage of completion: 100%

Research Goal 1: Determine whether Cav1 loss activates the Src/PEAK1 and Src/PI3K pathways, whose cooperation enhances the dynamics of invadopodia-like protrusions and thus ECM degradation and EV secretion.

Milestones:

1) Determine whether Cav1 silencing activates the Src-mediated PEAK1 and PI3K pathways.

2) Determine whether targeting Src, PEAK1, or PI3K inhibits the dynamics of invadopodia-like protrusions, ECM degradation, and EV secretion.

3) Determine whether targeting Src, PEAK1, or PI3K in CAFs delay PCa growth *in vivo*.

Target months: 12

Percentage of completion: 100%

Research Goal 2: Determine whether Cav1 loss regulates the release of certain extracellular proteins, in water-soluble or EV-confined form, that are important for PCa progression

Milestones:

1) Determine whether EVs, EV-depleted conditioned medium, or both are the functional mediators of angiogenesis and tumor cell migration and invasion.

2) Identify the differentially secreted proteins using a quantitative proteomics approach

3) Determine whether manipulating the expression or activity of select proteins may regulate PCa progression *in vitro* and *in vivo*.

Target months: 24

Percentage of completion: 100%

What was accomplishing under these goals?

This study describes a new mechanism of intercellular communication originating from extracellular vesicles (EVs). We demonstrate that in the context of prostate cancer, EV populations isolated from human patients harbor AKT1 and that AKT1 kinase activity is sustained in these particles, nominating them as active signaling platforms. Consistently, active AKT1 in circulating EVs from the plasma of metastatic prostate cancer patients was detected predominantly in atypically large, tumor-derived EVs, termed large oncosomes (LO). LO internalization induced reprogramming of human normal prostate fibroblasts, as reflected by increased levels of α-SMA, IL6, and MMP9. In turn, LO reprogrammed normal prostate fibroblasts to stimulate endothelial tube formation in vitro.

Major accomplishments include:

1) Src and PI3K pathway activation promotes EV secretion and AKT is selectively present in EVs

The loss of caveolin-1 is related with PI3K/Akt signaling pathway activation and increased shedding of EVs (4). Recent reports demonstrate that cells can shed different populations of EVs, with a potential distinct role mediating intercellular communication. To test independently EVs ability to modify TME, we isolated small exosomes (Exo) and large oncosomes (LO) using optimized protocols for EV purification (**Fig1**).

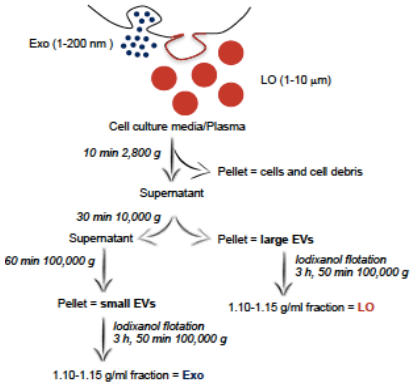

We used a protocol based on differential centrifugation to separate LO from Exo, followed by flotation to exclude proteins and other EV-attached molecules (Fig. 1)

Figure 1. Schematic representation of the protocol used for purification of LO and exosomes (Exo) starting from conditioned media (CM).

A recent report identified AKT1 and other kinases in EVs circulating in blood from patients with different epithelial tumor types (5). Because AKT1 is frequently activated in patients with metastatic PCa as a result of genomic aberrations in the phosphoinositide 3-kinase (PI3K) pathway we analyzed the distribution of EV-bound AKT1 in both LO and Exo. We found that LO harbor p-AKT1^{Ser473} at significantly higher levels than Exo (**Fig 2**).

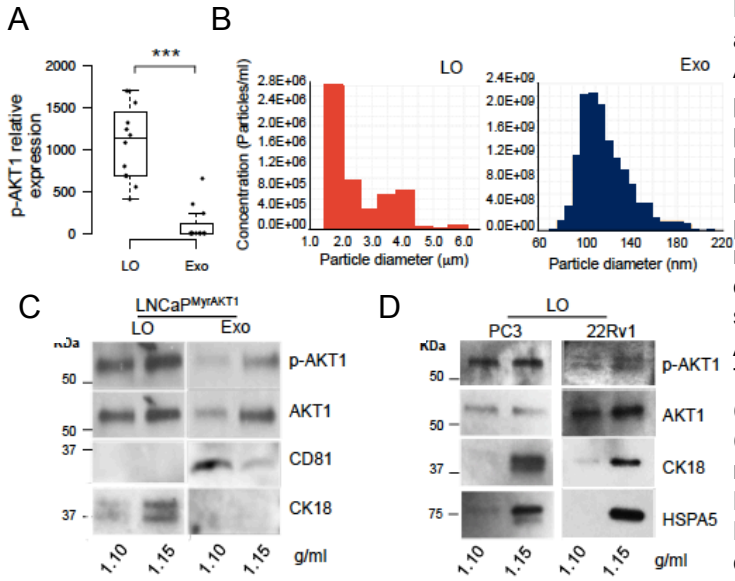

Figure 2. Large Oncosomes (LO) are EVs that harbor active AKT1. A, Protein lysates from LO and Exo purified from the plasma (500 μl) of patients with castration resistant prostate cancer (CRPC) (n=12) were blotted with a p-AKT1^{Ser473} antibody. p-AKT1^{Ser473} band intensity was normalized to protein content for each patient. Circulating LO carry significantly higher levels of active AKT1 than Exo (*** = $p < 0.002$). **C,** Tunable resistive pulse sensing (qNano) analysis of LO (left) and Exo (right) using NP2000 and NP100 membrane pores, respectively. **D,** LO and Exo were purified from LNCaP^{MyrAKT1} cell media by gradient centrifugation (iodixanol), and protein lysates (10 μg) from the indicated fractions (1.10 and 1.15 g/ml density of the 10k and 100k pellets) were blotted with the indicated antibodies, including LO marker CK18 and Exo marker CD81. **D,** Equal amounts of protein from PC3 and 22Rv1 derived LO were blotted with the indicated antibodies.

2) Src pathway activation promotes plasma membrane blebbing and EV secretion

Next, we addressed whether the activation of Src through epidermal-growth-factor (EGF) and IL-6 stimulation (6) could increase the number of invadiopodia-like protrusions (Figure 3A and 3B). We tested the activation of Src pathways by western blot, phosphorylation of ERK is a downstream event (Fig 3B). Increased plasma membrane blebbing and shedding of EVs was detected after EGF incubation. Plasma membrane blebbing is associated with amoeboid motility and increased metastatic propensity (Figure 3). By time lapse video microscopy we detected the increase shedding of LO after IL-6 and EGF stimulation (**Fig 3C**).

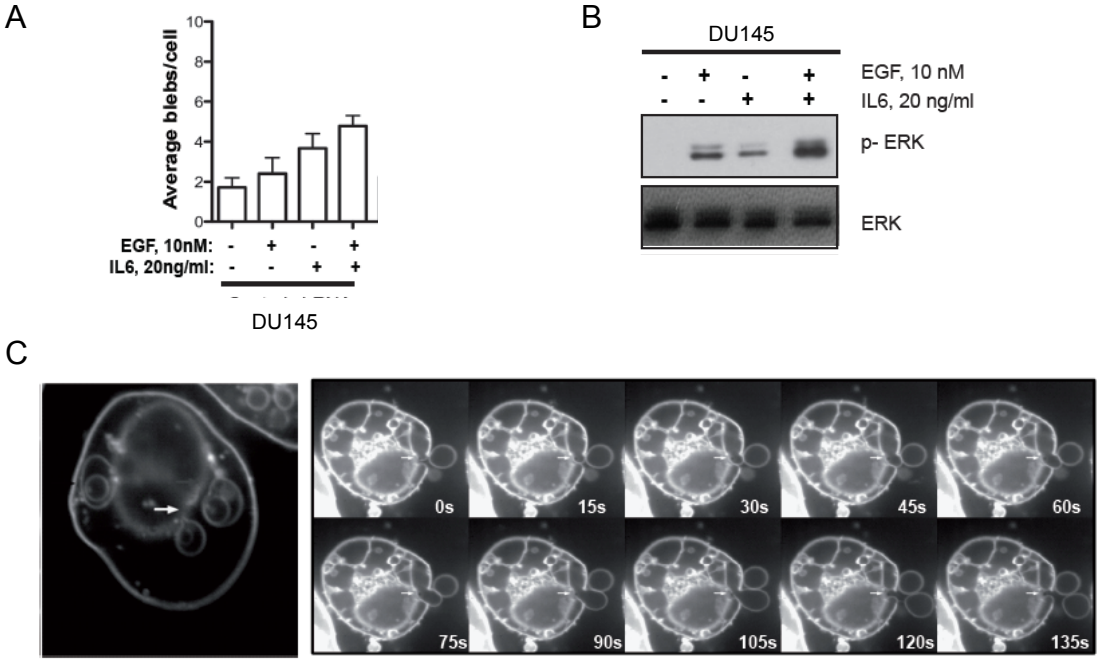

Figure 3. Increased plasma membrane blebbing and shedding of EVs through EGF and IL-6 stimulation. A, Average of blebs per cell in DU145 under EGF and IL-6 stimulation **B,** sustained ERK phosphorylation in response to EGF and IL-6, quantified by western blot in DU145 cells. **C,** Increased shedding of EVs under EGF stimulation in DU145 cells.

3) Inhibition of MAP kinase pathway prevents plasma protrusions

Next we used a selective inhibitor of MAP kinases, PD98059, to address whether we can prevent plasma membrane blebbing. The average number of blebs per cells was lower after incubation with PD98059 (**Fig 4**).

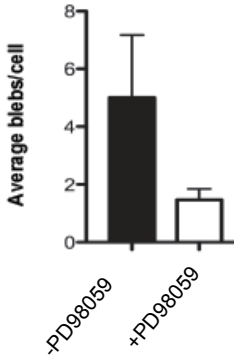

Figure 4. MAPK inhibition prevents plasma membrane blebbing. Average of blebs per cell in DU145 is prevented using PD98059 inhibitor.

4) LO are internalized by heterologous cells. EV uptake typically represents an important step for intercellular communication (7). In order to further investigate the consequences of LO uptake by cells from the microenvironment, we exposed immortalized WPMY-1 myofibroblasts to LO labeled with the fluorescent dye PKH26. LO uptake by target cells was quantitatively analyzed by flow cytometry (FACS) (**Fig. 5A**). Confocal imaging of FACS sorted LO-positive cells showed intact PKH26-labeled LO in the peripheral and perinuclear area (**Fig. 5B**). Increased PKH26 signal correlated with an increasing number of vesicles (**Fig. 5C**). Additionally, we found co-localization of PKH26 with MyrAKT1 (**Fig. 5D**), as detected with an HA-FITC antibody that binds with high specificity to the HA tag of the MyrAKT1 construct (8), which is expressed in the donor cells but absent in the target cells. These results suggest that the particles were intact LO rather than empty circular membrane structures capturing the lipid dye. We then determined whether cells other than myofibroblasts could also internalize LO. We tested normal human prostatic fibroblasts (NAF), human umbilical vein endothelial cells (HUVEC), CD8+ lymphocytes, and DU145 and LNCaP cancer cell lines. NAF are primary cells generated from prostatectomy tissues not associated with PCa. LO uptake varied among these cells, and was almost completely impaired in CD8+ lymphocytes (**Fig. 5E**), implying a selective mechanism of uptake. These observations suggest that LO enter target cells by a mechanism that might involve defined interactions between LO and the recipient cells.

To further rule out the possibility that LO uptake occurs by a passive fusion of EV and cell membranes, we incubated target cells with LO at 4^0C. This strategy has been previously used to inhibit ATP-dependent processes that are involved in EV endocytosis but not fusion (9). This approach efficiently prevented LO uptake (**Fig. 5A**) suggesting an active endocytic process. Due to their large size, we considered both phagocytosis and macropinocytosis as possible mechanisms, and tested the effect of known inhibitors of the major steps of these two processes on LO uptake.

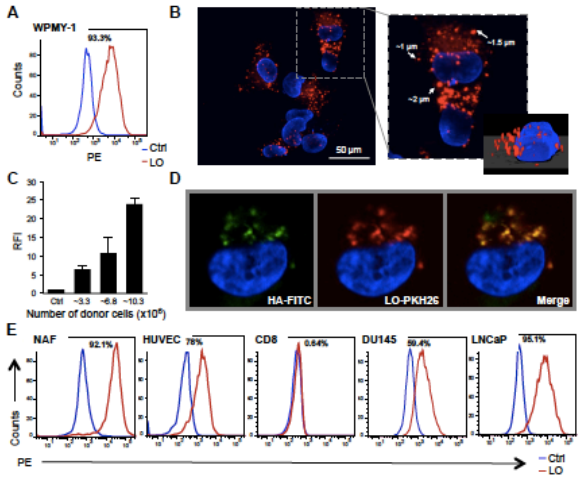

Figure 5: Internalization of LO by cells from the microenvironment. A, WPMY-1 fibroblasts were exposed to PKH26-labeled LO from LNCaP^{MyrAKT1} cells, or vehicle for 1h. The shift of the red line to the right, which is quantifiable, indicates LO internalization by the target cells. **B,** Cells positive for PKH26 were FACS-sorted and imaged by confocal microscopy demonstrating the presence of abundant vesicular structures in the LO size range. **C,** WPMY-1 cells were incubated with increasing doses of PKH26-labeled LO and then analyzed by FACS. Uptake rates, expressed as relative fluorescent intensity (RFI), correlate with LO doses. **D,** PKH26 positive WPMY-1 cells were sorted and stained with a HA-FITC antibody against the HA-tag on the MyrAKT1 construct. The two signals co-localize in internalized EVs. **E,** FACS analysis demonstrates variable uptake rate in the indicated cell lines exposed to PKH26-labeled LO.

The PI3K inhibitor, Wortmannin (WTN), and the actin polymerization inhibitor, cytochalasin-D (CYT-D) (10,11), typically used to block both phagocytosis and macropinocytosis (19), significantly perturbed LO uptake (**Fig 6**).

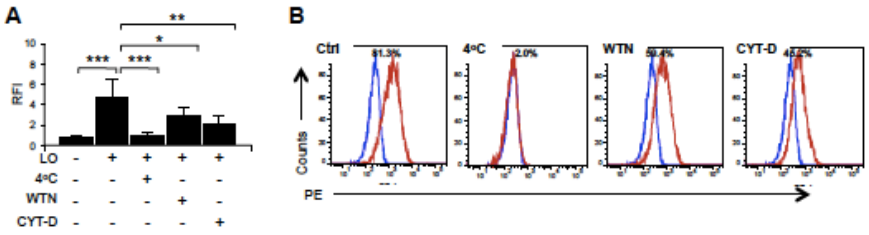

Figure 6. **A**, WPMY-1 fibroblasts were incubated with PKH26-labeled LO in presence or absence of Wortmannin (WTN) (1mM) or cytochalasin-D (CYT-D) (5mM), and then analyzed by FACS to quantify uptake inhibition. Bar plots show the mean of three biological replicates (*=p<0.05, **=p<0.02, ***=p<0.002). **B,** Representative FACS histograms of panel a.

To determine the relative contribution of these two processes, we used Dynasore-OH (Dyn) (12) and 5-(N-Ethyl-N-isopropyl) amiloride (EIPA) respectively. The primary and most ubiquitous target of Dyn is dynamin 2 (DNM2), which plays a role in the first stages of phagocytosis, including actin polymerization and augmenting of the membrane surface for particle engulfment (13,14). EIPA, which inhibits the Na+/H+ antiporter (15), is typically used to block macropinocytosis. LO uptake was significantly inhibited by Dyn but not by EIPA (**Fig. 7A and 7B**), suggesting that it occurs through a phagocytosis-like mechanism. The involvement of DNM2 in LO phagocytosis was further confirmed by a significant reduction in LO uptake upon transient silencing of DNM2 (**Fig. 7 and 8**).

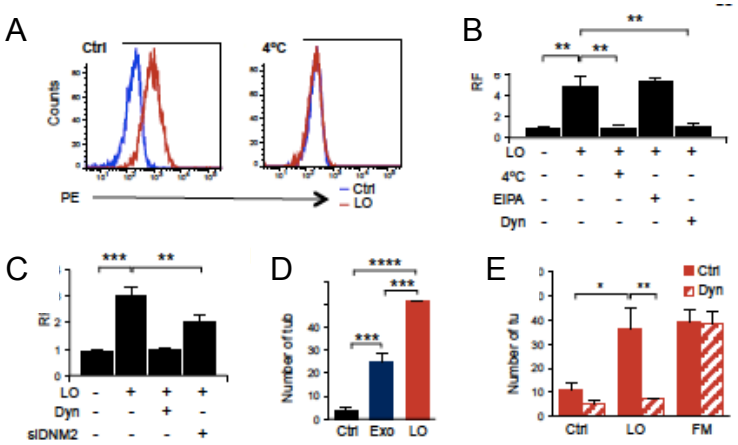

Figure 7. A, Treatment of WPMY-1 cells with LO at 4°C inhibits the uptake. **B,** LO uptake by WPMY-1 cells was significantly inhibited by Dynasore (Dyn) (20 μM) but not by 5-(N-Ethyl-N-isopropyl) amiloride (EIPA) (50 μM). As expected, uptake was inhibited at 4°C. **C,** Transient silencing of DNM2 (siDNM2) in WPMY-1 cells resulted in a significant reduction of LO uptake. **D,** Human umbilical vein endothelial cells (HUVEC) were seeded on matrigel-coated wells and exposed to Exo or LO (20 μg/ml). The number of branched tubes was significantly altered by both LO and Exo. **E,** Dyn treatment prevented the LO-induced tube formation. Bar plots show the average of three biological replicates (* = p < 0.05, ** = p < 0.02, *** = p < 0.002, **** = p < 0.000001)

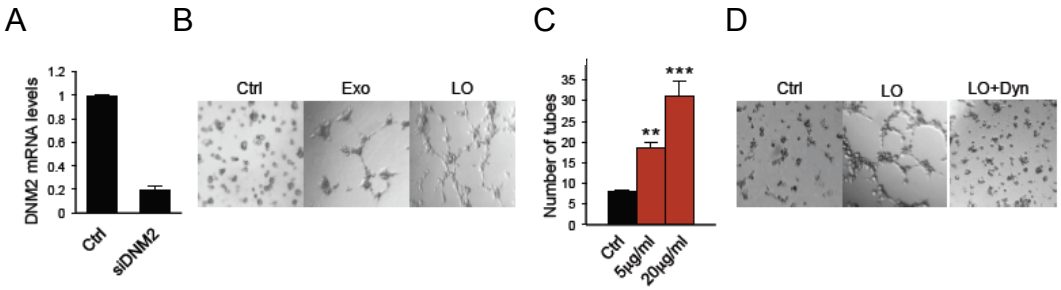

Figure 8. EVs induce angiogenesis. A) qRT-PCR in WPMY-q fibroblasts transiently silenced for DNM2, **B**) Representative images of the tube branching assay with HUVEC exposed to either Exo and LO from LNCAP ^{MyrAkt1} **C**) Tube branching assay with different doses of LO showing a dose-dependent response to LO treatment, which starts at 5 mg/ml. This dose corresponds to the use of LO from 10 door PCa cells to treat 1 recipient fibroblast, a result that is indicative of hogh biological potency. Bar plot shows the mean of three biological replicates **=p<0.02, ***=p<0.002). **D**) Representative images of the tube branching assay with Dyn. Bar plots show the mean of three biological replicates (8=p<0.05, 0.02, ***=p<0.002).

5) LO promotes tube branching ability in HUVEC

To determine whether the internalization is important for LO function, we employed tube formation assays, which have been previously used to show bioactivity of Exo (16) but have never been used to test LO function. Notably, LO stimulated a significant increase of the tube branching abilities of HUVEC. This effect was greater than that elicited by Exo, and was obtained with amounts of LO (5-20µg/ml) that are lower than those typically used for functional EV experiments (20-200 µg/ml) (17,18) (**Fig. 8D**). Dyn treatment of HUVEC cells prevented LO-induced tube branching, but did not prevent the branching induced by full media (FM), which contains abundant soluble molecules that stimulate angiogenesis (**Fig 7E**). Collectively, these results indicate that LO enter the target cells through a phagocytosis-like mechanism, and that this is necessary for LO-mediated biological functions.

6) LO enhanced the expression pro-vascularization factors on NAF

Because it is known that tumor-activated fibroblasts release factors that can influence tube formation (19), and having observed a potent induction of tube branching in response to LO used directly to condition endothelial cells, we tested whether this effect in endothelial cells could be elicited by the secretions of fibroblasts that had internalized LO. Conditioned media (CM) from NAF pre-treated with LO induced a more significant increase in tube branching than Exo (**Fig 7D**). To understand the molecular basis underlying the LO-induced result on NAF, we tested changes in expression of factors that are upregulated in fibroblasts activated by cancer cells (18,20). LO treatment resulted in enhanced expression of interleukin 6 (IL6), matrix metalloproteinase 9 (MMP9) (**Fig. 10E**) and α-smooth muscle actin (α-SMA) (**Fig.10C**). Conversely, transforming growth factor β1 (TGF-β1), MMP1, thrombospondin 1 (TSP1), which also have been recognized as markers of an activated, myofibroblast-like phenotype (18,21-24)

were not altered (data not shown) suggesting that LO induce a distinct reprogramming of the fibroblasts, which results in a pro-vascularization phenotype.

7) LO activate the transcription factor MYC in NAF. Transcription factor (TF) activation might be an important mechanism underlying the responses of target cells to EVs (25). However, how frequently this happens and whether this phenomenon is specific for a given subpopulation of EVs, or for a given TF, has not yet been investigated. We thus tested if LO treatment perturbed TF activity, with the underlying hypothesis that this could be the mechanism modulating the effects described above. Nuclear extracts of fibroblasts exposed to LO or vehicle were tested for functional binding of TFs to DNA. We employed an activity array for TFs with a known role in somatic cell reprogramming (including EGR1, Nanog, SOX2, ETS, KLF4, MEF2, MYC, Pax6, TCF/LEF). Independent trials revealed reproducible enhancement of MYC binding to DNA in response to LO (**Fig 10B**). To further validate this result, we measured MYC activity by examining the stimulation of MYC-dependent transcription. We used a luciferase assay that tests the activity of the cyclin-dependent kinase 4 (CDK4) promoter, which is regulated by MYC. Significant activation of this promoter was observed upon treatment with LO, but not with the same amount of Exo (Fig. 8D, $p < 0.05$).

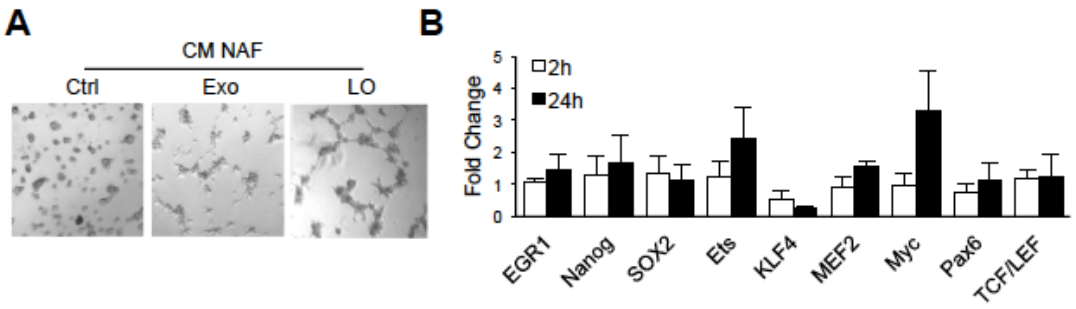

Figure 9) EVs promote angiogenic features. A) Representative images of tube branching assay in response to conditioned media (CM) from NAF previously incubated with Exo or LO. **B**) A transcription factor (TF) profiling array was applied to nuclear extracts of fibroblasts exposed to LO or vehicle for the indicated times to test FT activity in response to LO. Reporter activation was measured as relative luminescence activity in response to LO. Reporter activation was measured as relative to luminescence activity (RLU). The bar plot shows the ratio of the RLU between the treatment conditions and the control expressed as fold change.

This estimation was based on protein concentration (20 µg/ml), normalized to the number of cells. However, we reasoned that the array was composed of very few TFs, and a large-scale approach might be useful to unambiguously define the TF pathways involved in LO-mediated activation. RNA sequencing (RNA-seq) was carried out in NAF exposed to LO or vehicle to obtain an in-depth analysis of the transcriptome of these cells in response to LO. This analysis, performed in biological duplicate, identified 207 differentially expressed genes (DEG) (false discovery rate (FDR) < 0.1, fold change ≥ 1.5) in response to LO. Master regulator analysis (MRA) was then applied to the DEG set using TF-target

interaction information collected from public databases. This allowed us to infer functional interactions between TFs and their target genes following a strategy we previously employed to identify important transcriptional regulators (26). 16 out of a total of 274 activated TFs emerged as strong putative TFs (empirical test p-value < 0.01 and hypergeometric test p-value < 0.01). The number of putative TFs that were activated by LO is relatively small (~6%), suggesting that modulation of gene expression is selective. MYC emerged as a highly activated TF in response to LO (**Fig. 10E**), confirming our initial results. Furthermore, NAF exposed to LO exhibited increased levels of fibroblast growth factor 2 (FGF2), glutaminase (GLS) and lactate dehydrogenase (LDH), which are known transcriptional targets of MYC (**Fig 10F**). These results support an LO-dependent modulation of MYC activity in fibroblasts.

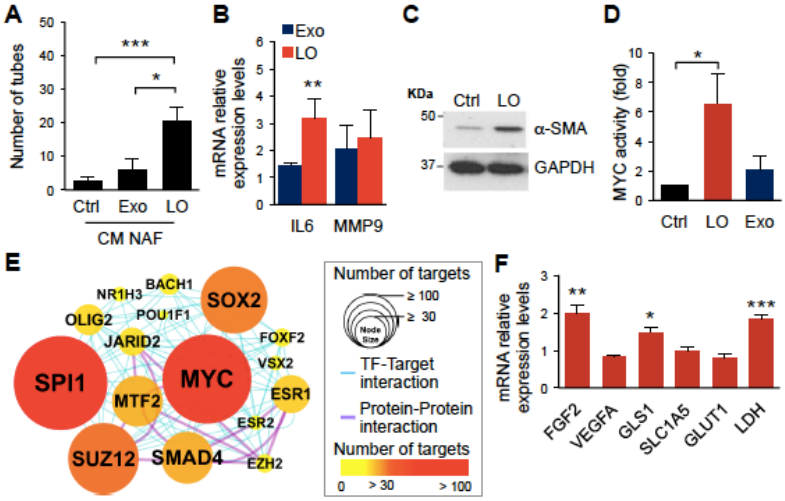

Figure 10) LO treatment of normal associated human prostatic fibroblasts (NAF) induces a MYC-dependent reprogramming. A, HUVEC cells were exposed to CM from NAF, previously incubated with LO and Exo. The CM from NAF pretreated with LO, but not Exo, induced tube formation. **B,** qRT-PCR of NAF exposed to LO or vehicle shows increased levels of IL6 and MMP9 mRNA in response to LO treatment. **C,** Immunoblot experiments demonstrated increased levels of α-SMA in NAF upon 24h exposure to LO. **D,** Luciferase activity of MYC regulated CDK4 promoter significantly increased in NAF exposed to LO but not Exo. **E,** Master regulator analysis (MRA) of differentially expressed genes (DEG) obtained after RNA-Sequencing in NAF treated with LO or vehicle. MYC is one of the most active TF in NAF in response to LO. TF network illustrating interactions between key TFs and the degree of influence to potential target genes among the DEGs (node size and color respectively). TFs with a large number of targets (> 105) is represented by big red nodes while TFs with smaller numbers of targets (< 50) are indicated with small yellow nodes. Cyan and purple connectors indicate TF-target and protein-protein interactions, respectively. **F,** qRT-PCR in NAF, exposed to LO or vehicle, shows increase levels of MYC targets in response to LO. **G,** Immunoblot analysis showing that MYC inhibition, using either the MYC inhibitor 10058F4 (MYC-i) (20 μM) or siRNA specific for MYC (siMYC) prevents LO-dependent induction of α-SMA. **H,** MYC inhibition (MYC-i, siMYC) induces a reduction of tube formation in response to LO. **I,** Luciferase activity of the MYC-regulated promoter in response to LO is inhibited by Dyn.

8) LO-induced NAF activation is mediated by MYC

The above results prompted us to test whether MYC plays a functional role in LO-mediated fibroblast reprogramming. Both genetic silencing of MYC using MYC inhibition by the low molecular weight compound 10058-F4 (27) and two independent siRNAs (**Fig 11A**) in NAF were sufficient to block the LO-induced a-SMA increase and the ability of these cells to stimulate branching morphogenesis (**Fig 11B-D**). The LO-induced MYC activity was blocked by the MYC inhibitor confirming the specific effect of the compound (**Fig 11G**). A tumor supportive role for stromal MYC was also independently demonstrated by animal experiments in which overexpression of MYC in wild-type mouse primary prostatic fibroblasts induced hyperplasia of the adjacent normal prostatic epithelium in tissue recombinants grafted into the subrenal capsule of syngeneic C57BL/6 mice (**Fig 11H**). Interestingly, the LO-induced MYC activation was reduced in NAF by blocking LO uptake with Dyn (**Fig 11I**).

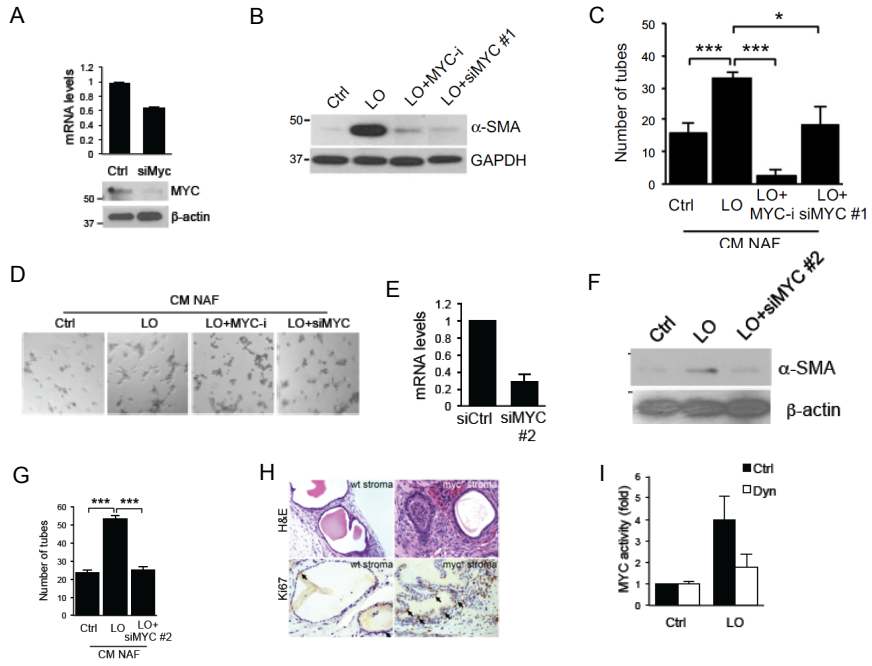

Figure 11. LO-induced NAF activation is mediated by MYC A, qRT-PCR and WB in NAF transiently silenced for MYC. **B**, Immunoblot analysis showing that MYC inhibition, using either the MYC inhibitor 10058F4 (MYC-i; 20 mmol/L) or siRNA specific for MYC (siMYC), prevents LO-dependent induction of a-SMA. **C,** HUVEC cells were exposed to CM from NAF previously incubated with LO with or without MYC inhibition. MYC inhibition (MYC-i, siMYC) induces a reduction of tube formation in response to LO. **D**, Representative images of tube branching in HUVEC cells exposed to CM from NAF, previously incubated with LO with or without MYC inhibition (MYC-i, siMYC). **E**, qRT-PCR in NAF transiently silenced for MYC using a different siRNA. **F**, Immunoblot analysis showing that MYC inhibition, a second siRNA specific for MYC (siMYC) prevents LO-dependent induction of a-SMA. **G** HUVEC cells exposed to CM from NAF, previously incubated with LO with or without MYC inhibition using a second MYC siRNA. MYC inhibition induces a reduction of tube formation in response to LO. **H** Tissue sections from mice grafted with chimeric fibroblasts stably transfected with a MYC construct or an empty vector show increased proliferating activity in MYC overexpressing conditions. Representative Hematoxylin & Eosin (H&E) and Ki67 staining are shown (Magnification: 20X). I Luciferase activity of the MYC-regulated promoter in response to LO is inhibited by Dyn.

To investigate the contribution of LO–stroma interactions in vivo, DU145 cells, alone or recombined with NAF, were injected subcutaneously in nude mice, and

tumor growth was measured for up to 35 days. Recombination of tumor cells with NAF led to an approximately 1.5-fold increase of the mean tumor volume compared with the tumor cells alone. Notably, ex vivo pretreatment of NAF for 3 days with LO isolated from LNCaP^{MyrAKT1} significantly enhanced tumor growth (~3-fold higher than tumor cells alone). This effect was completely prevented by blocking LO uptake with Dyn and reduced by treatment with the MYC inhibitor (**Fig 11A and B**). Treatment with the MYC inhibitor alone also prevented the NAF-supported tumor growth (data not shown). Together, these data provide evidence of an important functional role for MYC in fibroblast reprogramming and modulation of tumor growth mediated by AKT1-loaded LO.

9) MYC activation in the stroma is dependent on AKT1 kinase activity

Because most of the results described so far were elicited by LO originating from cells expressing a constitutively active AKT1, and because we found high levels of p-AKT1^{Ser473} in LO, we wondered whether this kinase was functionally active in the particles. We first demonstrated that MyrAKT1 can be readily immunoprecipitated in LO (**Fig 11C**). Then, the AKT1 immunoprecipitation products from the two EV populations, cultured in cell and serum-free culture conditions for up to 72 hours, were submitted to a AKT1 kinase activity assay, which demonstrated abundant phosphorylation of the AKT1 target glycogen synthase kinase 3a/b (GSK3a/b) in LO, but not in Exo (**Fig 11D**). In support of the hypothesis that LO might function as mobile platforms for active kinase, LO induced upregulation of p-AKT1^{Ser473} in NAF (**Fig 11E and 11F**).

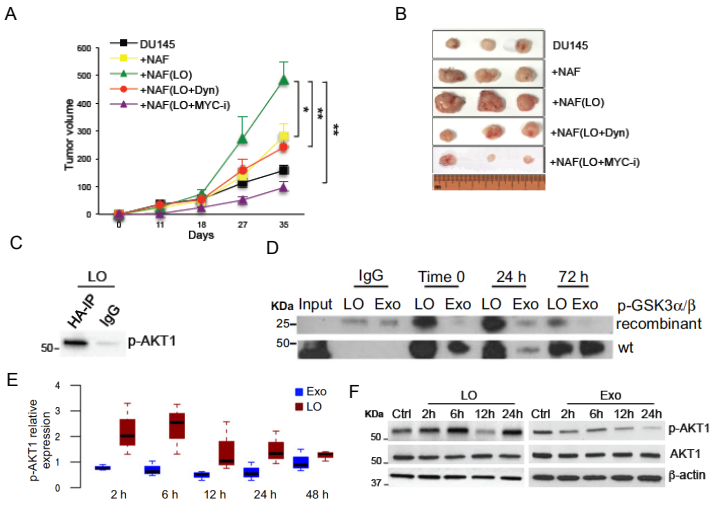

Figure 11 A) DU145 cells were injected subcutaneously into nude mice with or without NAF (ratio 4:1) and the tumor volume (mean ± SE) measured at the indicated intervals (tumors n≥5 per group). The NAF were either untreated or exposed, *ex vivo*, to LO in the presence or absence of Dyn or MYCi for 72 hours. LO treatment increased significantly the tumor volume, an effect inhibited by both Dyn and MYC-i. **B**) Representative gross photographs of the tumors. Plots shows the average of three biological replicate (*, $P < 0.05$; **, $P < 0.02$; ***, $P < 0.002$). **C**) Protein lysates were immunoprecipitated using an anti-HA antibody and blotted with p-AKT1^{Ser473}. **D**) NAF exposed to LO or Exo for the indicated times were immunoblotted with p-AKT1^{Ser473} and AKT1 antibodies. The box plot shows the average of the p-AKT1Ser473 band intensity, normalized over b-actin, from three different experiments. **E**) NAF exposed to LO or Exo for the indicated times were immunoblotted with p-AKT1Ser473 and AKT1 antibodies. The box plot shows the average of the p-AKT1^{Ser473} band intensity, normalized over b-actin, from three different experiments. **F)** Western blot with AKT1 and p-AKT1Ser473 antibodies in NAF exposed to the same amount of LO or Exo at the indicated times. Representative images, from three independent replicates, are shown.

We then tested whether AKT1 activity is necessary for the LO-mediated effects on the stroma. MYC activity (**Fig. 12A**), α-SMA levels (**Fig. 12B**), and tube branching (**Fig. 12C-E**) were reduced in NAF exposed to LO in the presence of the AKT1 inhibitor AZD5363 (28) in comparison with vehicle treatment. The result on tube branching was reproduced with LO derived from an unrelated prostate cancer cell line that endogenously expresses an active AKT1 (**Fig. 12F**). Collectively, these data suggest that the LO-induced fibroblast reprogramming is dependent on AKT1 kinase activity.

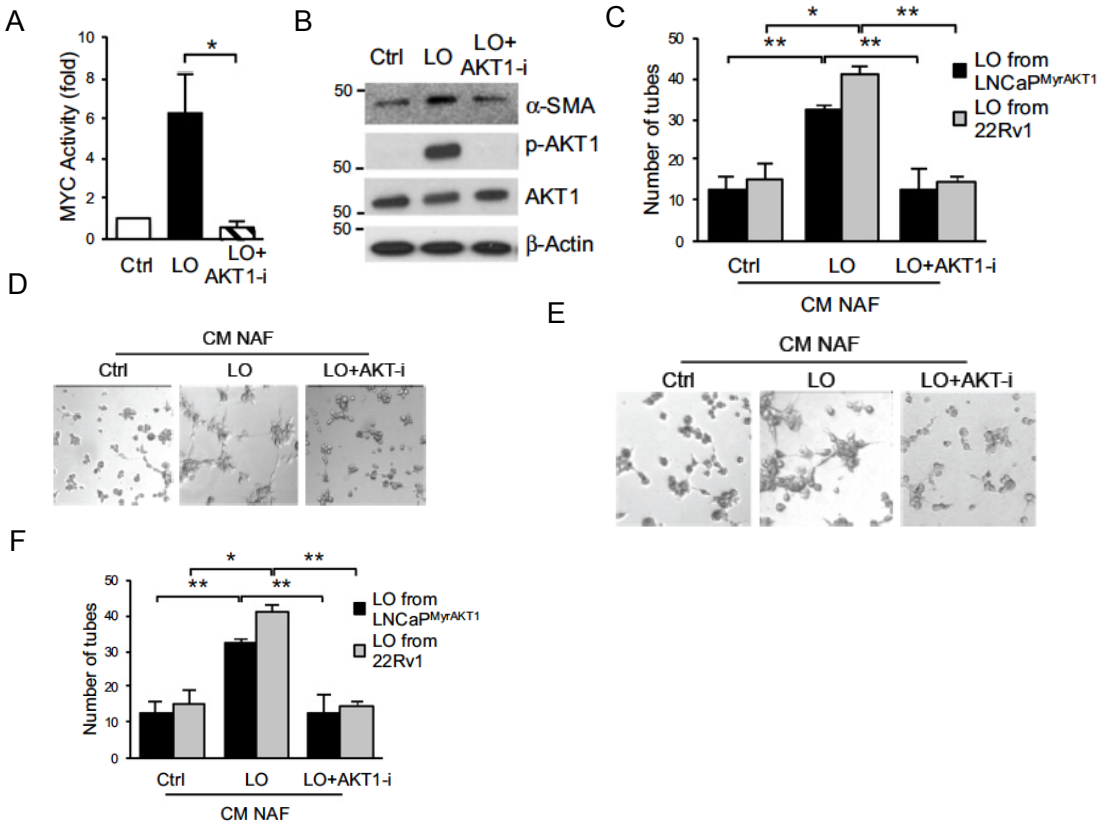

Figure 12. A) Luciferase activity of the MYC-regulated promoter in response to LO inhibited by the AKT1 inhibitor AZD5363 (AKT1-i; 1 μmol/L). Bar plot shows the average of three biological replicates (*, $P < 0.05$). **B**) NAF exposed to LO or Exo for the indicated times were immunoblotted with p-AKT1^{Ser473} and AKT1 antibodies. The box plot shows the average of the p-AKT1Ser473 band intensity, normalized over b-actin, from three different experiments. **C**) Luciferase activity of the MYC-regulated promoter in response to LO inhibited by the AKT1 inhibitor AZD5363 (AKT1-i; 1 μmol/L). Bar plot shows the average of three biological replicates (*, $P < 0.05$). Representative images of HUVEC cells seeded on matrigel-coated wells and exposed to CM from NAF previously incubated with LO from LNCaP^{MyrAKT1} (**D**) or 22Rv1 (**E**) in presence or absence of the AKT1 inhibitor AZD5363 (AKT1-i). Tube branching in response to LO is reduced by AKT1-i. Bar plots show the average of three biological replicates (*, P < 0.05; **, P < 0.02).

8. <u>Key research accomplishments.</u> We have demonstrated:

- Activation of PI3K and Src pathways promotes shedding of LO
- Inhibition of MAP kinase pathway prevents plasma protrusions, involved in cancer cells motility
- LO are EVs that harbor active AKT1
- Active AKT1 was detected in circulating EV from the plasma of metastatic prostate cancer patients and was LO specific.
- LO can be internalized by cells from the PCa microenvironment
- LO internalization induced reprogramming of human normal prostate fibroblasts as reflected by high levels of α-SMA, IL6, and MMP9.
- The internalization of LO can be prevented by inhibiting phagocytic-like events
- LO enhanced the expression of pro-vascularization factors on normal associated human prostatic fibroblasts
- LO treatment of normal associated human prostatic fibroblasts induces a MYC-dependent reprogramming
- MYC activation in the stroma is dependent on AKT1 kinase activity
- LO-reprogrammed normal prostate fibroblasts promoted tumor growth in mice
- Inhibition of LO internalization prevented activation of MYC and impaired the tumor-supporting properties of fibroblasts

9. Conclusion

Overall, our data show that prostate cancer-derived LO powerfully promote establishment of a tumor-supportive environment by inducing a novel reprogramming of the stroma. This mechanism offers potential alternative options for patient treatment.

10. Other achievements

1) Stromal cells caveolin-1 silenced uptake higher percentage of tumor derived LO. Previous findings demonstrated that Cav-1 expression in the stroma can decline in advanced and metastatic prostate cancer, taking together this finding suggests that the loss of Cav-1 in stroma can facilitate the cells reprograming and tumor progression (Figure 12).

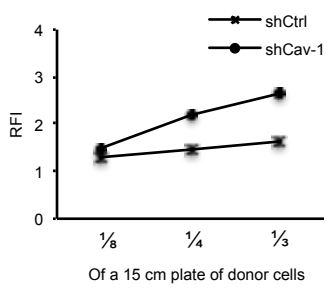

Figure 12. LO are preferentially internalized by stromal cells with low Cav1. Fibroblasts WPMY-1 Cav-1 silenced and controls using shRNA were exposed to increase concentration of LO tumor cells derived.

2) Because nuclear deformability is a rate liming-step during cancer cell migration (29) we studied the nuclear shape of LO-shedding cells. We stained the nuclear envelope and we detected increased nuclear membrane instability (Figure 13A). We observed emerin mislocalization in association with disruption of the nuclear envelope contour in LO-shedding cells, as well as nuclear envelope blebbing. We also observed increased levels of emerin in LO purified by gradient ultracentrifugation from the cell media (Figure 13B). Our data suggest that emerin can be a marker for extracellular vesicles originated from cells with nuclear membrane instability. Cav-1 has been previously described as EV marker and recent reports shown that Cav-1 directly interacts with emerin. Taken together, these observations reinforce the idea that nuclear derived material can be found in EVs and emerin can be a biomarker of aggressive cancer.

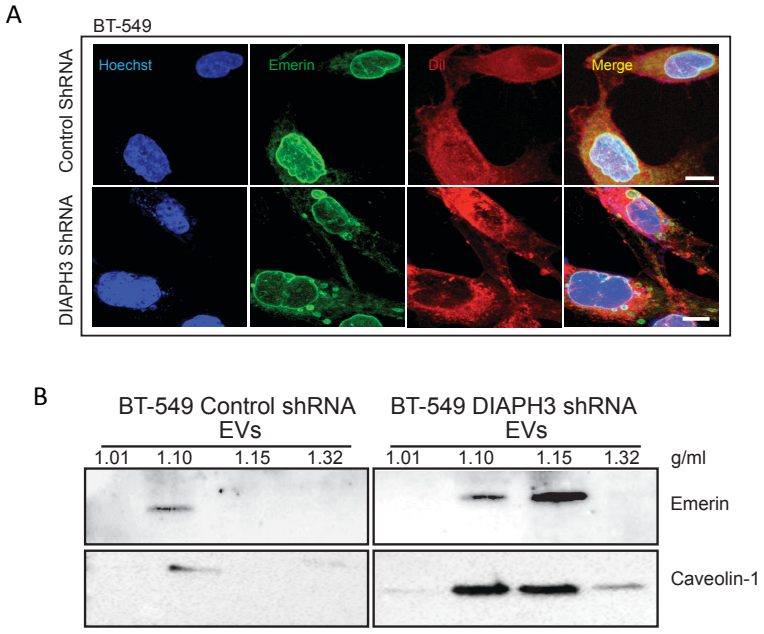

Figure 13. Nuclear membrane instability in cancer LO-shedding cells. **A**) Confocal 3D images of BT-549 control shRNA and DIAPH3 shRNA cells. DNA (Hoechst, blue), emerin (FITC, green) and membrane (DiI, red) staining are shown, scale bar 10 mm. **B**) emerin immunoblot of secreted EVs from BT-549 control shRNA and BT DIAPH3 shRNA cells culture for 24h in EVs-free complete culture medium. Equal numbers of cells were plated and the EVs were purified with layers of OptiPrepTM with the indicated densities.

References

1. Zhang, J. and J. Liu, Tumor stroma as targets for cancer therapy. Pharmacol Ther, 2013. 137(2): p.200-15.
2. Li, H., X. Fan, and J. Houghton, Tumor microenvironment: the role of the tumor stroma in cancer. J Cell Biochem, 2007. 101(4): p. 805-15.
3. Vader, P., X.O. Breakefield, and M.J. Wood, Extracellular vesicles: emerging targets for cancer therapy. Trends Mol Med, 2014. 20(7): p. 385-93.
4. Di Vizio, D., et al., An absence of stromal caveolin-1 is associated with advanced prostate cancer, metastatic disease and epithelial Akt activation. Cell Cycle, 2009. 8(15): p. 2420-4.

5. van der Mijn JC, Sol N, Mellema W, Jimenez CR, Piersma SR, Dekker H, et al. Analysis of AKT and ERK1/2 protein kinases in extracellular vesicles isolated from blood of patients with cancer. J Extracell Vesicles 2014;3:25657 doi 10.3402/jev.v3.25657.
6. Osherov, N., and Levitzki, A., Epidermal-growth-factor-dependent activation of the src-family kinases. Eur J Biochem, 1994; 1;225(3):1047-53.
7. Abels ER, Breakefield XO. Introduction to Extracellular Vesicles: Biogenesis, RNA Cargo Selection, Content, Release, and Uptake. Cell Mol Neurobiol 2016;36(3):301-12 doi 10.1007/s10571-016-0366-z.
8. Di Vizio D, Morello M, Dudley AC, Schow PW, Adam RM, Morley S, et al. Large oncosomes in human prostate cancer tissues and in the circulation of mice with metastatic disease. Am J Pathol 2012;181(5):1573-84 doi 10.1016/j.ajpath.2012.07.030.
9. Svensson KJ, Christianson HC, Wittrup A, Bourseau-Guilmain E, Lindqvist E, Svensson LM, et al. Exosome uptake depends on ERK1/2-heat shock protein 27 signaling and lipid Raft-mediated endocytosis negatively regulated by caveolin-1. J Biol Chem 2013;288(24):17713-24 doi 10.1074/jbc.M112.445403.
10. Araki N, Johnson MT, Swanson JA. A role for phosphoinositide 3-kinase in the completion of macropinocytosis and phagocytosis by macrophages. J Cell Biol 1996;135(5):1249-60.
11. Swanson JA. Shaping cups into phagosomes and macropinosomes. Nat Rev Mol Cell Biol 2008;9(8):639-49 doi 10.1038/nrm2447.
12. Macia E, Ehrlich M, Massol R, Boucrot E, Brunner C, Kirchhausen T. Dynasore, a cell-permeable inhibitor of dynamin. Dev Cell 2006;10(6):839-50 doi 10.1016/j.devcel.2006.04.002.
13. Kinchen JM, Doukoumetzidis K, Almendinger J, Stergiou L, Tosello-Trampont A, Sifri CD, et al. A pathway for phagosome maturation during engulfment of apoptotic cells. Nat Cell Biol 2008;10(5):556-66 doi 10.1038/ncb1718.
14. Kinchen JM, Ravichandran KS. Phagosome maturation: going through the acid test. Nat Rev Mol Cell Biol 2008;9(10):781-95 doi 10.1038/nrm2515.
15. Commisso C, Davidson SM, Soydaner-Azeloglu RG, Parker SJ, Kamphorst JJ, Hackett S, et al. Macropinocytosis of protein is an amino acid supply route in Ras-transformed cells. Nature 2013;497(7451):633-7 doi 10.1038/nature12138.
16. Kosaka N, Iguchi H, Yoshioka Y, Takeshita F, Matsuki Y, Ochiya T. Secretory mechanisms and intercellular transfer of microRNAs in living cells. J Biol Chem 2010;285(23):17442-52 doi 10.1074/jbc.M110.107821.
17. Webber JP, Spary LK, Sanders AJ, Chowdhury R, Jiang WG, Steadman R, et al. Differentiation of tumour-promoting stromal myofibroblasts by cancer exosomes. Oncogene 2015;34(3):290-302 doi 10.1038/onc.2013.560.

18. Webber J, Steadman R, Mason MD, Tabi Z, Clayton A. Cancer exosomes trigger fibroblast to myofibroblast differentiation. Cancer Res 2010;70(23):9621-30 doi 10.1158/0008-5472.CAN-10-1722.
19. Orimo A, Gupta PB, Sgroi DC, Arenzana-Seisdedos F, Delaunay T, Naeem R, et al. Stromal fibroblasts present in invasive human breast carcinomas promote tumor growth and angiogenesis through elevated SDF-1/CXCL12 secretion. Cell 2005;121(3):335-48 doi 10.1016/j.cell.2005.02.034.
20. Giannoni E, Bianchini F, Masieri L, Serni S, Torre E, Calorini L, et al. Reciprocal activation of prostate cancer cells and cancer-associated fibroblasts stimulates epithelial-mesenchymal transition and cancer stemness. Cancer Res 2010;70(17):6945-56 doi 10.1158/0008-5472.CAN-10-0785.
21. Orimo A, Gupta PB, Sgroi DC, Arenzana-Seisdedos F, Delaunay T, Naeem R, et al. Stromal fibroblasts present in invasive human breast carcinomas promote tumor growth and angiogenesis through elevated SDF-1/CXCL12 secretion. Cell 2005;121(3):335-48 doi 10.1016/j.cell.2005.02.034.
22. Giannoni E, Bianchini F, Masieri L, Serni S, Torre E, Calorini L, et al. Reciprocal activation of prostate cancer cells and cancer-associated fibroblasts stimulates epithelial-mesenchymal transition and cancer stemness. Cancer Res 2010;70(17):6945-56 doi 10.1158/0008-5472.CAN-10-0785.
23. Kalluri R, Zeisberg M. Fibroblasts in cancer. Nat Rev Cancer 2006;6(5):392-401 doi 10.1038/nrc1877.
24. Serini G, Gabbiani G. Mechanisms of myofibroblast activity and phenotypic modulation. Exp Cell Res 1999;250(2):273-83 doi 10.1006/excr.1999.4543.
25. Cossetti C, Iraci N, Mercer TR, Leonardi T, Alpi E, Drago D, et al. Extracellular vesicles from neural stem cells transfer IFN-gamma via Ifngr1 to activate Stat1 signaling in target cells. Mol Cell 2014;56(2):193-204 doi 10.1016/j.molcel.2014.08.020.
26. Yang W, Ramachandran A, You S, Jeong H, Morley S, Mulone MD, et al. Integration of proteomic and transcriptomic profiles identifies a novel PDGF-MYC network in human smooth muscle cells. Cell Commun Signal 2014;12:44 doi 10.1186/s12964-014-0044-z.
27. Yin X, Giap C, Lazo JS, Prochownik EV. Low molecular weight inhibitors of Myc-Max interaction and function. Oncogene 2003;22(40):6151-9 doi 10.1038/sj.onc.1206641.
28. Lamoureux F, Thomas C, Crafter C, Kumano M, Zhang F, Davies BR, et al. Blocked autophagy using lysosomotropic agents sensitizes resistant prostate tumor cells to the novel Akt inhibitor AZD5363. Clin Cancer Res 2013;19:833–44.
29. Davidson PM, Denais C, Bakshi MC, Lammerding J. Nuclear deformability a rate-limiting step during cell migration in 3-D environments. Cell Mol Bioeng 2014; 1;7(3):293-306.

30. Sanna E, Miotti S, Mazzi M, De Santis G, Canevari S, Tomassetti A. Binding of nuclear caveolin-1 to promoter elements of growth-associated genes in ovarian carcinoma cells. Exp Cell Res 2007; 313(7):1307-17.

What opportunities for training and professional development has the project provided?

I am a co-author of 2 published studies and I am preparing a first author study describing the relation between nuclear membrane instability, extracellular vesicles shedding and metastasis (see PRODUCTS section). I presented the results of this study at the 2016 and 2017 International Society of Extracellular Vesicles (ISEV). I gave presentations in lab meetings, journal club, and cancer biology workgroup meetings.

How were the results disseminated to communities of interest?

From this work, we demonstrated for the first time that LO circulates in blood from prostate cancer patients, containing active AKT1. This is a major discovery in the field, which has allowed collaborations with other nationally prominent prostate cancer research teams, including UCLA. This work elucidates of the function of LO in the modulation of the tumor microenvironment and identifies the nodes that could be targeted to prevent tumor progression and metastasis. Manipulating the expression or activity of select proteins may regulate PCa progression *in vivo*. We will also identify the differentially secreted proteins and we applied a set of experimental and bioinformatics strategies to understand the function of LO in the tumor microenvironment and develop approaches directed toward targeting it.

4. IMPACT.

What was the impact on the development of the principal discipline(s) of the project?

I have made an important conceptual and clinically relevant advance by characterizing the role of LO uptake in cells from PCa microenvironment. Consequently, this project is high impact and high reward, with potentially immediate opportunities to alter clinical practice if the classification scheme can be shown to have clinical utility. We additionally identify new markers to isolate EVs in patients.

What was the impact on other disciplines?

Nothing to Report.

What was the impact on technology transfer?

Nothing to Report.

What was the impact on society beyond science and technology?
Nothing to Report.

5. CHANGES/PROBLEMS

Changes in approach and reasons for change
Nothing to Report.

Actual or anticipated problems or delays and actions or plans to resolve them
Nothing to Report.

Changes that had a significant impact on expenditures
Nothing to Report.

Significant changes in use or care of human subjects, vertebrate animals, biohazards, and/or select agents
Nothing to Report.

6. PRODUCTS:

Publications, conference papers, and presentations

Other publications, conference papers, and presentations.
Journal publications.

1. **Reis-Sobreiro M**, Chen JC, Zijlstra A, Morley S, You S, Stedman K, Gill NK, Chu C-Y, Chung LWK, Tanaka H, Yang W, Rowat AC, Tseng H-R, Knudsen BS, Posadas EM, Di Vizio D, Freeman MR. The nuclear envelope protein is a critical mediator of nuclear instability and metastasis (in preparation).
2. Minciacchi VR, Spinelli C, **Reis-Sobreiro M**, Cavallini L, You S, Zandian M, Li X, Chiarugi P, Adam RM, Posadas EM, Viglietto G, Freeman MR, Cocucci E, Bhowmick NA, Dolores Di Vizio. Prostate fibroblast reprograming induced by large oncosomes is mediated by MYC. Cancer Research. 2017; 77(9) 2306-2317.
3. Ciardiello C, Cavallini L, Spinelli C, Yang J, **Reis-Sobreiro M**, de Candia P, Minciacchi VR, Di Vizio. Focus on Extracellular Vesicles: New Frontiers of Cell-to-Cell Communication in Cancer. Int J Mol Sci. 2016; 17(2):175.2.
4. Minciacchi VR, You S, Spinelli C, Morley S, Zandian M, Aspuria PJ, Cavallini L, Ciardiello C, **Reis-Sobreiro M**, Morello M, Kharmate G, Jang SC, Kim DK, Hosseini-Beheshti E, Tomlinson Guns E, Gleave M, Gho YS, Mathivanan S, Yang W, Freeman MR, Di Vizio D. Large oncosomes contain distinct protein cargo and represent a separate functional class of tumor-derived extracellular vesicles. Oncotarget. 2015; 6(13): 11327-41.

Books or other non-periodical, one-time publications.
Nothing to Report.

Other publications, conference papers, and presentations.
Poster presentation:

1. **Reis-Sobreiro M**, Chen JC, Zijlstra A, Morley S, You S, Stedman K, Gill NK, Chu C-Y, Chung LWK, Tanaka H, Yang W, Rowat AC, Tseng H-R, Knudsen BS, Posadas EM, Di Vizio D, Freeman MR. Amoeboid cancer cells shed extracellular vesicles enriched with nuclear derived material. International Society of Extracellular Vesicles (ISEV),Toronto, Canada, 2017 (Selected for oral presentation and poster secion)
2. **Reis-Sobreiro M**, Morley S, Steadman K, Chen JF, You S, Yang W, Posadas E, Di Vizio, D, and Freeman M.R. Disruption of the LINC complex drives transition to the amoeboid phenotype. Cancer Research Poster Day Cedars Sinai Medical Center, Los Angeles, USA, 9 June 2016.
3. **Reis-Sobreiro M**, Morley S, Steadman K, Chen JK, You S, Posadas E, Di Vizio D, Freeman MR. Disruption of the LINC complex in cancer cells drives the genesis of extracellular vesicles with nuclear content. International Society of Extracellular Vesicles (ISEV), Rotterdam, The Netherlands, 2016 (Selected for oral presentation)
4. Minciacchi VR, You S, Yang W, Morello M, **Reis-Sobreiro M**, Spinelli C, Zandian M, Kim J, Rotinen M, Morley S, Freeman MR, Di Vizio D. Functional and quantitative proteomic analysis of two distinct populations of extracellular vesicles from the same cell source. International Society of Extracellular Vesicles (ISEV), Melbourne, Australia, 2014 (Oral presentation).
5. Minciacchi VR, Spinelli C, Morello M, You S, Yang W, **Reis-Sobreiro M**, Zandian M, Rotinen M, Morley S, Adam RM, Freeman MR, Di Vizio D. Large oncosomes are internalized and functionally modulate transcription factors in recipient cells. SELECTBIO meeting on Circulating Biomarkers, Boston, Massachusetts, USA, 2014 (Poster).
6. Minciacchi VR, Spinelli C, Morello M, You S, Yang W, **Reis-Sobreiro M**, Zandian M, Rotinen M, Morley S, Adam RM, Freeman MR, Di Vizio D. Large oncosomes are internalized and functionally modulate transcription factors in recipients cells. Annual meeting of the American Association for Cancer Research (AACR), San Diego, USA, 2014 (Poster).
7. Minciancchi VR, Morello M, **Reis-Sobreiro M**, Spinelli C, Zandian M, Yang J, Rotinen M, Morley S, Adam RM, Freeman MR, Di Vizio D. Large oncosomes are internalized and modulate transcription factors in recipient cells. Annual meeting of the International Society of Extracellular Vesicles (ISEV), Rotterdam, The Netherlands, 2014 (Oral presentation).
8. Minciacchi VR, Spinelli C, Cavallini L, **Reis-Sobreiro M**, Zandian M, Adam RM, Posadas EM, Freeman MR, Cocucci E, Bhowmick NA, Di Vizio D. Large oncosomes reprogram prostate fibroblasts towards an angiogenic phenotype.

Annual meeting of the International Society of Extracellular Vesicles (ISEV), Rotterdam, The Netherlands, 2016 (Oral).

Lectures:

Reis-Sobreiro M "Nuclear membrane instability and cancer amoeboid motility" in the program Cell Biophysics in Physiology and Disease, held in University of California, Los Angeles, California (UCLA), May 2017.

Reis-Sobreiro M "Amoeboid motility and cancer metastasis" in the program Cell Biophysics in Physiology and Disease, held in University of California, Los Angeles, California (UCLA), March 2016.

Website(s) or other Internet site(s)
Nothing to Report.

Technologies or techniques
Nothing to Report.

Inventions, patent applications, and/or licenses
Nothing to Report.

Other Products
Nothing to Report.

7. PARTICIPANTS & OTHER COLLABORATING ORGANIZATIONS

Nothing to Report.

Has there been a change in the active other support of the PD/PI(s) or senior/key personnel since the last reporting period?
Nothing to Report.

What other organizations were involved as partners?
Nothing to Report.

8. SPECIAL REPORTING REQUIREMENTS: Nothing to Report.

9. APPENDICES: A copy of the journal publications

Statement of Work – 20/11/2014
Proposed Start Date 1 Sep, 2015

Site 1: Cedars-Sinai Medical Center [CSMC]
8700 Beverly Blvd.

Los Angeles, CA, 90048
PI: Mariana Reis-Sobreiro, PhD
Mentors: Michael R. Freeman, PhD
Dolores Di Vizio, PhD
Wei Yang, PhD

International Journal of
Molecular Sciences

MDPI

Review

Focus on Extracellular Vesicles: New Frontiers of Cell-to-Cell Communication in Cancer

Chiara Ciardiello [1,2], Lorenzo Cavallini [1,3], Cristiana Spinelli [1], Julie Yang [1], Mariana Reis-Sobreiro [1], Paola de Candia [4], Valentina Renè Minciacchi [1] and Dolores Di Vizio [1,5,6,*]

1 Division of Cancer Biology and Therapeutics, Departments of Surgery, Biomedical Sciences and Pathology and Laboratory Medicine, Samuel Oschin Comprehensive Cancer Institute, Cedars-Sinai Medical Center, Los Angeles, CA 90048, USA; chiara.ciardiello@hotmail.it (C.C.); lorecava@hotmail.it (L.C.); cristiana.spinelli@cshs.org (C.S.); julie.yang@cshs.org (J.Y.); mariana.sobreiro@cshs.org (M.R.-S.); valentina.minciacchi@cshs.org (V.R.M.)
2 Experimental Pharmacology Unit, Department of Research, IRCCS-Istituto Nazionale Tumori Fondazione G. Pascale, 80131 Naples, Italy
3 Department of Experimental and Clinical Biomedical Science, University of Florence, 50121 Florence, Italy
4 Istituto Nazionale Genetica Molecolare "Romeo ed Enrica Invernizzi", 20122 Milan, Italy; paoladecandia@yahoo.com
5 The Urological Diseases Research Center, Boston Children's Hospital, Boston, MA 02115, USA
6 Department of Surgery, Harvard Medical School, Boston, MA 02115, USA
* Correspondence: dolores.divizio@cshs.org; Tel.: +1-310-423-7709; Fax: +1-310-967-3809

Academic Editor: Ritva Tikkanen
Received: 12 August 2015; Accepted: 16 October 2015; Published: 6 February 2016

Abstract: Extracellular Vesicles (EVs) have received considerable attention in recent years, both as mediators of intercellular communication pathways that lead to tumor progression, and as potential sources for discovery of novel cancer biomarkers. For many years, research on EVs has mainly investigated either the mechanism of biogenesis and cargo selection and incorporation, or the methods of EV isolation from available body fluids for biomarker discovery. Recent studies have highlighted the existence of different populations of cancer-derived EVs, with distinct molecular cargo, thus pointing to the possibility that the various EV populations might play diverse roles in cancer and that this does not happen randomly. However, data attributing cancer specific intercellular functions to given populations of EVs are still limited. A deeper functional, biochemical and molecular characterization of the various EV classes might identify more selective clinical markers, and significantly advance our knowledge of the pathogenesis and disease progression of many cancer types.

Keywords: extracellular vesicles; exosomes; ectosomes; large oncosomes; microvesicles; cancer; intercellular communication; tumor microenvironment

1. Introduction

Extracellular vesicles (EVs) are structures of variable size (from 30 nm to a few μm), surrounded by a lipid bilayer, which are released from any type of cell into the extracellular space and are detectable in body fluids. EVs can exert pleiotropic biological functions, and can influence the microenvironment via the horizontal transfer of bioactive molecules, including proteins, lipids, DNA, and RNA [1,2]. EVs have been implicated in several physiological and pathological processes, such as inflammation, immune disorders, neurological diseases, and cancer [3–5]. One of the first lines of evidence that tumor cells shed membrane-vesicles was provided in 1978, when Friend and colleagues described them as "rare, pleomorphic membrane-lined particles ranging broadly in size between 400 and 1200 Å", in cell

lines derived from patients with Hodgkin's disease [6]. A year later an independent study identified plasma-derived vesicles released by murine leukemia cells [7]. At the beginning of the 1980s, the shedding of plasma membrane EVs from pig hepatocellular carcinoma and mouse breast carcinoma cells helped to demonstrate that tumor EVs are carriers of procoagulant activity and thus participate in cancer thrombogenicity by activating the clotting system [8]. However, only twenty years later it was formally proven that EVs are not artifacts and can affect tumor progression by promoting angiogenesis, tumor invasion, and immune escape [9,10]. Since then, the number of reports on cancer-derived EVs has surged, and it is now well established that EVs contain functional proteins, microRNA, DNA, and mutated transcripts with oncogenic properties. In particular, it has been proposed by several studies that EV DNA may serve as a biomarker for cancer detection [11,12] and targeted therapy [13]. In addition, this very active field of investigation recently culminated in the demonstration that EVs can condition the pre-metastatic niche *in vivo*, a report that unequivocally corroborates active participation of EVs in cancer lethality [14].

2. The Variegated World of Extracellular Vesicles

Tumor cells release several types of EVs, which differ in size, biogenesis, and molecular composition. Two main categories of EVs have been described: exosomes and ectosomes. In addition, recent data point to the existence of additional subpopulations of EVs, which may express quantitatively and/or qualitatively different types of molecular cargo [15–18]. Moreover, Nakano and colleagues have recently observed that different subtypes of glioblastoma may activate different pathways of EVs biogenesis, due to the activation of diverse intracellular signaling [19].

Establishing an "EV population fingerprint" is highly relevant for two main reasons. On one hand, the definition of specific biological roles associated with specific EV categories may significantly advance our knowledge about the pathogenesis and the progression of disease. On the other hand, a deeper functional, biochemical and molecular characterization of diverse populations of EVs might identify more selective clinical markers, finely defining specific steps of tumorigenesis and potential avenues for therapeutic intervention.

2.1. Exosomes

Exosomes are nano-sized EVs (30–100 nm) that originate from the late endosomal trafficking machinery, are gathered intracellularly into multivesicular bodies (MVBs) and ultimately released as a result of MVB fusion with the plasma membrane [20]. An analysis of the proteins most frequently identified in exosomes and deposited in the online EV databases *ExoCarta*, *Vesiclepedia* and *EVPedia* [21–25] highlights the presence of the tetraspanin family members CD9, CD63 and CD81, the small actin-binding protein Cofilin1, heat shock proteins such as Hsp70 and Hsp90, and enzymes involved in cell metabolism, including Enolase1, Aldolase A, phosphoglycerate kinase 1 (PGK1) and lactate dehydrogenase A (LDHA) [26]. While most of these proteins have been shown to play a role in cancer progression, their identification in exosomes is not specific for cancer. Additional proteins that have more recently emerged as specifically associated with exosomes, and often absent in EVs other than exosomes, are Tsg101 and Programmed Cell Death-6 Interacting Protein (PDCD6IP), also known as ALG-2 Interacting Protein or, more commonly, as ALIX. Interestingly, these proteins are part of the ESCRT complex (ESCRT I and ESCRT III, respectively) that has been recently shown to play a direct role in exosomes biogenesis, with specific components differently affecting vesicle shedding [27]. While silencing of Tsg101 induces a decrease in exosomes production, the absence of ALIX leads to a specific increase in the release of larger EVs [27], suggesting a role for both proteins in the biogenesis of exosomes. However, conclusive results on the absence of Tsg101 and ALIX in non MVB-derived EVs are still lacking, neither is it clearly known whether they can be identified in exosomes from all cell systems, including cancer. Moreover, despite findings demonstrating that Tsg101 and ALIX can interact, Tsg101 seems to play a direct role in cancer [28], whereas the function of ALIX is generally associated with programmed cell death [29]. Interestingly, both genes are mostly mutated, albeit at

extremely rare frequency, in human tumors, as demonstrated by data generated by the TCGA Research Network (Available online: http://cancergenome.nih.gov/) (Figure 1).

2.2. Ectosomes

Ectosomes, also reported as membrane particles, nanoparticles, matrix vesicles and microvesicles (MV), are cell surface-derived EVs typically larger than exosomes, originating from direct budding from the plasma membrane [30]. This category includes apoptotic bodies (ABs) and possibly large oncosomes (LO), which derive from apoptotic and non-apoptotic membrane blebbing processes, respectively [31–33]. Ectosome shedding can be induced by alterations in the asymmetric distribution of phospholipids in the plasma membrane, which results in the exposure of phosphatidylserine (PS) and phosphatidylethanolamine (PE) in the extracellular layer of the membrane. This information derives mostly from studies on MV [34,35] and the phenomenon of ectosome shedding is stimulated by increased levels of intracellular Ca^{2+} in different cell types including cancer [36]. Cancer-derived MV are enriched in the ADP-ribosylation factor 6 (ARF6), which functions as a promoter of EV shedding from prostate and breast cancer cell lines [37]. Importantly, interrogation of publicly available prostate cancer expression datasets demonstrates that ARF6 mRNA levels are higher in prostate cancer compared with benign tissue [38].

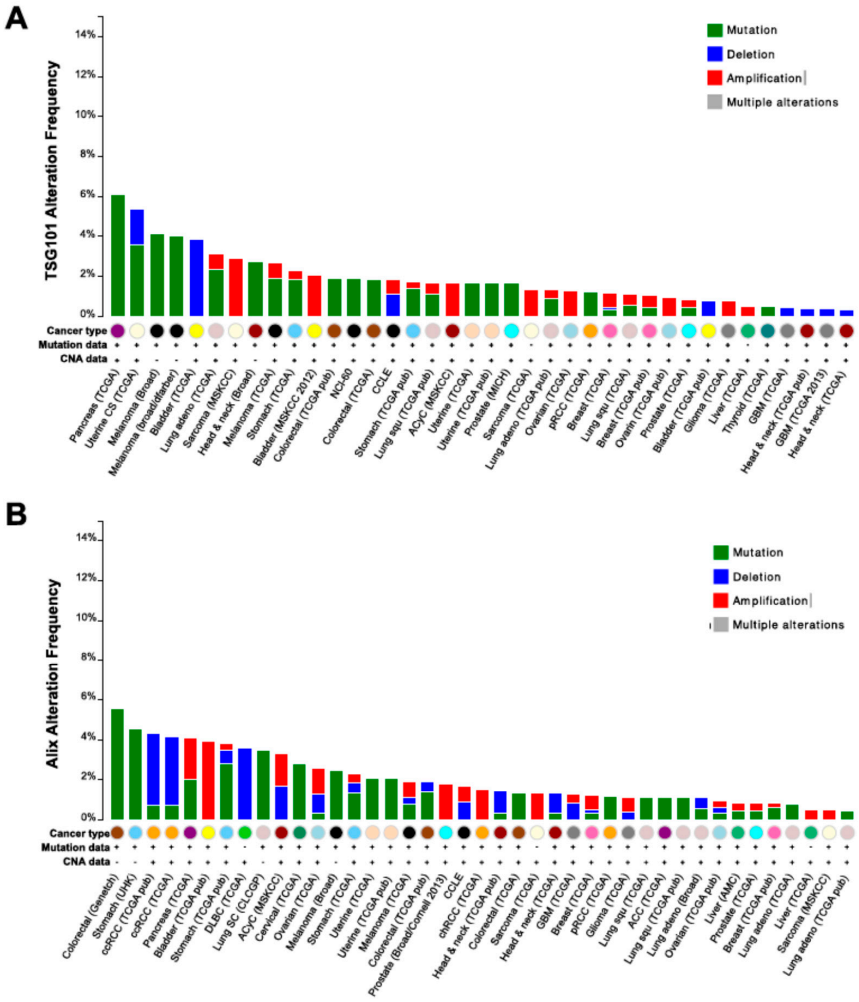

Figure 1. Genomic alterations of Tsg101 and ALIX in cancer. Frequency of copy number alterations and mutations of Tsg101 (**A**); and ALIX (**B**) across several tumor types. The results shown here are based upon data generated by the TCGA Research Network (Available online: http://cancergenome.nih.gov/).

Cancer ectosomes, similarly to other EV populations, represent a valuable reservoir for molecules functionally involved in cancer progression and are representative of their cell of origin [37,39,40] hence they make appealing candidates for the identification of circulating biomarkers. Despite the similarities in the molecular composition of ectosomes and donor cells, it is becoming evident that the internal composition of ectosomes, as well as the composition of the ectosome membrane, are not a mere reflection of the cytosol and cell membrane of the cell of origin [37,39]. Unraveling the mechanisms of molecular sorting in ectosomes could shed light on "intercellular messaging" that might occur at high rates in cancer.

2.3. Apoptotic Bodies

Apoptotic bodies (*ABs*) are particles of relatively large size (1–4 μm), released by tumor cells and other cell types upon the trigger of the cellular collapse that results in *karyorrhexis* (nuclear fragmentation), increase in membrane permeability, and externalization of phosphatidylserine (PS) [41,42]. Apoptotic membrane blebbing is a well-studied phenomenon that occurs during the late stages of programmed cell death, and is the result of caspase-mediated cleavage and consequent activation of ROCK1 [43]. It has been reported that ABs contain nuclear material, which might be functional. However, the results suggesting that ABs, through the horizontal transfer of oncogenes from cancer to recipient cells, participate in cancer development [44] needs further investigation *in vitro* and possibly *in vivo* [45]. Importantly, although an exchange of cancer-derived DNA has been reported in prostate cancer cells [46], whether this mechanism has functional consequences is still unknown. Another role suggested for ABs is that they can act by "dispatching suicide notes" to the surrounding environment. In fact, in early phases of apoptosis, AB membranes display increased permeabilization, allowing them to release proteins into the microenvironment. This, in turn, prepares the surrounding cells for the catastrophic loss of membrane integrity that affects apoptotic cells during secondary necrosis [47].

2.4. Large Oncosomes

Large Oncosomes (LO) represent an additional class of tumor-derived EVs, so called because of an atypically large size and abundant oncogenic cargo [31,38]. Similarly to ectosomes, this EV population might originate directly from plasma membrane budding and, like MV, these particles express ARF6 [38]. LO formation is particularly evident in highly migratory, aggressive tumor cells with an amoeboid phenotype [31,38], and experiments in different cell lines indicate that LO can form as bioproducts of non-apoptotic membrane blebs used by amoeboid cells as propulsive forces to migrate [32]. Quantitative analyses of LO has shown that even if LO diameter can vary from 1 to 10 μm and larger, the mode of distribution of LO diameters, calculated on hundreds of cells, is 3–4 μm, and some of them can reach several μm in size, considerably larger than any type of EV described so far. LO have been identified in several cancer systems, and comparative experiments between tumor and benign cells indicate that they are specifically released by tumor cells, whereas their detection in benign cell systems is negligible. Consistently, LO-like features have been described in human prostate cancer sections *in situ*, but not detected in benign tissue [38]. LO shedding is common to several tumor types, including prostate, breast, bladder, lung cancer, and other tumors ([38] and unpublished observations) and is enhanced by silencing of the gene encoding the cytoskeletal regulator Diaphanous related formin-3 (DIAPH3), or by activation of the epidermal growth factor receptor (EGFR) and overexpression of a membrane-targeted, constitutively active form of Akt1. Importantly, LO have been identified in the circulation of mice and patients with metastatic prostate cancer, suggesting that these EVs are potentially useful sources of clinical biomarkers [48].

EVs in the size range and appearance of LO have been recently described with different names including: (1) giant vesicles, identified in ERα-positive breast cancer cells and tumor tissues [49]; (2) migrasomes, large round structures containing numerous vesicles (pomegranate-like structures), which depart from retraction fibers of migratory benign cells [50]; and (3) tumor-derived MV

originating from amoeboid-like tumor cells, in which VAMP3 seems to regulate the delivery of MV cargo to regions of high plasma membrane blebbing. MV appear to be released through blebbing during migration [51]. Whether these three types of EVs are distinct from LO and use different mechanisms to play their extracellular functions is currently unknown.

Despite the effort to reach a consensus on vesicle nomenclature and classification, it is becoming evident that the biochemical composition and the biological function of different EV populations derived from the same cellular system overlap, at least in part [52]. Furthermore, current methods of isolation do not discriminate between exosomes and ectosomes because physical properties that can unambiguously distinguish between the two EV types have not been fully characterized and specific molecular markers are still lacking [37,53,54]. However, despite the current limitations, a recent study indicates that RNA profiles of exosomes, ectosomes, and ABs differ [55]. Therefore, regardless of the confusing and frequently inappropriate terminology used to define particular EV populations, it is clear that tumor cells release a spectrum of EVs that might all functionally participate in the biology of the disease. A partial snapshot of the vesicle types described above is presented in Table 1. A more comprehensive introduction into EVs, particularly exosomes, is provided in a focus edition by Kalra *et al.* [56].

Table 1. Populations of Extracellular Vesicles.

Vesicle Type	Size	Origin	Pathway	Cargo	Ref.
Exosomes	30–300 nm	MVB fusion with the plasma membrane	Tsg101 and ALIX dependent	Tsg101, ALIX, CD9, CD63, CD81	[27,57]
Ectosomes	0.05–1 μm	Budding from the plasma membrane	ARF6, RhoA, PS exposure dependent	ARF6	[37,40]
Apoptotic Bodies	1–4 μm	Budding from the plasma membrane	Apoptosis-related pathway	Annexin V, Caspase 3	[42]
Large Oncosomes	1–10 μm	Budding from the plasma membrane	EGFR, Akt1, Cav-1 and DIAPH3-loss dependent	ARF6, CK18, GAPDH	[31,38,48]
Giant Vesicles	3–42 μm	Budding from the plasma membrane	17-β-estradiol dependent	Not Identified	[49]
Migrasomes	0.5–3 μm	Budding from retraction fibers	Integrin and migration dependent	TSPAN4	[50]

3. Cancer Extracellular Vesicles and the Tumor Microenvironment

The molecular mechanisms regulating the functional interaction between cancer cells and the microenvironment have been the subject of active investigation, and historically are considered to be mediated by small molecules, cytokines and growth factors. Today we know that cancer cells also communicate through EVs, thus transferring functional information from cell to cell at the paracrine level (Figure 2). Recent reports are leading to the conclusion that EV cargo influences the stroma by activating molecular pathways that differ, at least in part, from the ones modulated by soluble factors [58].

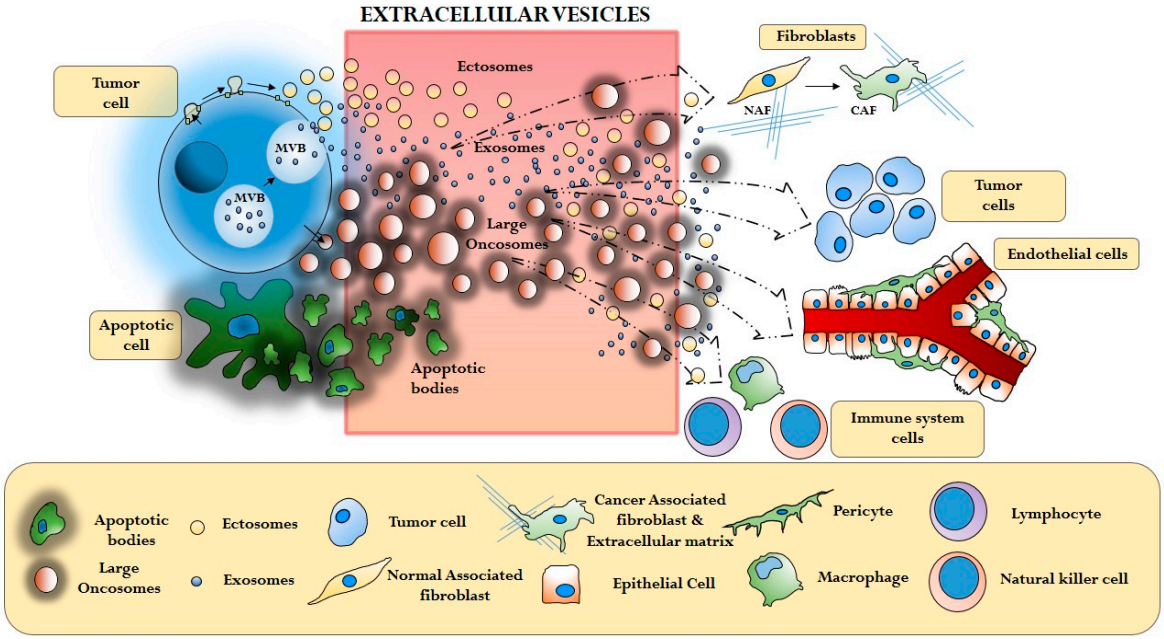

Figure 2. Extracellular Vesicle (EV)-mediated interaction between cancer cells and different components of the tumor microenviroment (Cancer Associated Fibroblasts—CAF, extracellular matrix—ECM, Tumor cells, Endothelial cells, Immune system cells).

3.1. Cancer Cells and Cancer Associated Fibroblasts (CAFs)

Cancer associated fibroblasts (CAFs) are one of the most abundant cell type in the tumor microenvironment. Upon exposure to cancer cells, CAFs alter their phenotypes [59]. In turn, when co-cultured or exposed to conditioned media from CAFs, cancer cells demonstrate increased aggressiveness, which might depend on CAF-induced stemness and metabolic reprogramming [60–63]. Both cancer cells and fibroblasts can produce different species of EVs, which seem to actively participate in the mutual interplay between these cells, and this is crucial to tumor progression [58,64–67].

A recent study demonstrated that tumor-derived exosomes can modify the stroma to promote tumor growth by supporting angiogenesis and accelerating tumor cell proliferation [58]. Furthermore, the TGF-β associated with tumor exosomes can trigger fibroblast differentiation into a myofibroblast or CAF phenotype, with increased levels of α-smooth muscle actin (α-SMA). The uptake of tumor-derived exosomes by fibroblasts also results in the deposition of a hyaluronic acid pericellular coat leading to increased contractile activity [64]. Similarly, treatment with ovarian and breast cancer cell-derived exosomes induces, in adipose tissue derived stem cells, the typical characteristics of tumor-associated myofibroblasts [68,69]. Additionally, the Extracellular Matrix Metalloproteinase Inducer (EMMPRIN) [65] contained in exosomes and released by lung carcinoma cells is able to enhance the expressionof Matrix Metalloproteases (MMPs) in fibroblasts, with dramatic repercussions on tumor progression and metastasis.

Increasing attention has been placed to the role of cancer-derived ectosomes on the tumor microenvironment. Tumor ectosomes have been reported as carriers of cathepsins [70], MMPs, uPA and have been studied as promoters of the proteolytic cascade required by cancer cells to degrade the extracellular matrix and invade the surrounding environment [71]. Antonyak and colleagues demonstrated that ectosome-like MV, derived from different human cancer cells (breast carcinoma and glioma cells), can transform normal fibroblasts and enhance their survival abilities by transferring tissue transglutaminase (tTG), an enzyme that can cross-link Fibronectin (FN) on the ectosomes, enhancing the role of FN in potentiating activation of integrins and their downstream effectors, focal adhesion kinase (FAK) and ERK [72]. Additionally, LO can functionally influence the stroma, inducing

Akt1 signaling pathway activation, expression of genes implicated in prostate cancer metastasis and functional changes in cancer-associated fibroblasts [38,73].

Evidence that exosomes derived from fibroblasts exert a conditioning activity on cancer cells is still very limited. One of the very first studies on the topic, showing that CAF-derived exosomes stimulate breast cancer cell motility, protrusive activity and metastasis, was published in 2012 [66]. The salient discovery of this seminal study is that CAF-derived exosomes can be taken up by breast cancer cells and then loaded with Wnt11 produced by the recipient cells. This results in CAF-derived exosomes, in which CD81 and Wnt11 colocalize in trans, which can activate planar cell polarity (PCP) signaling in an autocrine manner in cancer cells, thus promoting migration. A more recent report demonstrates that exosomes produced by dermal fibroblasts, in which the tissue inhibitor of MMPs (TIMP) gene family has been knocked down with consequent acquisition of a CAF phenotype, are enriched in Disintegrinand metalloproteinase domain-containing protein 10 (ADAM10), and can enhance breast cancer cell motility by activating RhoA and Notch signaling [67]. Notably, mass spectrometry analysis of fibroblast-derived exosomes indicates that these EVs stimulate migration and invasion of target cells and can also play a role in metabolic reprogramming and extracellular acidification [66,67]. All together, these findings indicate that EVs can be exchanged reciprocally between cancer cells and CAFs, and that most of the biological changes that occur in either compartment as a result of cancer progression, including stemness, invasion, extracellular acidification, and metabolism reprogramming are mediated by specialized EVs. However, comparative functional analysis of the functional influence exerted by different populations of EVs on the stroma are still almost completely missing.

3.2. Immune System Regulation by Cancer Extracellular Vesicles

The uptake of tumor derived EVs by immune cells seems to have functional consequences on the immune microenvironment, which can result in either escaping the immune response or in activating immune suppression. Whether different populations of EVs elicit distinct types of immune responses, and the molecular mechanisms underlying the transferring to and the modulation of the immune microenvironment by receptors, proteins, RNA, and DNA carried in EVs, are all still largely unknown. Nonetheless, studying how immune cells are educated by tumor-derived EVs, thus facilitating tumor cell escape strategies, is crucial in order to develop cancer vaccines and new cancer treatments.

One way tumor EVs educate the immune microenvironment is by transfer of information to monocytes. Baj-Krzywirzeka and colleagues [74] characterized a number of cell surface markers and mRNA transcripts in EVs from pancreatic adenocarcinoma (HPC-4), colorectal carcinoma (DeTa), and lung carcinoma (A549) cells and they found that IL8, VEGF, HGF, and CD44 mRNA were expressed at high levels in EVs, suggesting a function for these messengers in monocyte re-education. Moreover, the interaction of EV cell surface proteins with monocytes alters CCR6 and CD44v7/8 expression and activates Akt, resulting in increased chemo-taxis and cell survival. All these events may result in the recruitment of monocytes into the tumor tissue, where they can differentiate into tumor-associated macrophages and support tumor initiation, local progression, and distant metastasis [75].

Frequent targets of tumor-derived exosomes are CD8+ T lymphocytes. Wieckowski and colleagues [76] demonstrated that MV from head and neck squamous cell carcinoma (PCI-13) carry the cancer testis antigen MAGE 3/6, and FasL that, once transferred to CD8+ T cells, induce their cell death. Another study demonstrated that EVs can be collected from the sera of patients with acute myeloid leukemia (AML), which contains higher levels of membrane associated TGFβ-1 and FasL than control sera [77] and that the treatment of Natural Killer cells with AML patients'exosomes results in TGFβ-1-mediated cytotoxicity of the target cells. On the other hand, tumor exosomes have also the ability to induce immune suppression by activating CD4+/CD25+Foxp3+ regulatory T cells (*Treg*) via TGFβ-1.

The induction of an efficient adaptive immune response against the tumor requires dendritic cell cross-processing and presentation of tumor antigens to T cells. Rughetti and colleagues characterized a population of EVs containing the tumor associated MUC1, a glycoprotein that can bind the MHC

groove and induce activation of CD8+ T cells, which can influence its processing, in dendritic cells. Importantly, dendritic cells can also internalize MUC1-positive EVs obtained from ascites of patients with stage III or IV ovarian cancer [78]. It is evident that, by eliminating the lymphocytes that have the ability to recognize and kill tumor cells, or by activating the regulatory suppressive branch of the adaptive response, cancer can escape immune attack and enhance its own survival [79].

3.3. Cancer Extracellular Vesicles and the Endothelium

The genesis of new blood vessels, known as angiogenesis, is an important step in cancer progression. Establishing the tumor vascular network is essential for cancer cell proliferation because tumor cells depend on blood for the supply of oxygen and nutrients and for the removal of waste products. The vascular supply becomes even more crucial to the cells during metastatic invasion, and facilitates the entrance of tumor cells in the bloodstream to colonize distant organs in the body [80,81].

Importantly, tumor exosomes contain key pro-angiogenic factors directly linked to endothelial cell migration and the induction of new blood vessel formation, such as Vascular Endothelial Growth Factor (VEGF), overexpressed in the majority of tumors [82,83], Epidermal Growth Factor like domains (EDIL-3/Del1) in bladder cancer cell-derived exosomes [84] and Annexin A2 (ANXA2), one of the most abundant proteins of glioblastoma cell-derived exosomes [85]. Kucharzewska and colleagues showed that exosomes derived from glioblastoma cells in hypoxic conditions are potent inducers of angiogenesis through phenotypic modulation of endothelial cells [86]. Furthermore, it has been shown that exosomes derived from renal cancer cells induce up-regulation of VEGF mRNA and protein levels in human umbilical vein endothelial cells (HUVECs), thus promoting angiogenesis [87].

Recent studies have demonstrated that tumor exosomes contribute to angiogenesis by transferring miRNAs [88]. Taverna and colleagues reported that exosomes derived from chronic myeloid leukemia are enriched with miR-126, which can be delivered to endothelial cells and down-regulate its molecular targets, CXCL12 and VCAM1. This results in enhanced migration of the cancer cells toward the endothelial cells in a co-culture model [89]. The release of exosomes enriched with miR-92a from leukemic cells induces down regulation of integrin α5 in endothelial cells and increases angiogenesis [90]. Additionally, exosomes derived from lung adenocarcinoma, enriched with miR-210, promote tube formation in HUVECs by down-regulating its target Ephrin A3, a known inhibitor of angiogenesis [91].

Recently, a functional role for large oncosomes (LO) in endothelial cell signaling and activities has been described: LO have been observed to induce migration of mouse dermal endothelial (MDEC) and tumor endothelial cells (TEC), suggesting that these EVs might disrupt the integrity of endothelial cell junctions and thereby increase blood vessel permeability *in vivo* [38]. However, additional studies to test whether the results on endothelial cell migration can be reproduced by using canonical angiogenesis assays *in vitro* are needed to fully understand the biological consequences of the cross-talk between LO and the endothelium. Further experiments are also necessary to determine if these atypically large EVs can be internalized into endothelial cells. Finally, although it has been demonstrated that LO extracted from the plasma of mice with prostate cancer can stimulate migration of endothelial cells, the capability of these EVs to cause endothelial leakage in animal models has yet to be tested. Additionally, the molecular mechanisms underscoring this and other biological functions of LO are still largely unknown [38].

While different EV populations have been studied and demonstrated to be involved in angiogenesis, whether they cooperate or not, and to what extent each population intervenes in specific phases of angiogenesis and metastasis is still a topic of investigation.

3.4. Extracellular Vesicles and the Transfer of Biological Information between Cancer Cells

EV-mediated intercellular communication is not limited to the interactions between tumor cells and the microenvironment described above, but rather occurs within the composite puzzle of heterogeneous cells that populate the tumor. Among the different roles EVs can play in extracellular

communication in cancer, one fascinating hypothesis is that EVs might function by horizontal transfer of genes with pre-existent mutations. While the intercellular transfer of oncogenic DNA has often been attributed to the uptake of apoptotic bodies (ABs) [44], reports indicate that EV populations corresponding to exosome and MV subtypes can mediate single- and double-stranded DNA transfer respectively [92,93]. In particular, H-ras-transformed rat epithelial cells can shed EVs containing chromatin-associated double-stranded DNA fragments covering the entire host genome, which can transfer full-length H-ras to recipient cells, stimulating their proliferation and inducing phenotype changes [92]. Another emerging important function seems to be related to the transfer and propagation of drug resistance. Almost unavoidably, chemotherapy results in changes in the biology of cancer cells, which consequently leads to chemoresistance. The traditional view believes that cells with endogenously acquired chemoresistance will survive and propagate upon treatment. In addition, a new hypothesis suggests that chemoresistance can also be transmitted horizontally from one cell to another through the exchange of EVs. Indeed, Zhang and colleagues recently described EV-mediated transfer of resistance to Paclitaxel in ovarian cancer [94]. P-glycoprotein (P-gP), encoded by the multidrug resistance gene-1 (MDR-1), which is associated with resistance to a variety of anticancer agents, is delivered through EVs from resistant to sensitive cells that then acquire the resistant phenotype. Using a different mechanism, exosomes can indirectly modulate P-gP by transferring to recipient cells TrpC5, a Ca^{2+} permeable channel [95]. This leads to increased concentrations of intracellular Ca^{2+} and consequent increase of P-gP levels, and intercellular transfer of drug resistance. This seems to occur between different cell types, including cancer and endothelial cells [96]. Intriguingly, an additional novel molecular mechanism by which sensitive cells become chemoresistant via exosome-mediated horizontal communication is mediated by miRNA and other non-coding RNAs [97]. For example, miR-222, which is cargo of breast cancer exosomes can target PTEN, thus activating the PI3K pathway, stimulating cell proliferation and promoting chemoresistance to Adryamycin and Docetaxel in cells sensitive to these drugs. However, the specific mechanism by which the sensitive cells became resistant is not known [98]. EVs can also play a protective role in chemoresistance. This is the case for a study demonstrating that EVs can be directly involved in the sequestration, transport and expulsion of Cisplatin from cancer cells [99], suggesting that, by using a sophisticated disposal mechanism, cancer cells might escape drug treatments.

In the future, it would be useful to investigate the extent to which specific types of EVs are implicated in drug chemoresistance and if the transfer of entire genes can modify the genomic make up of the recipient cells thus modulating response to the drugs intrinsically, before initiating drug treatment [100]. Further information on various aspects of EVs is provided in the other reviews of this focus edition [56,101–104].

4. Extracellular Vesicle Associated Cargo with Particular Emphasis on MicroRNA

The molecular content of EVs seems to be highly dependent on the source and conditions of the system at the time of vesicle biogenesis. For example, the abundance of the RNA and protein content of endothelial cell-derived exosomes is altered after exposure of the endothelial cells to different types of stress, including hypoxia, treatment with TNFα, or exposure to high concentrations of glucose and mannose [105]. Moreover, the overexpression of the ErbB2/HER2 receptor tyrosine kinase can alter the proteome of two different populations of EVs derived from mammary luminal epithelial cell lines in comparison with parental cells, suggesting complementary roles for certain biological pathways, and possibly a different response to HER2 upregulation in different types of EVs [106]. A plethora of studies arose on proteomic analyses of EVs from different organ systems [107,108], as it has been discussed by recent reviews [109].

Particular attention has recently been paid to the study of microRNAs (miRNAs) as key regulatory molecules in several diseases, including cancer. In bodily fluids, miRNAs have been identified either in complex with the argonaute RISC catalytic factor AGO2 [110,111] or within EVs [39,112]. Kosaka and colleagues demonstrated that incorporation of miRNA into intraluminal vesicles of MVBs is

controlled by neutral sphingomyelinase 2 (nSMase2), a regulator of ceramide biosynthesis [113]. Exosome shedding is potentiated by nSMase2, and its inhibition reduces the release of exosomes containing miRNA. This result has been confirmed in another study, demonstrating that RAB27A and RAB27B, two small GTPases that regulate secretory pathways, increase miRNA export from bladder carcinoma cells [114]. Vallarroya-Beltri and colleagues demonstrated that the miRNA sequence motif is important for miRNA loading into exosomes. This conclusion derives from mutagenesis experiments demonstrating that the heterogeneous nuclear ribonucleoprotein A2B1 (hnRNPA2B1) binds miRNAs directly through the recognition of their mature sequence, and controls their sorting in EVs. In exosomes, hnRNPA2B1 is sumoylated, and this post-translational modification facilitates its binding to miRNAs [115]. The EV-loading efficiency seems to depend not only on the RNA sequence but also on the cell type and physiological state. As a consequence, some small RNAs appear to be preferentially exported into EVs, while others are retained within the cell [116]. Whether these crucial mechanistic insights are applicable to cancer EVs remains to be proven.

Numerous studies have reported enrichment of miRNAs in EVs released by different types of cancer cells and present in biological fluids from cancer patients, resulting in the identification of promising markers of disease prognosis [117]. These EV miRNAs also play a functional role that is becoming increasingly recognized. A recent study suggests that decreased export of tumor suppressor miRNAs might be a mechanism of pro-metastatic function exerted by EVs *in vivo* [114]. One example is represented by miR-200, highly expressed in EVs from metastatic breast cancer cell lines, and responsible for enhanced metastatic abilities of less aggressive cells upon intercellular transfer [118].

Remarkably, Melo and colleagues have recently demonstrated the presence, in cancer but not in normal cell-derived exosomes, of AGO2 that, together with the RISC-Loading Complex (RLC), display cell-independent capacity to process pre-miRNAs in mature transcripts [119]. This study provides evidence that cancer exosomes, including those derived from breast cancer patient sera, can confer tumorigenic behavior to epithelial cells in a Dicer-dependent manner, and strongly reinforces the rationale for the development of exosome based therapies.

Surprisingly, the first quantitative and stoichiometric evaluation of exosome-derived miRNA demonstrates the presence of less than one miRNA copy per exosomes [120]. The authors propose two alternative models, a low-occupancy/low-miRNA concentration model, where a small number of exosomes carries a low concentration of miRNA, and a low-occupancy/high-miRNA concentration model, where rare exosomes carry many copies of a given miRNA. This study highlights the necessity to expand our current methodologies and approaches to more deeply investigate the functional role of EV miRNA cargo along with its potential use as a biomarker. It also corroborates the hypothesis that large EVs might contain higher amounts of miRNA [73]. Quantification of miRNA in EVs is an exciting topic in cancer research also because the amount of extracellular miRNA seems to be upregulated in the plasma of patients bearing tumors [121,122].

5. Conclusions

EVs are involved in several, if not all aspects, of tumor development and progression due to their apparently fundamental role in packaging and delivering molecular messages intercellularly. The potential implications, both diagnostic and therapeutic, of a deeper EV characterization, are widespread. Despite the current limitations, our abilities to specifically characterize EV populations are constantly improving. Furthermore, different EVs might all coexist at the same time within the tumor microenvironment and possibly cooperate or antagonize each other in the intercellular exchange of messages. In line with this concept, it might be helpful to functionally study different EV populations in a comparative manner or in combination. Finally, additional studies are necessary to clarify whether EV release is primarily a mechanism for spreading cancer-associated activities within the tumor microenvironment and in the circulation, if it is a mechanism of defense adopted by cancer cells to survive during disease progression, or both.

Acknowledgments: The authors apologize for not having cited many original research articles on this topic. Dolores Di Vizio is supported by the National Institutes of Health NCI NIH R00 CA131472; NIH UCLA SPORE in Prostate Cancer award P50 CA092131; the Avon Foundation Fund 02-2013-043; the Martz Translational Breast Cancer Research Fund, and by the Steven Spielberg Discovery Fund in Prostate Cancer Research.

Author Contributions: The manuscript was written through contributions of all authors. All authors approved the final version of the manuscript.

Conflicts of Interest: Dolores Di Vizio: Inventor of patents on EVs as circulating biomarkers of cancer.

References

1. Turturici, G.; Tinnirello, R.; Sconzo, G.; Geraci, F. Extracellular membrane vesicles as a mechanism of cell-to-cell communication: Advantages and disadvantages. *Am. J. Physiol. Cell Physiol.* **2014**, *306*, C621–C633. [CrossRef] [PubMed]
2. Kanada, M.; Bachmann, M.H.; Hardy, J.W.; Frimannson, D.O.; Bronsart, L.; Wang, A.; Sylvester, M.D.; Schmidt, T.L.; Kaspar, R.L.; Butte, M.J.; *et al*. Differential fates of biomolecules delivered to target cells via extracellular vesicles. *Proc. Natl. Acad. Sci. USA* **2015**, *112*, E1433–E1442. [CrossRef] [PubMed]
3. Cossetti, C.; Iraci, N.; Mercer, T.R.; Leonardi, T.; Alpi, E.; Drago, D.; Alfaro-Cervello, C.; Saini, H.K.; Davis, M.P.; Schaeffer, J.; *et al*. Extracellular vesicles from neural stem cells transfer IFN-γ via IFNGR1 to activate STAT1 signaling in target cells. *Mol. Cell* **2014**, *56*, 193–204. [CrossRef] [PubMed]
4. Hazan-Halevy, I.; Rosenblum, D.; Weinstein, S.; Bairey, O.; Raanani, P.; Peer, D. Cell-specific uptake of mantle cell lymphoma-derived exosomes by malignant and non-malignant B-lymphocytes. *Cancer Lett.* **2015**, *364*, 59–69. [CrossRef] [PubMed]
5. Zomer, A.; Maynard, C.; Verweij, F.J.; Kamermans, A.; Schafer, R.; Beerling, E.; Schiffelers, R.M.; de Wit, E.; Berenguer, J.; Ellenbroek, S.I.; *et al*. *In vivo* imaging reveals extracellular vesicle-mediated phenocopying of metastatic behavior. *Cell* **2015**, *161*, 1046–1057. [CrossRef] [PubMed]
6. Friend, C.; Marovitz, W.; Henie, G.; Henie, W.; Tsuei, D.; Hirschhorn, K.; Holland, J.G.; Cuttner, J. Observations on cell lines derived from a patient with hodgkin's disease. *Cancer Res.* **1978**, *38*, 2581–2591. [PubMed]
7. Van Blitterswijk, W.J.; Emmelot, P.; Hilkmann, H.A.; Hilgers, J.; Feltkamp, C.A. Rigid plasma-membrane-derived vesicles, enriched in tumour-associated surface antigens (MLR), occurring in the ascites fluid of a murine leukaemia (GRSL). *Int. J. Cancer* **1979**, *23*, 62–70. [CrossRef] [PubMed]
8. Dvorak, H.F.; Quay, S.C.; Orenstein, N.S.; Dvorak, A.M.; Hahn, P.; Bitzer, A.M.; Carvalho, A.C. Tumor shedding and coagulation. *Science* **1981**, *212*, 923–924. [CrossRef] [PubMed]
9. Kim, C.W.; Lee, H.M.; Lee, T.H.; Kang, C.; Kleinman, H.K.; Gho, Y.S. Extracellular membrane vesicles from tumor cells promote angiogenesis via sphingomyelin. *Cancer Res.* **2002**, *62*, 6312–6317. [PubMed]
10. Cocucci, E.; Racchetti, G.; Meldolesi, J. Shedding microvesicles: Artefacts no more. *Trends Cell Biol.* **2009**, *19*, 43–51. [CrossRef] [PubMed]
11. Kahlert, C.; Melo, S.A.; Protopopov, A.; Tang, J.; Seth, S.; Koch, M.; Zhang, J.; Weitz, J.; Chin, L.; Futreal, A.; *et al*. Identification of double-stranded genomic DNA spanning all chromosomes with mutated KRAS and p53 DNA in the serum exosomes of patients with pancreatic cancer. *J. Biol. Chem.* **2014**, *289*, 3869–3875. [CrossRef] [PubMed]
12. Thakur, B.K.; Zhang, H.; Becker, A.; Matei, I.; Huang, Y.; Costa-Silva, B.; Zheng, Y.; Hoshino, A.; Brazier, H.; Xiang, J.; *et al*. Double-stranded DNA in exosomes: A novel biomarker in cancer detection. *Cell Res.* **2014**, *24*, 766–769. [CrossRef] [PubMed]
13. Montermini, L.; Meehan, B.; Garnier, D.; Lee, W.J.; Lee, T.H.; Guha, A.; Al-Nedawi, K.; Rak, J. Inhibition of oncogenic epidermal growth factor receptor kinase triggers release of exosome-like extracellular vesicles and impacts their phosphoprotein and DNA content. *J. Biol. Chem.* **2015**. [CrossRef] [PubMed]
14. Peinado, H.; Aleckovic, M.; Lavotshkin, S.; Matei, I.; Costa-Silva, B.; Moreno-Bueno, G.; Hergueta-Redondo, M.; Williams, C.; Garcia-Santos, G.; Ghajar, C.; *et al*. Melanoma exosomes educate bone marrow progenitor cells toward a pro-metastatic phenotype through met. *Nat. Med.* **2012**, *18*, 883–891. [CrossRef] [PubMed]

15. Lazaro-Ibanez, E.; Sanz-Garcia, A.; Visakorpi, T.; Escobedo-Lucea, C.; Siljander, P.; Ayuso-Sacido, A.; Yliperttula, M. Different GDNA content in the subpopulations of prostate cancer extracellular vesicles: Apoptotic bodies, microvesicles, and exosomes. *Prostate* **2014**, *74*, 1379–1390. [CrossRef] [PubMed]
16. Lunavat, T.R.; Cheng, L.; Kim, D.K.; Bhadury, J.; Jang, S.C.; Lasser, C.; Sharples, R.A.; Lopez, M.D.; Nilsson, J.; Gho, Y.S.; *et al*. Small RNA deep sequencing discriminates subsets of extracellular vesicles released by melanoma cells—Evidence of unique microrna cargos. *RNA Biol.* **2015**, *12*, 810–823. [CrossRef] [PubMed]
17. Tosar, J.P.; Gambaro, F.; Sanguinetti, J.; Bonilla, B.; Witwer, K.W.; Cayota, A. Assessment of small RNA sorting into different extracellular fractions revealed by high-throughput sequencing of breast cell lines. *Nucleic Acids Res.* **2015**, *43*, 5601–5616. [CrossRef] [PubMed]
18. Xu, R.; Greening, D.W.; Rai, A.; Ji, H.; Simpson, R.J. Highly-purified exosomes and shed microvesicles isolated from the human colon cancer cell line lim1863 by sequential centrifugal ultrafiltration are biochemically and functionally distinct. *Methods* **2015**. [CrossRef] [PubMed]
19. Nakano, I.; Garnier, D.; Minata, M.; Rak, J. Extracellular vesicles in the biology of brain tumour stem cells—Implications for inter-cellular communication, therapy and biomarker development. *Semin. Cell Dev. Biol.* **2015**, *40*, 17–26. [CrossRef] [PubMed]
20. Pan, B.T.; Teng, K.; Wu, C.; Adam, M.; Johnstone, R.M. Electron microscopic evidence for externalization of the transferrin receptor in vesicular form in sheep reticulocytes. *J. Cell Biol.* **1985**, *101*, 942–948. [CrossRef] [PubMed]
21. Kalra, H.; Simpson, R.J.; Ji, H.; Aikawa, E.; Altevogt, P.; Askenase, P.; Bond, V.C.; Borras, F.E.; Breakefield, X.; Budnik, V.; *et al*. Vesiclepedia: A compendium for extracellular vesicles with continuous community annotation. *PLoS Biol.* **2012**, *10*, e1001450. [CrossRef] [PubMed]
22. Kim, D.K.; Kang, B.; Kim, O.Y.; Choi, D.S.; Lee, J.; Kim, S.R.; Go, G.; Yoon, Y.J.; Kim, J.H.; Jang, S.C.; *et al*. EVpedia: An integrated database of high-throughput data for systemic analyses of extracellular vesicles. *J. Extracell. Vesicles* **2013**, *2*. [CrossRef] [PubMed]
23. Kim, D.K.; Lee, J.; Kim, S.R.; Choi, D.S.; Yoon, Y.J.; Kim, J.H.; Go, G.; Nhung, D.; Hong, K.; Jang, S.C.; *et al*. EVpedia: A community web portal for extracellular vesicles research. *Bioinformatics* **2014**, *31*, 933–939. [CrossRef] [PubMed]
24. Andreu, Z.; Yanez-Mo, M. Tetraspanins in extracellular vesicle formation and function. *Front. Immunol.* **2014**, *5*, 442. [CrossRef] [PubMed]
25. Simpson, R.J.; Kalra, H.; Mathivanan, S. ExoCarta as a resource for exosomal research. *J. Extracell. Vesicles* **2012**, *1*. [CrossRef] [PubMed]
26. Welton, J.L.; Khanna, S.; Giles, P.J.; Brennan, P.; Brewis, I.A.; Staffurth, J.; Mason, M.D.; Clayton, A. Proteomics analysis of bladder cancer exosomes. *Mol. Cell. Proteom.* **2010**, *9*, 1324–1338. [CrossRef] [PubMed]
27. Colombo, M.; Moita, C.; van Niel, G.; Kowal, J.; Vigneron, J.; Benaroch, P.; Manel, N.; Moita, L.F.; Thery, C.; Raposo, G. Analysis of ESCRT functions in exosome biogenesis, composition and secretion highlights the heterogeneity of extracellular vesicles. *J. Cell Sci.* **2013**, *126*, 5553–5565. [CrossRef] [PubMed]
28. Young, T.W.; Rosen, D.G.; Mei, F.C.; Li, N.; Liu, J.; Wang, X.F.; Cheng, X. Up-regulation of tumor susceptibility gene 101 conveys poor prognosis through suppression of p21 expression in ovarian cancer. *Clin. Cancer Res.* **2007**, *13*, 3848–3854. [CrossRef] [PubMed]
29. Strappazzon, F.; Torch, S.; Chatellard-Causse, C.; Petiot, A.; Thibert, C.; Blot, B.; Verna, J.M.; Sadoul, R. ALIX is involved in caspase 9 activation during calcium-induced apoptosis. *Biochem. Biophys. Res. Commun.* **2010**, *397*, 64–69. [CrossRef] [PubMed]
30. Stein, J.M.; Luzio, J.P. Ectocytosis caused by sublytic autologous complement attack on human neutrophils. The sorting of endogenous plasma-membrane proteins and lipids into shed vesicles. *Biochem. J.* **1991**, *274 Pt 2*, 381–386. [CrossRef] [PubMed]
31. Di Vizio, D.; Kim, J.; Hager, M.H.; Morello, M.; Yang, W.; Lafargue, C.J.; True, L.D.; Rubin, M.A.; Adam, R.M.; Beroukhim, R.; *et al*. Oncosome formation in prostate cancer: Association with a region of frequent chromosomal deletion in metastatic disease. *Cancer Res.* **2009**, *69*, 5601–5609. [CrossRef] [PubMed]
32. Fackler, O.T.; Grosse, R. Cell motility through plasma membrane blebbing. *J. Cell Biol.* **2008**, *181*, 879–884. [CrossRef] [PubMed]
33. Zernecke, A.; Bidzhekov, K.; Noels, H.; Shagdarsuren, E.; Gan, L.; Denecke, B.; Hristov, M.; Koppel, T.; Jahantigh, M.N.; Lutgens, E.; *et al*. Delivery of microRNA-126 by apoptotic bodies induces CXCL12-dependent vascular protection. *Sci. Signal.* **2009**, *2*. [CrossRef] [PubMed]

34. Larson, M.C.; Woodliff, J.E.; Hillery, C.A.; Kearl, T.J.; Zhao, M. Phosphatidylethanolamine is externalized at the surface of microparticles. *Biochim. Biophys. Acta* **2012**, *1821*, 1501–1507. [CrossRef] [PubMed]
35. Lima, L.G.; Chammas, R.; Monteiro, R.Q.; Moreira, M.E.; Barcinski, M.A. Tumor-derived microvesicles modulate the establishment of metastatic melanoma in a phosphatidylserine-dependent manner. *Cancer Lett.* **2009**, *283*, 168–175. [CrossRef] [PubMed]
36. Pap, E.; Pallinger, E.; Pasztoi, M.; Falus, A. Highlights of a new type of intercellular communication: Microvesicle-based information transfer. *Inflamm. Res.* **2009**, *58*, 1–8. [CrossRef] [PubMed]
37. Muralidharan-Chari, V.; Clancy, J.; Plou, C.; Romao, M.; Chavrier, P.; Raposo, G.; D'Souza-Schorey, C. ARF6-regulated shedding of tumor cell-derived plasma membrane microvesicles. *Curr. Biol.* **2009**, *19*, 1875–1885. [CrossRef] [PubMed]
38. Di Vizio, D.; Morello, M.; Dudley, A.C.; Schow, P.W.; Adam, R.M.; Morley, S.; Mulholland, D.; Rotinen, M.; Hager, M.H.; Insabato, L.; *et al*. Large oncosomes in human prostate cancer tissues and in the circulation of mice with metastatic disease. *Am. J. Pathol.* **2012**, *181*, 1573–1584. [CrossRef] [PubMed]
39. Skog, J.; Wurdinger, T.; van Rijn, S.; Meijer, D.H.; Gainche, L.; Sena-Esteves, M.; Curry, W.T., Jr.; Carter, B.S.; Krichevsky, A.M.; Breakefield, X.O. Glioblastoma microvesicles transport RNA and proteins that promote tumour growth and provide diagnostic biomarkers. *Nat. Cell Biol.* **2008**, *10*, 1470–1476. [CrossRef] [PubMed]
40. Li, B.; Antonyak, M.A.; Zhang, J.; Cerione, R.A. RhoA triggers a specific signaling pathway that generates transforming microvesicles in cancer cells. *Oncogene* **2012**, *31*, 4740–4749. [CrossRef] [PubMed]
41. Elmore, S. Apoptosis: A review of programmed cell death. *Toxicol. Pathol.* **2007**, *35*, 495–516. [CrossRef] [PubMed]
42. Turiak, L.; Misjak, P.; Szabo, T.G.; Aradi, B.; Paloczi, K.; Ozohanics, O.; Drahos, L.; Kittel, A.; Falus, A.; Buzas, E.I.; *et al*. Proteomic characterization of thymocyte-derived microvesicles and apoptotic bodies in BALB/C mice. *J. Proteom.* **2011**, *74*, 2025–2033. [CrossRef] [PubMed]
43. Mills, J.C.; Stone, N.L.; Erhardt, J.; Pittman, R.N. Apoptotic membrane blebbing is regulated by myosin light chain phosphorylation. *J. Cell Biol.* **1998**, *140*, 627–636. [CrossRef] [PubMed]
44. Bergsmedh, A.; Szeles, A.; Henriksson, M.; Bratt, A.; Folkman, M.J.; Spetz, A.L.; Holmgren, L. Horizontal transfer of oncogenes by uptake of apoptotic bodies. *Proc. Natl. Acad. Sci. USA* **2001**, *98*, 6407–6411. [CrossRef] [PubMed]
45. Kerr, J.F.; Wyllie, A.H.; Currie, A.R. Apoptosis: A basic biological phenomenon with wide-ranging implications in tissue kinetics. *Br. J. Cancer* **1972**, *26*, 239–257. [CrossRef] [PubMed]
46. De la Taille, A.; Chen, M.W.; Burchardt, M.; Chopin, D.K.; Buttyan, R. Apoptotic conversion: Evidence for exchange of genetic information between prostate cancer cells mediated by apoptosis. *Cancer Res.* **1999**, *59*, 5461–5463. [PubMed]
47. Wickman, G.R.; Julian, L.; Mardilovich, K.; Schumacher, S.; Munro, J.; Rath, N.; Zander, S.A.; Mleczak, A.; Sumpton, D.; Morrice, N.; *et al*. Blebs produced by actin-myosin contraction during apoptosis release damage-associated molecular pattern proteins before secondary necrosis occurs. *Cell Death Differ.* **2013**, *20*, 1293–1305. [CrossRef] [PubMed]
48. Minciacchi, V.R.; You, S.; Spinelli, C.; Morley, S.; Zandian, M.; Aspuria, P.J.; Cavallini, L.; Ciardiello, C.; Reis Sobreiro, M.; Morello, M.; *et al*. Large oncosomes contain distinct protein cargo and represent a separate functional class of tumor-derived extracellular vesicles. *Oncotarget* **2015**, *6*, 11327–11341. [CrossRef] [PubMed]
49. Wright, P.K.; Jones, S.B.; Ardern, N.; Ward, R.; Clarke, R.B.; Sotgia, F.; Lisanti, M.P.; Landberg, G.; Lamb, R. 17β-estradiol regulates giant vesicle formation via estrogen receptor-α in human breast cancer cells. *Oncotarget* **2014**, *5*, 3055–3065. [CrossRef] [PubMed]
50. Ma, L.; Li, Y.; Peng, J.; Wu, D.; Zhao, X.; Cui, Y.; Chen, L.; Yan, X.; Du, Y.; Yu, L. Discovery of the migrasome, an organelle mediating release of cytoplasmic contents during cell migration. *Cell Res.* **2015**, *25*, 24–38. [CrossRef] [PubMed]
51. Clancy, J.W.; Sedgwick, A.; Rosse, C.; Muralidharan-Chari, V.; Raposo, G.; Method, M.; Chavrier, P.; D'Souza-Schorey, C. Regulated delivery of molecular cargo to invasive tumour-derived microvesicles. *Nat. Commun.* **2015**, *6*, 6919. [CrossRef] [PubMed]

52. Klein-Scory, S.; Tehrani, M.M.; Eilert-Micus, C.; Adamczyk, K.A.; Wojtalewicz, N.; Schnolzer, M.; Hahn, S.A.; Schmiegel, W.; Schwarte-Waldhoff, I. New insights in the composition of extracellular vesicles from pancreatic cancer cells: Implications for biomarkers and functions. *Proteome Sci.* **2014**, *12*. [CrossRef] [PubMed]
53. Choi, D.S.; Choi, D.Y.; Hong, B.S.; Jang, S.C.; Kim, D.K.; Lee, J.; Kim, Y.K.; Kim, K.P.; Gho, Y.S. Quantitative proteomics of extracellular vesicles derived from human primary and metastatic colorectal cancer cells. *J. Extracell. Vesicles* **2012**, *1*. [CrossRef] [PubMed]
54. Haqqani, A.S.; Delaney, C.E.; Tremblay, T.L.; Sodja, C.; Sandhu, J.K.; Stanimirovic, D.B. Method for isolation and molecular characterization of extracellular microvesicles released from brain endothelial cells. *Fluids Barriers CNS* **2013**, *10*. [CrossRef] [PubMed]
55. Crescitelli, R.; Lasser, C.; Szabo, T.G.; Kittel, A.; Eldh, M.; Dianzani, I.; Buzas, E.I.; Lotvall, J. Distinct RNA profiles in subpopulations of extracellular vesicles: Apoptotic bodies, microvesicles and exosomes. *J. Extracell. Vesicles* **2013**, *2*. [CrossRef] [PubMed]
56. Kalra, H.; Drummen, G.P.C.; Mathivanan, S. Focus on extracellular vesicles: Exosomes, the next small big thing. *Int. J. Mol. Sci.* **2016**, *17*. [CrossRef] [PubMed]
57. Baietti, M.F.; Zhang, Z.; Mortier, E.; Melchior, A.; Degeest, G.; Geeraerts, A.; Ivarsson, Y.; Depoortere, F.; Coomans, C.; Vermeiren, E.; *et al*. Syndecan-syntenin-ALIX regulates the biogenesis of exosomes. *Nat. Cell Biol.* **2012**, *14*, 677–685. [CrossRef] [PubMed]
58. Webber, J.P.; Spary, L.K.; Sanders, A.J.; Chowdhury, R.; Jiang, W.G.; Steadman, R.; Wymant, J.; Jones, A.T.; Kynaston, H.; Mason, M.D.; *et al*. Differentiation of tumour-promoting stromal myofibroblasts by cancer exosomes. *Oncogene* **2015**, *34*, 290–302. [CrossRef] [PubMed]
59. Otranto, M.; Sarrazy, V.; Bonte, F.; Hinz, B.; Gabbiani, G.; Desmouliere, A. The role of the myofibroblast in tumor stroma remodeling. *Cell Adhes. Migr* **2012**, *6*, 203–219. [CrossRef] [PubMed]
60. Shimoda, M.; Mellody, K.T.; Orimo, A. Carcinoma-associated fibroblasts are a rate-limiting determinant for tumour progression. *Semin. Cell Dev. Biol.* **2010**, *21*, 19–25. [CrossRef] [PubMed]
61. Giannoni, E.; Bianchini, F.; Masieri, L.; Serni, S.; Torre, E.; Calorini, L.; Chiarugi, P. Reciprocal activation of prostate cancer cells and cancer-associated fibroblasts stimulates epithelial-mesenchymal transition and cancer stemness. *Cancer Res.* **2010**, *70*, 6945–6956. [CrossRef] [PubMed]
62. Hanahan, D.; Weinberg, R.A. Hallmarks of cancer: The next generation. *Cell* **2011**, *144*, 646–674. [CrossRef] [PubMed]
63. Fiaschi, T.; Marini, A.; Giannoni, E.; Taddei, M.L.; Gandellini, P.; de Donatis, A.; Lanciotti, M.; Serni, S.; Cirri, P.; Chiarugi, P. Reciprocal metabolic reprogramming through lactate shuttle coordinately influences tumor-stroma interplay. *Cancer Res.* **2012**, *72*, 5130–5140. [CrossRef] [PubMed]
64. Webber, J.; Steadman, R.; Mason, M.D.; Tabi, Z.; Clayton, A. Cancer exosomes trigger fibroblast to myofibroblast differentiation. *Cancer Res.* **2010**, *70*, 9621–9630. [CrossRef] [PubMed]
65. Sidhu, S.S.; Mengistab, A.T.; Tauscher, A.N.; LaVail, J.; Basbaum, C. The microvesicle as a vehicle for EMMPRIN in tumor-stromal interactions. *Oncogene* **2004**, *23*, 956–963. [CrossRef] [PubMed]
66. Luga, V.; Zhang, L.; Viloria-Petit, A.M.; Ogunjimi, A.A.; Inanlou, M.R.; Chiu, E.; Buchanan, M.; Hosein, A.N.; Basik, M.; Wrana, J.L. Exosomes mediate stromal mobilization of autocrine WNT-PCP signaling in breast cancer cell migration. *Cell* **2012**, *151*, 1542–1556. [CrossRef] [PubMed]
67. Shimoda, M.; Principe, S.; Jackson, H.W.; Luga, V.; Fang, H.; Molyneux, S.D.; Shao, Y.W.; Aiken, A.; Waterhouse, P.D.; Karamboulas, C.; *et al*. Loss of the TIMP gene family is sufficient for the acquisition of the CAF-like cell state. *Nat. Cell Biol.* **2014**, *16*, 889–901. [CrossRef] [PubMed]
68. Cho, J.A.; Park, H.; Lim, E.H.; Kim, K.H.; Choi, J.S.; Lee, J.H.; Shin, J.W.; Lee, K.W. Exosomes from ovarian cancer cells induce adipose tissue-derived mesenchymal stem cells to acquire the physical and functional characteristics of tumor-supporting myofibroblasts. *Gynecol. Oncol.* **2011**, *123*, 379–386. [CrossRef] [PubMed]
69. Cho, J.A.; Park, H.; Lim, E.H.; Lee, K.W. Exosomes from breast cancer cells can convert adipose tissue-derived mesenchymal stem cells into myofibroblast-like cells. *Int. J. Oncol.* **2012**, *40*, 130–138. [PubMed]
70. Giusti, I.; D'Ascenzo, S.; Millimaggi, D.; Taraboletti, G.; Carta, G.; Franceschini, N.; Pavan, A.; Dolo, V. Cathepsin B mediates the pH-dependent proinvasive activity of tumor-shed microvesicles. *Neoplasia* **2008**, *10*, 481–488. [CrossRef] [PubMed]
71. Inal, J.M.; Ansa-Addo, E.A.; Stratton, D.; Kholia, S.; Antwi-Baffour, S.S.; Jorfi, S.; Lange, S. Microvesicles in health and disease. *Arch. Immunol. Ther. Exp.* **2012**, *60*, 107–121. [CrossRef] [PubMed]

72. Antonyak, M.A.; Li, B.; Boroughs, L.K.; Johnson, J.L.; Druso, J.E.; Bryant, K.L.; Holowka, D.A.; Cerione, R.A. Cancer cell-derived microvesicles induce transformation by transferring tissue transglutaminase and fibronectin to recipient cells. *Proc. Natl. Acad. Sci. USA* **2011**, *108*, 4852–4857. [CrossRef] [PubMed]
73. Morello, M.; Minciacchi, V.R.; de Candia, P.; Yang, J.; Posadas, E.; Kim, H.; Griffiths, D.; Bhowmick, N.; Chung, L.W.; Gandellini, P.; *et al*. Large oncosomes mediate intercellular transfer of functional microRNA. *Cell Cycle* **2013**, *12*, 3526–3536. [CrossRef] [PubMed]
74. Baj-Krzyworzeka, M.; Szatanek, R.; Weglarczyk, K.; Baran, J.; Urbanowicz, B.; Branski, P.; Ratajczak, M.Z.; Zembala, M. Tumour-derived microvesicles carry several surface determinants and mRNA of tumour cells and transfer some of these determinants to monocytes. *Cancer Immunol. Immunother. CII* **2006**, *55*, 808–818. [CrossRef] [PubMed]
75. Richards, D.M.; Hettinger, J.; Feuerer, M. Monocytes and macrophages in cancer: Development and functions. *Cancer Microenviron.* **2013**, *6*, 179–191. [CrossRef] [PubMed]
76. Wieckowski, E.U.; Visus, C.; Szajnik, M.; Szczepanski, M.J.; Storkus, W.J.; Whiteside, T.L. Tumor-derived microvesicles promote regulatory T cell expansion and induce apoptosis in tumor-reactive activated CD8+ T lymphocytes. *J. Immunol.* **2009**, *183*, 3720–3730. [CrossRef] [PubMed]
77. Szczepanski, M.J.; Szajnik, M.; Welsh, A.; Whiteside, T.L.; Boyiadzis, M. Blast-derived microvesicles in sera from patients with acute myeloid leukemia suppress natural killer cell function via membrane-associated transforming growth factor-β1. *Haematologica* **2011**, *96*, 1302–1309. [CrossRef] [PubMed]
78. Rughetti, A.; Rahimi, H.; Belleudi, F.; Napoletano, C.; Battisti, F.; Zizzari, I.G.; Antonilli, M.; Bellati, F.; Wandall, H.H.; Benedetti Panici, P.; *et al*. Microvesicle cargo of tumor-associated MUC1 to dendritic cells allows cross-presentation and specific carbohydrate processing. *Cancer Immunol. Res.* **2014**, *2*, 177–186. [CrossRef] [PubMed]
79. Croci, D.O.; Zacarias Fluck, M.F.; Rico, M.J.; Matar, P.; Rabinovich, G.A.; Scharovsky, O.G. Dynamic cross-talk between tumor and immune cells in orchestrating the immunosuppressive network at the tumor microenvironment. *Cancer Immunol. Immunother.* **2007**, *56*, 1687–1700. [CrossRef] [PubMed]
80. Gombos, F.; Serpico, R.; Gaeta, G.M.; Budetta, F.; de Luca, P. The importance of direct immunofluorescence in the diagnosis of oral lichen planus. A clinical study and proposal of new diagnostic criteria. *Miner. Stomatol.* **1992**, *41*, 23–32.
81. Nishida, N.; Yano, H.; Nishida, T.; Kamura, T.; Kojiro, M. Angiogenesis in cancer. *Vascul. Health Risk Manag.* **2006**, *2*, 213–219. [CrossRef]
82. Ekstrom, E.J.; Bergenfelz, C.; von Bulow, V.; Serifler, F.; Carlemalm, E.; Jonsson, G.; Andersson, T.; Leandersson, K. WNT5A induces release of exosomes containing pro-angiogenic and immunosuppressive factors from malignant melanoma cells. *Mol. Cancer* **2014**, *13*. [CrossRef] [PubMed]
83. Liu, Y.; Zhao, L.; Li, D.; Yin, Y.; Zhang, C.Y.; Li, J.; Zhang, Y. Microvesicle-delivery miR-150 promotes tumorigenesis by up-regulating VEGF, and the neutralization of miR-150 attenuate tumor development. *Protein Cell* **2013**, *4*, 932–941. [CrossRef] [PubMed]
84. Beckham, C.J.; Olsen, J.; Yin, P.N.; Wu, C.H.; Ting, H.J.; Hagen, F.K.; Scosyrev, E.; Messing, E.M.; Lee, Y.F. Bladder cancer exosomes contain EDIL-3/DEL1 and facilitate cancer progression. *J. Urol.* **2014**, *192*, 583–592. [CrossRef] [PubMed]
85. Bronisz, A.; Wang, Y.; Nowicki, M.O.; Peruzzi, P.; Ansari, K.I.; Ogawa, D.; Balaj, L.; de Rienzo, G.; Mineo, M.; Nakano, I.; *et al*. Extracellular vesicles modulate the glioblastoma microenvironment via a tumor suppression signaling network directed by miR-1. *Cancer Res.* **2014**, *74*, 738–750. [CrossRef] [PubMed]
86. Kucharzewska, P.; Christianson, H.C.; Belting, M. Global profiling of metabolic adaptation to hypoxic stress in human glioblastoma cells. *PLoS ONE* **2015**, *10*, e0116740. [CrossRef] [PubMed]
87. Zhang, L.; Wu, X.; Luo, C.; Chen, X.; Yang, L.; Tao, J.; Shi, J. The 786-0 renal cancer cell-derived exosomes promote angiogenesis by downregulating the expression of hepatocyte cell adhesion molecule. *Mol. Med. Rep.* **2013**, *8*, 272–276. [PubMed]
88. Figliolini, F.; Cantaluppi, V.; De Lena, M.; Beltramo, S.; Romagnoli, R.; Salizzoni, M.; Melzi, R.; Nano, R.; Piemonti, L.; Tetta, C.; *et al*. Isolation, characterization and potential role in β cell-endothelium cross-talk of extracellular vesicles released from human pancreatic islets. *PLoS ONE* **2014**, *9*, e102521. [CrossRef] [PubMed]

89. Taverna, S.; Amodeo, V.; Saieva, L.; Russo, A.; Giallombardo, M.; de Leo, G.; Alessandro, R. Exosomal shuttling of miR-126 in endothelial cells modulates adhesive and migratory abilities of chronic myelogenous leukemia cells. *Mol. Cancer* **2014**, *13*. [CrossRef] [PubMed]
90. Umezu, T.; Ohyashiki, K.; Kuroda, M.; Ohyashiki, J.H. Leukemia cell to endothelial cell communication via exosomal miRNAs. *Oncogene* **2013**, *32*, 2747–2755. [CrossRef] [PubMed]
91. Cui, H.; Seubert, B.; Stahl, E.; Dietz, H.; Reuning, U.; Moreno-Leon, L.; Ilie, M.; Hofman, P.; Nagase, H.; Mari, B.; *et al*. Tissue inhibitor of metalloproteinases-1 induces a pro-tumourigenic increase of miR-210 in lung adenocarcinoma cells and their exosomes. *Oncogene* **2014**, *34*, 3640–3650. [CrossRef] [PubMed]
92. Lee, T.H.; Chennakrishnaiah, S.; Audemard, E.; Montermini, L.; Meehan, B.; Rak, J. Oncogenic ras-driven cancer cell vesiculation leads to emission of double-stranded DNA capable of interacting with target cells. *Biochem. Biophys. Res. Commun.* **2014**, *451*, 295–301. [CrossRef] [PubMed]
93. Balaj, L.; Lessard, R.; Dai, L.; Cho, Y.J.; Pomeroy, S.L.; Breakefield, X.O.; Skog, J. Tumour microvesicles contain retrotransposon elements and amplified oncogene sequences. *Nat. Commun.* **2011**, *2*. [CrossRef] [PubMed]
94. Zhang, F.F.; Zhu, Y.F.; Zhao, Q.N.; Yang, D.T.; Dong, Y.P.; Jiang, L.; Xing, W.X.; Li, X.Y.; Xing, H.; Shi, M.; *et al*. Microvesicles mediate transfer of p-glycoprotein to paclitaxel-sensitive a2780 human ovarian cancer cells, conferring paclitaxel-resistance. *Eur. J. Pharmacol.* **2014**, *738*, 83–90. [CrossRef] [PubMed]
95. Ma, X.; Cai, Y.; He, D.; Zou, C.; Zhang, P.; Lo, C.Y.; Xu, Z.; Chan, F.L.; Yu, S.; Chen, Y.; *et al*. Transient receptor potential channel TrpC5 is essential for p-glycoprotein induction in drug-resistant cancer cells. *Proc. Natl. Acad. Sci. USA* **2012**, *109*, 16282–16287. [CrossRef] [PubMed]
96. Dong, Y.; Pan, Q.; Jiang, L.; Chen, Z.; Zhang, F.; Liu, Y.; Xing, H.; Shi, M.; Li, J.; Li, X.; *et al*. Tumor endothelial expression of p-glycoprotein upon microvesicular transfer of TrpC5 derived from adriamycin-resistant breast cancer cells. *Biochem. Biophys. Res. Commun.* **2014**, *446*, 85–90. [CrossRef] [PubMed]
97. Takahashi, K.; Yan, I.K.; Kogure, T.; Haga, H.; Patel, T. Extracellular vesicle-mediated transfer of long non-coding RNA ror modulates chemosensitivity in human hepatocellular cancer. *FEBS Open Biol.* **2014**, *4*, 458–467. [CrossRef] [PubMed]
98. Chen, W.X.; Liu, X.M.; Lv, M.M.; Chen, L.; Zhao, J.H.; Zhong, S.L.; Ji, M.H.; Hu, Q.; Luo, Z.; Wu, J.Z.; *et al*. Exosomes from drug-resistant breast cancer cells transmit chemoresistance by a horizontal transfer of microRNAs. *PLoS ONE* **2014**, *9*, e95240. [CrossRef] [PubMed]
99. Safaei, R.; Larson, B.J.; Cheng, T.C.; Gibson, M.A.; Otani, S.; Naerdemann, W.; Howell, S.B. Abnormal lysosomal trafficking and enhanced exosomal export of cisplatin in drug-resistant human ovarian carcinoma cells. *Mol. Cancer Ther.* **2005**, *4*, 1595–1604. [CrossRef] [PubMed]
100. Gottesman, M.M. Mechanisms of cancer drug resistance. *Annu. Rev. Med.* **2002**, *53*, 615–627. [CrossRef] [PubMed]
101. Iraci, N.; Leonardi, T.; Gessler, F.; Vega, B.; Pluchino, S. Focus on extracellular vesicles: Physiological role and signaling properties of extracellular membrane vesicles. *Int. J. Mol. Sci.* **2016**, *17*. [CrossRef] [PubMed]
102. Ohno, S.I.; Drummen, G.P.C.; Kuroda, M. Focus on extracellular vesicles: Development of exosome-based therapeutic systems. *Int. J. Mol. Sci.* **2016**, *17*. [CrossRef] [PubMed]
103. Vella, L.J.; Hill, A.F.; Cheng, L. Focus on extracellular vesicles: Exosomes and their role in protein trafficking in Alzheimer's and Parkinson's disease. *Int. J. Mol. Sci.* **2016**, *17*. [CrossRef] [PubMed]
104. Zhang, B.; Tan, K.H.; Lim, S.K. Focus on extracellular vesicles: Therapeutic efficacy of stem cell-derived extracellular vesicles. *Int. J. Mol. Sci.* **2016**, *17*. [CrossRef] [PubMed]
105. De Jong, O.G.; Verhaar, M.C.; Chen, Y.; Vader, P.; Gremmels, H.; Posthuma, G.; Schiffelers, R.M.; Gucek, M.; van Balkom, B.W. Cellular stress conditions are reflected in the protein and RNA content of endothelial cell-derived exosomes. *J. Extracell. Vesicles* **2012**, *1*. [CrossRef] [PubMed]
106. Amorim, M.; Fernandes, G.; Oliveira, P.; Martins-de-Souza, D.; Dias-Neto, E.; Nunes, D. The overexpression of a single oncogene (ErbB2/HER2) alters the proteomic landscape of extracellular vesicles. *Proteomics* **2014**, *14*, 1472–1479. [CrossRef] [PubMed]
107. Zhu, Y.; Chen, X.; Pan, Q.; Wang, Y.; Su, S.; Jiang, C.; Li, Y.; Xu, N.; Wu, L.; Lou, X.; *et al*. A comprehensive proteomics analysis reveals a secretory path- and status-dependent signature of exosomes released from tumor-associated macrophages. *J. Proteome Res.* **2015**, *14*, 4319–4331. [CrossRef] [PubMed]
108. Thery, C.; Boussac, M.; Veron, P.; Ricciardi-Castagnoli, P.; Raposo, G.; Garin, J.; Amigorena, S. Proteomic analysis of dendritic cell-derived exosomes: A secreted subcellular compartment distinct from apoptotic vesicles. *J. Immunol.* **2001**, *166*, 7309–7318. [CrossRef] [PubMed]

109. D'Souza-Schorey, C.; di Vizio, D. Biology and proteomics of extracellular vesicles: Harnessing their clinical potential. *Expert Rev. Proteom.* **2014**, *11*, 251–253. [CrossRef] [PubMed]
110. Turchinovich, A.; Weiz, L.; Langheinz, A.; Burwinkel, B. Characterization of extracellular circulating microRNA. *Nucleic Acids Res.* **2011**, *39*, 7223–7233. [CrossRef] [PubMed]
111. Arroyo, J.D.; Chevillet, J.R.; Kroh, E.M.; Ruf, I.K.; Pritchard, C.C.; Gibson, D.F.; Mitchell, P.S.; Bennett, C.F.; Pogosova-Agadjanyan, E.L.; Stirewalt, D.L.; *et al*. Argonaute2 complexes carry a population of circulating microRNAs independent of vesicles in human plasma. *Proc. Natl. Acad. Sci. USA* **2011**, *108*, 5003–5008. [CrossRef] [PubMed]
112. Valadi, H.; Ekstrom, K.; Bossios, A.; Sjostrand, M.; Lee, J.J.; Lotvall, J.O. Exosome-mediated transfer of mRNAs and microRNAs is a novel mechanism of genetic exchange between cells. *Nat. Cell Biol.* **2007**, *9*, 654–659. [CrossRef] [PubMed]
113. Kosaka, N.; Iguchi, H.; Yoshioka, Y.; Takeshita, F.; Matsuki, Y.; Ochiya, T. Secretory mechanisms and intercellular transfer of microRNAs in living cells. *J. Biol. Chem.* **2010**, *285*, 17442–17452. [CrossRef] [PubMed]
114. Ostenfeld, M.S.; Jeppesen, D.K.; Laurberg, J.R.; Boysen, A.T.; Bramsen, J.B.; Primdal-Bengtson, B.; Hendrix, A.; Lamy, P.; Dagnaes-Hansen, F.; Rasmussen, M.H.; *et al*. Cellular disposal of miR23b by RAB27-dependent exosome release is linked to acquisition of metastatic properties. *Cancer Res.* **2014**, *74*, 5758–5771. [CrossRef] [PubMed]
115. Villarroya-Beltri, C.; Gutierrez-Vazquez, C.; Sanchez-Cabo, F.; Perez-Hernandez, D.; Vazquez, J.; Martin-Cofreces, N.; Martinez-Herrera, D.J.; Pascual-Montano, A.; Mittelbrunn, M.; Sanchez-Madrid, F. Sumoylated hnRNPA2B1 controls the sorting of miRNAs into exosomes through binding to specific motifs. *Nat. Commun.* **2013**, *4*. [CrossRef] [PubMed]
116. Guduric-Fuchs, J.; O'Connor, A.; Camp, B.; O'Neill, C.L.; Medina, R.J.; Simpson, D.A. Selective extracellular vesicle-mediated export of an overlapping set of microRNAs from multiple cell types. *BMC Genom.* **2012**, *13*. [CrossRef] [PubMed]
117. Kosaka, N.; Yoshioka, Y.; Hagiwara, K.; Tominaga, N.; Katsuda, T.; Ochiya, T. Trash or treasure: Extracellular microRNAs and cell-to-cell communication. *Front. Genet.* **2013**, *4*. [CrossRef] [PubMed]
118. Le, M.T.; Hamar, P.; Guo, C.; Basar, E.; Perdigao-Henriques, R.; Balaj, L.; Lieberman, J. miR-200-containing extracellular vesicles promote breast cancer cell metastasis. *J. Clin. Investig.* **2014**, *124*, 5109–5128. [CrossRef] [PubMed]
119. Melo, S.A.; Sugimoto, H.; O'Connell, J.T.; Kato, N.; Villanueva, A.; Vidal, A.; Qiu, L.; Vitkin, E.; Perelman, L.T.; Melo, C.A.; *et al*. Cancer exosomes perform cell-independent microRNA biogenesis and promote tumorigenesis. *Cancer Cell* **2014**, *26*, 707–721. [CrossRef] [PubMed]
120. Chevillet, J.R.; Kang, Q.; Ruf, I.K.; Briggs, H.A.; Vojtech, L.N.; Hughes, S.M.; Cheng, H.H.; Arroyo, J.D.; Meredith, E.K.; Gallichotte, E.N.; *et al*. Quantitative and stoichiometric analysis of the microRNA content of exosomes. *Proc. Natl. Acad. Sci. USA* **2014**, *111*, 14888–14893. [CrossRef] [PubMed]
121. Geng, Q.; Fan, T.; Zhang, B.; Wang, W.; Xu, Y.; Hu, H. Five microRNAs in plasma as novel biomarkers for screening of early-stage non-small cell lung cancer. *Respir. Res.* **2014**, *15*. [CrossRef] [PubMed]
122. Shen, L.; Wan, Z.; Ma, Y.; Wu, L.; Liu, F.; Zang, H.; Xin, S. The clinical utility of microRNA-21 as novel biomarker for diagnosing human cancers. *Tumour Biol. J. Int. Soc. Oncodev. Biol. Med.* **2015**, *36*, 1993–2005. [CrossRef] [PubMed]

Published OnlineFirst February 15, 2017; DOI: 10.1158/0008-5472.CAN-16-2942

Microenvironment and Immunology

Cancer Research

MYC Mediates Large Oncosome-Induced Fibroblast Reprogramming in Prostate Cancer

Valentina R. Minciacchi[1], Cristiana Spinelli[1], Mariana Reis-Sobreiro[1], Lorenzo Cavallini[1,2], Sungyong You[1], Mandana Zandian[1], Xiaohong Li[3], Rajeev Mishra[6,9], Paola Chiarugi[2], Rosalyn M. Adam[4,5], Edwin M. Posadas[6], Giuseppe Viglietto[7], Michael R. Freeman[1,4,6], Emanuele Cocucci[8], Neil A. Bhowmick[9], and Dolores Di Vizio[1,4,5]

Abstract

Communication between cancer cells and the tumor microenvironment results in the modulation of complex signaling networks that facilitate tumor progression. Here, we describe a new mechanism of intercellular communication originating from large oncosomes (LO), which are cancer cell–derived, atypically large (1–10 μm) extracellular vesicles (EV). We demonstrate that, in the context of prostate cancer, LO harbor sustained AKT1 kinase activity, nominating them as active signaling platforms. Active AKT1 was detected in circulating EV from the plasma of metastatic prostate cancer patients and was LO specific. LO internalization induced reprogramming of human normal prostate fibroblasts as reflected by high levels of α-SMA, IL6, and MMP9. In turn, LO-reprogrammed normal prostate fibroblasts stimulated endothelial tube formation *in vitro* and promoted tumor growth in mice. Activation of stromal MYC was critical for this reprogramming and for the sustained cellular responses elicited by LO, both *in vitro* and *in vivo* in an AKT1-dependent manner. Inhibition of LO internalization prevented activation of MYC and impaired the tumor-supporting properties of fibroblasts. Overall, our data show that prostate cancer–derived LO powerfully promote establishment of a tumor-supportive environment by inducing a novel reprogramming of the stroma. This mechanism offers potential alternative options for patient treatment. *Cancer Res; 77(9); 2306–17.* ©*2017 AACR.*

Introduction

During the development of prostate cancer, the host microenvironment co-evolves with the tumor in establishing a positive feedback loop that plays a key role in disease onset and progression (1, 2). Extracellular vesicles (EV) are membrane-enclosed particles that contribute to tumor progression by establishing a tumor-supportive environment. Exosomes (Exo) are nano-sized EVs that have been implicated in angiogenesis, tolerogenic immune response, fibroblast activation, and preparation of the metastatic niche (3–6).

Highly migratory prostate cancer cells exhibit a pattern of motility characterized by dynamic formation of nonapoptotic membrane blebs. Pinching off of these blebs results in the release of abnormally large EVs (1–10 μm), which are referred to as "large oncosomes" (LO; refs. 7, 8). LO formation and release is enhanced by loss of the cytoskeletal regulator diaphanous related formin-3 (DIAPH3), which induces a transition from a mesenchymal to a more rapid, invasive, and metastatic "amoeboid" phenotype (9). Increased LO shedding is also observed in association with enforced expression of a membrane-bound myristoylated form of the serine-threonine protein kinase AKT1 (MyrAKT1), which is constitutively active, in LNCaP cells (7, 10).

LO released from amoeboid cancer cells are abundant in tumor tissues and plasma of patients and mice with metastatic prostate cancer, and are not detected in benign samples (10–12). LO are also bioactive, as demonstrated by their capacity to degrade extracellular matrices *in vitro* (10). However, whether these vesicles play specific functional roles in the tumor microenvironment is completely unknown. LO harbor distinct protein cargo in comparison with Exo, suggesting that LO might activate specific molecular pathways (11).

Here, we focused on defining whether and how LO facilitate the propagation of oncogenic signaling originating from the tumor cells and affecting the stroma. We demonstrate that LO are the EV population that harbors functionally active AKT1 and that these particles can be internalized by stromal cells, even given their large size in comparison with Exo. Internalization seems to occur via phagocytosis and is necessary for the consequent biological and

[1]Division of Cancer Biology and Therapeutics, Departments of Surgery, Biomedical Sciences and Pathology and Laboratory Medicine, Samuel Oschin Comprehensive Cancer Institute, Cedars-Sinai Medical Center, Los Angeles, California. [2]Department of Experimental and Clinical Biomedical Sciences, University of Florence, Florence, Italy. [3]Van Andel Institute, Grand Rapids, Michigan. [4]The Urological Diseases Research Center, Boston Children's Hospital, Boston, Massachusetts. [5]Department of Surgery, Harvard Medical School, Boston, Massachusetts. [6]Urologic Oncology Program and Uro-Oncology Research Laboratories, Samuel Oschin Comprehensive Cancer Institute, Cedars-Sinai Medical Center, Los Angeles, California. [7]Department of Experimental and Clinical Medicine, University Magna Graecia, Catanzaro, Italy. [8]Division of Hematology, Department of Internal Medicine, The Ohio State University, Columbus, Ohio. [9]Department of Medicine, Cedars-Sinai Medical Center, Los Angeles, California.

Note: Supplementary data for this article are available at Cancer Research Online (http://cancerres.aacrjournals.org/).

Corresponding Author: Dolores Di Vizio, Cedars-Sinai Medical Center/Boston Children's Hospital, 8700 Beverly Blvd, Los Angeles, CA 90048. Phone: 310-423-7709; Fax: 310-423-5454; E-mail: dolores.divizio@cshs.org

doi: 10.1158/0008-5472.CAN-16-2942

Published OnlineFirst February 15, 2017; DOI: 10.1158/0008-5472.CAN-16-2942

functional effects. LO uptake induces a specific "reprogramming" of the fibroblasts that results in their increased ability to stimulate tube formation in endothelial cells and to promote tumor growth *in vivo*. Activation of the transcription factor (TF) MYC in the fibroblasts is necessary to sustain the effects elicited by LO *in vitro* and *in vivo*. Our study shows for the first time that LO are capable of activating specific functional pathways in the microenvironment. Inhibiting these pathways prevents the horizontal propagation of oncogenic signals *in vitro* and *in vivo*.

Materials and Methods

Cell culture and reagents

LNCaP^{MyrAKT1} cells were obtained and cultured as previously described (13). WPMY-1, PC3, 22Rv1 cells, and human umbilical vein endothelial cells (HUVEC) were purchased from the ATCC and cultured as previously described (7, 10). The normal associated human prostatic fibroblasts (NAF) were generated from surgical explants of patients diagnosed with benign prostatic hyperplasia (14). All cell lines were authenticated by short tandem repeat profiling, *in vivo* growth, and histology, and they were negative mycoplasma upon periodical testing (Lonza). Primary wild-type mouse fibroblasts were expanded and transduced with a commercially available c-MYC lentiviral vector. A detailed description of the reagents can be found in the Supplementary Materials and Methods section.

Patient specimens

Human studies were approved by a Cedars-Sinai Medical Center Institutional Review Board protocol (n. 00030191), in compliance with the declaration of Helsinki. All subjects provided informed consent for blood donation to be used for research purposes. Patient samples were obtained from the Urologic Oncology Program and the Cedars-Sinai BioBank.

EV isolation

EVs were isolated from platelet-poor plasma specimens or cell culture supernatants (obtained after 24 hours in serum-free media) as previously described (11). For functional studies, the EVs were used at a working concentration of 20 μg/mL, unless otherwise specified. This dose corresponds to the use of LO from 30 donor prostate cancer cells to treat 1 recipient cell, a result that is indicative of high biological potency.

Immunoblot analysis

Samples were lysed with RIPA cell lysis buffer supplemented with Octyl β-D-glucopyranoside (OCG), protease, and phosphatase inhibitors. Note that 10 μg per lane were loaded, and samples were blotted for indicated antibodies.

Tunable resistive pulse sensing measurements

EV preparations were submitted to tunable resistive pulse sensing (TRPS) analysis using a qNano instrument (IZON Science) as described previously (15).

PKH26 staining

For LO uptake experiments, LO were fluorescently labeled using the lipophilic membrane dye PKH26. LO were incubated with the dye for 3 minutes at room temperature, and the reaction was blocked by BSA 1%. LO were then washed in 5 mL of PBS to remove any unbound dye, concentrated by filtration as previously described (12), and collected in PBS.

Flow cytometry

For LO uptake detection, target cells were incubated with PKH26-labeled LO (from $\sim 3.3 \times 10^6$ LNCaP^{MyrAKT1} cells) for 1 hour at 37°C or at 4°C. Cells were washed several times, trypsinized to remove surface-associated LO, and then analyzed using a Becton Dickinson LSR II, or analyzed and sorted using a Becton Dickinson FACSAria III. In experiments with pharmacologic inhibitors, the indicated compounds were added simultaneously with PKH26-labeled LO. Data analysis was performed using FlowJo software (Treestar). Relative fluorescent intensity (RFI) was calculated as the ratio between the mean fluorescence intensity of the treated cells and control cells. Experiments were performed in triplicate.

Confocal microscopy

WPMY-1 cells, after internalization of PKH26-labeled LO or treated with vehicle control, were sorted and plated on coverslip, fixed, and permeabilized in 4% paraformaldehyde and then imaged by confocal microscopy. In select experiments, cells were incubated with a FITC-conjugated HA antibody. Images were acquired on a Leica TCS SP spectral confocal microscope with white light laser (10).

RNA interference

Cells were transfected with specific siRNA oligos to transiently inhibit expression of DNM2 or MYC. The oligos were diluted in Lipofectamine RNAiMAX (Thermo Fisher Scientific) at a final concentration of 40 nmol/L and 100 nmol/L for 72 hours (DNM2; ref. 16) or 24 hours (MYC), in accordance to the manufacturer's instruction. The cells, tested for silencing efficiency, were used in select experiments.

RNA extraction and qRT-PCR

RNA was extracted using the RNeasy Mini Kit and then quantified using NanoDrop2000 (Thermo Scientific). Five hundred nanogram of total RNA were retro-transcribed into complementary DNA (cDNA) using the iScript Kit. The primer sequences are listed in Supplementary Table S1. qRT-PCR was run on a ABI Prism 7900HT Sequence Detection System (Applied Biosystems). The relative levels of each mRNA were calculated using the ΔΔCt, and either GAPDH or β-actin levels were used for normalizing data.

Tube-branching assay

A total of 20,000 HUVEC cells/well were plated on Growth Factor Reduced Matrigel coated wells (96-well plate; ref. 17) with (1) SF DMEM in the presence or absence of LO and Exo, (2) Dynasore-OH (Dyn) (20 μmol/L) in SFM, with LO or full media (FM; EGM-2, 2% serum), and (3) conditioned media (CM) from NAF previously exposed to LO and Exo. To obtain the CM, NAF were washed 3 times and then cultured in fresh SFM for 24 hours after treatment with LO (6 hours in SFM). The CM was cleared of cell debris prior to being placed on endothelial cells. After 6 hours of incubation at 37°C, images were recorded with an inverted Leica microscope equipped with an Olympus camera. Results were quantified by measuring the number of tubes per field (at least 4 fields) by phase-contrast microscopy and Image J.

Published OnlineFirst February 15, 2017; DOI: 10.1158/0008-5472.CAN-16-2942

TF array

Nuclear extract of WPMY-1 treated with LO or vehicle was obtained with a Nuclear Extraction Kit (Thermo Fisher Scientific). Note that 10 μg of nuclear extracts were assayed for the activity of 16 TFs using a Stem Cell TF Activation Profiling Plate Array I (Signosis) following the manufacturer's instruction.

Luciferase reporter assay

To perform the luciferase reporter assay, the pBV-Luc wt MBS1-4 vector containing the MYC-regulated cyclin-dependent kinase 4 (CDK4) promoter element (18) or the pBV-Luc empty vector was transfected into primary NAF with the pRL-SV40 vector expressing renilla luciferase as internal control. Twenty-four hours after transfection, the media were changed, and the cells were exposed to LO or vehicle for 6 hours. In select experiments, cells were pretreated with either Dyn for 30 minutes or p-AKT1 inhibitor AZD5363 for 12 hours before LO treatment. In the case of Dyn, after treating the cells with LO +/– Dyn, they were cultured in fresh media for 6 hours before measuring MYC activity. The luciferase activity was determined with the Dual-Luciferase Reporter Assay System following the manufacturer's instructions. The relative luciferase activity was calculated as ratio of firefly versus renilla luciferase activity. At least three biological replicates were performed for each assay.

RNA sequencing

NAF were exposed to LO or vehicle for 6 hours prior to RNA extraction as described above. RNA concentration and quality were tested respectively with Nanodrop 8000 (Thermo Scientific) and 2100 Bioanalyzer (Agilent). One microgram of total RNA per sample was used for library construction with the Illumina TruSeq Stranded mRNA Library Prep Kit. Libraries were thus multiplexed and sequenced across 4 lanes of a NextSeq 500 platform (Illumina) using 75 single-end sequencing. On average, about 20 million reads were generated from each sample.

Data processing and master regulator analysis

Raw reads obtained from RNA sequencing (RNA-seq) were aligned to the custom human GRCh38 transcriptome reference (http://www.gencodegenes.org) using Bowtie (version 1.1.1; ref. 19) and RSEM (version 1.2.20; ref. 20) with default parameters. The data were filtered in low or unexpressed genes and ribosomal RNAs, normalized, and then subjected to differential expression analysis in limma-voom. Data files from the RNA-seq analysis were deposited in the gene expression omnibus data bank under the accession code GSE87563. Master regulator analysis (MRA) was performed as previously described, using TF-target interaction information collected from public databases (21).

Mouse studies

All mouse studies were performed in accordance to the institutional guidelines (animal protocol #5911). Animals were monitored for abnormal tissue growth and euthanized if excessive health deterioration was observed. Subrenal capsule grafting was done in C57BL/6 male mice as previously reported (22). Alternatively, tumor cells were recombined with or without fibroblasts (4:1) and injected subcutaneously athymic nude mice. Pretreatment with LO was performed at a concentration of 100 μg/mL. Dyn and the MYC-i (10058-F4) were used at a concentration of 20 μmol/L. Tumor size was measured twice a week and calculated as: $^1/_2$ x width^2 x length. Tumor tissues were either stained with hematoxylin and eosin or immunostained with Ki67 antibody using established protocols (23).

Immunoprecipitation

Protein lysates were incubated with IgG or HA antibodies (4°C for 2 hours) followed by overnight incubation (4°C) with protein G agarose beads. The immunoprecipitate was analyzed through gel electrophoresis and immunoblotting or used for the kinase activity assay.

Kinase activity assay

To analyze kinase activity, a nonradioactive AKT Kinase Assay Kit (Cell Signaling Technology) was used following the manufacturer's instruction. GSK3α/β phosphorylation was detected by using the phospho-GSK3α/β (Ser21/9) antibody.

Statistical analysis

Plots show an average of at least three independent biological replicate. Experimental groups were compared using a two-tailed, unpaired, Student *t* test.

Results

EV-bound AKT1 is selectively present in LO

A recent report identified AKT1 and other kinases in blood EVs from patients with different epithelial tumor types (24). Because AKT1 is frequently activated in patients with metastatic prostate cancer as a result of genomic aberrations in the PI3K pathway, and the above report did not separate large from small EVs, we analyzed the distribution of EV-bound AKT1 in LO and Exo. Immunoblotting for AKT1 phosphorylated on Ser473 (a marker of kinase activation) was performed in LO and Exo obtained from the plasma of patients ($n = 12$) with metastatic prostate cancer. We used a protocol based on differential centrifugation to separate LO from Exo, followed by flotation (upward displacement) to exclude proteins and other EV-attached molecules (Fig. 1A; ref. 11). We found that LO harbor p-AKT1^{Ser473} at significantly higher levels than Exo (Fig. 1B; Supplementary Fig. S1A), despite high similarities in the total protein amount in most of the samples (Supplementary Fig. S1B). To further characterize the active AKT1 content in EVs, we isolated LO and Exo from LNCaP^{MyrAKT1} cells. TRPS analysis identified particles with a diameter ranging from 1.5 to 6.0 μm, in the LO fraction, and from 80 to 180 nm, in the Exo fraction (Fig. 1C). High levels of p-AKT1^{Ser473} were readily detectable in LO, whereas they were significantly lower in Exo (Fig. 1D). p-AKT1^{Ser473} was also detected in LO from PC3 and 22Rv1 prostate cancer cells, which express the active protein endogenously (Fig. 1E). These results reveal that active AKT1 is primarily localized in LO, when compared with Exo, in both cell line–derived and patient plasma samples, suggesting that LO might serve as mobile platforms for active kinases, and that the enzyme travels in the circulation protected in EVs.

LO are internalized by heterologous cells

EV uptake typically represents an important step for intercellular communication. However, very little is currently known about the mechanisms that cells adopt to internalize EVs larger than Exo (25). We exposed immortalized WPMY-1 myofibroblasts to LO labeled with the fluorescent dye PKH26 and quantitatively analyzed LO uptake by flow cytometry. LO uptake by

Published OnlineFirst February 15, 2017; DOI: 10.1158/0008-5472.CAN-16-2942

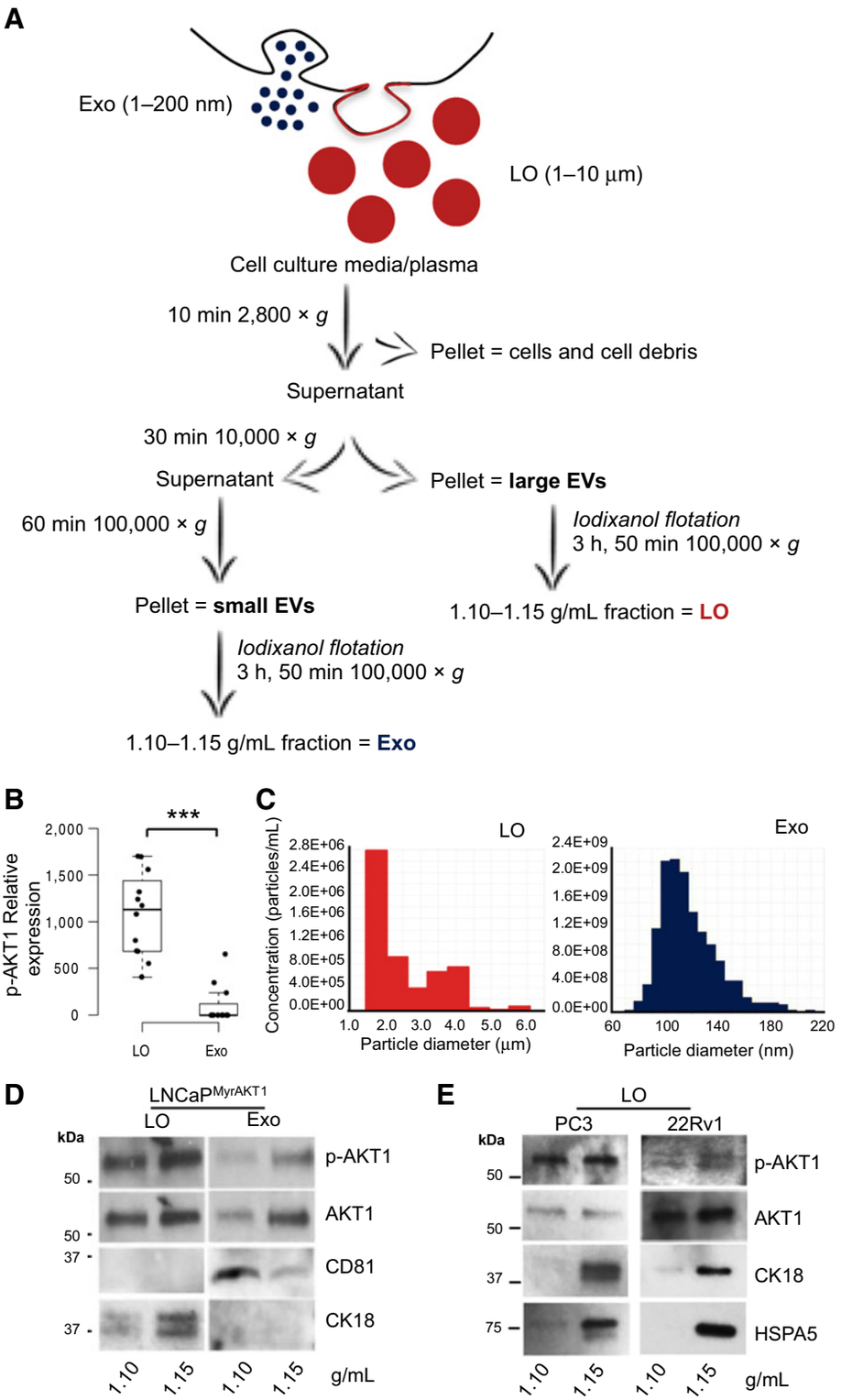

Figure 1.
LO are EVs that harbor active AKT1. **A,** Schematic representation of the protocol used for purification of LO and Exo starting from CM and patient plasma. **B,** Protein lysates from LO and Exo purified from the plasma (500 μL) of patients with castration-resistant prostate cancer ($n = 12$) were blotted with a p-AKT1^{Ser473} antibody. p-AKT1^{Ser473} band intensity was normalized to protein content for each patient. Circulating LO carry significantly higher levels of active AKT1 than Exo (***, $P < 0.002$). **C,** TRPS (qNano) analysis of LO (left) and Exo (right) using NP2000 and NP100 membrane pores, respectively. **D,** LO and Exo were purified from LNCaP^{MyrAKT1} cell media by gradient centrifugation (iodixanol), and protein lysates (10 μg) from the indicated fractions (1.10 and 1.15 g/mL density of the 10k and 100k pellets) were blotted with the indicated antibodies, including LO marker CK18 and Exo marker CD81. **E,** Equal amounts of protein from PC3- and 22Rv1-derived LO were blotted with the indicated antibodies.

target cells was quantitatively analyzed by flow cytometry (FACS; Fig. 2A). Confocal imaging of FACS-sorted LO-positive cells showed intact PKH26-labeled LO in the peripheral and perinuclear area (Fig. 2B). Increased PKH26 signal correlated with an increasing number of vesicles (Fig. 2C). In addition, we found colocalization of PKH26 with MyrAKT1 (Fig. 2D; Supplementary Fig. S2A), as detected with an HA-FITC antibody that binds with high specificity to the HA tag of the MyrAKT1 construct (10),

Published OnlineFirst February 15, 2017; DOI: 10.1158/0008-5472.CAN-16-2942

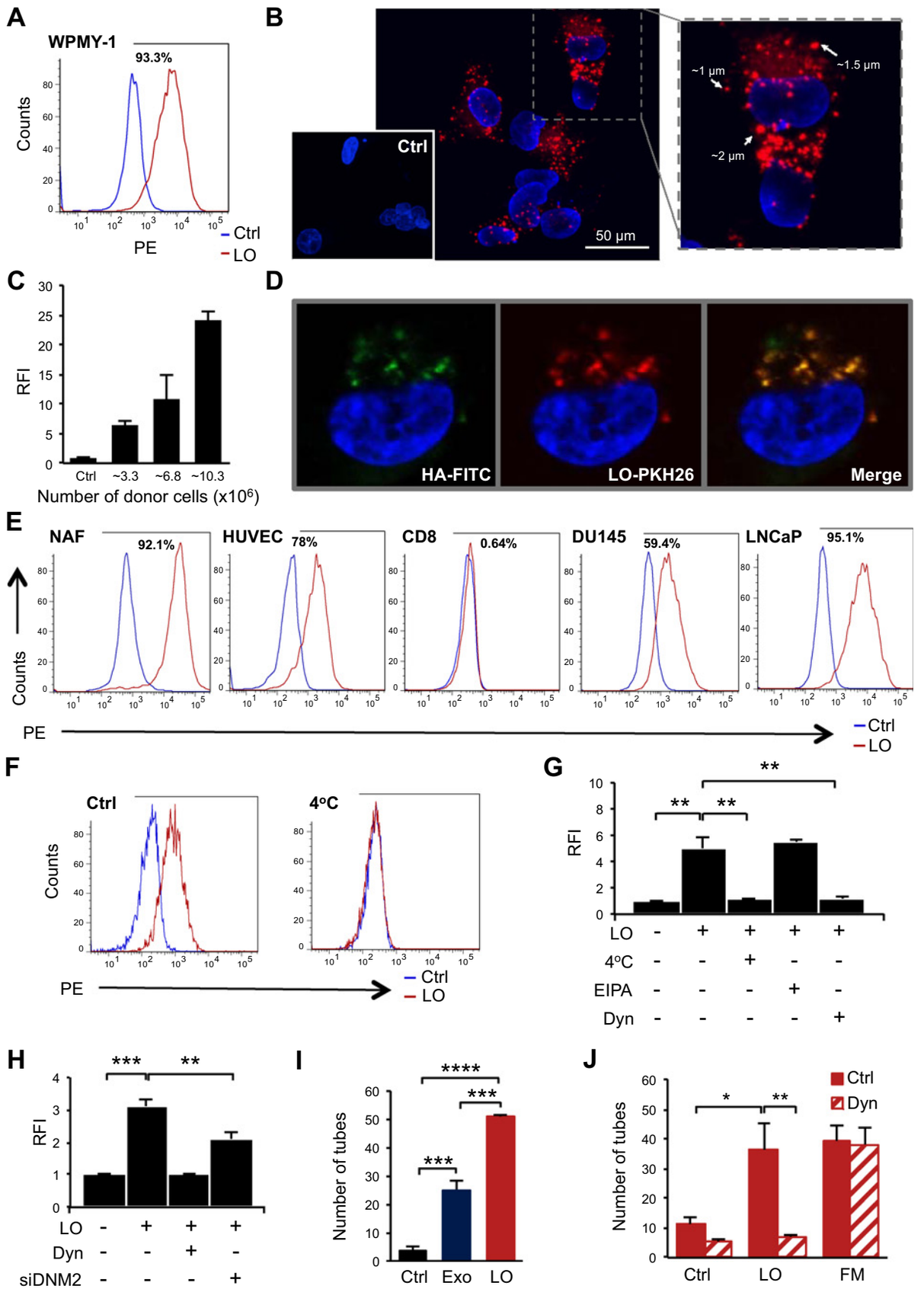

Published OnlineFirst February 15, 2017; DOI: 10.1158/0008-5472.CAN-16-2942

which is expressed in the donor cells but absent in the target cells. These results suggest that the particles were intact LO rather than empty circular membrane structures capturing the lipid dye. We then determined whether cells other than myofibroblasts could also internalize LO. We tested NAF, HUVEC, $CD8^+$ lymphocytes, and DU145 and LNCaP cancer cell lines. NAF are primary cells generated from prostatectomy tissues not associated with prostate cancer. LO uptake varied among these cells and was almost completely impaired in $CD8^+$ lymphocytes (Fig. 2E), implying a selective mechanism of uptake. These observations suggest that LO enter target cells by a mechanism that might involve defined interactions between LO and the recipient cells.

The biological effects of LO can be inhibited by blocking LO uptake

To further rule out the possibility that LO uptake occurs by a passive fusion of EV and cell membranes, we incubated target cells with LO at 4°C. This strategy has been previously used to inhibit ATP-dependent processes that are involved in EV endocytosis but not fusion (26). This approach efficiently prevented LO uptake (Fig. 2F), suggesting an active endocytic process. Due to their large size, we considered both phagocytosis and macropinocytosis as possible mechanisms. The PI3K inhibitor, Wortmannin (WTN), and the actin polymerization inhibitor, cytochalasin-D (CYT-D; refs. 27, 28), typically used to block both phagocytosis and macropinocytosis (29), significantly perturbed LO uptake (Supplementary Fig. S2B and S2C). To determine the relative contribution of these two processes, we used Dyn (30) and 5-(N-Ethyl-N-isopropyl) amiloride (EIPA), respectively. The primary and most ubiquitous target of Dyn is dynamin 2 (DNM2), which plays a role in the first stages of phagocytosis, including actin polymerization and augmenting of the membrane surface for particle engulfment (31, 32). EIPA, which inhibits the Na^+/H^+ antiporter (33), is typically used to block macropinocytosis. LO uptake was significantly inhibited by Dyn but not by EIPA (Fig. 2G; Supplementary Fig. S2D and S2E), suggesting that it occurs through a phagocytosis-like mechanism. The involvement of DNM2 in LO phagocytosis was further confirmed by a significant reduction in LO uptake upon specific silencing of DNM2 (Fig. 2H; Supplementary Fig. S2F). To determine whether the internalization is important for LO function, we employed tube formation assays, which have been previously used to show bioactivity of Exo (34) but have never been used to test LO function. Notably, LO stimulated a significant increase of the tube-branching abilities of HUVEC (Fig. 2I; Supplementary Fig. S2G). This effect was greater than that elicited by Exo and was obtained with amounts of LO (5–20 μg/mL) that are lower than those typically used for functional EV experiments (20–200 μg/mL; Supplementary Fig. S2H; refs. 6, 35). Dyn treatment of HUVEC cells prevented LO-induced tube branching, but did not prevent the branching induced by full media, which contains abundant soluble molecules that stimulate angiogenesis (Fig. 2J; Supplementary Fig. S2I). Collectively, these results indicate that LO enter the target cells through a phagocytosis-like mechanism, and that this is necessary for LO-mediated biological functions.

LO internalization induces a distinct fibroblast phenotype

Because it is known that tumor-activated fibroblasts release factors that can influence tube formation (36), and having observed a potent induction of tube branching in response to LO used directly to condition endothelial cells, we tested whether this effect in endothelial cells could be elicited by the secretions of fibroblasts that had internalized LO. CM from NAF pretreated with LO induced a more significant increase in tube branching than Exo (Fig. 3A; Supplementary Fig. S3A). To understand the molecular basis underlying the LO-induced result on NAF, we tested changes in expression of factors that are upregulated in fibroblasts activated by cancer cells (6, 14). LO treatment resulted in enhanced expression of IL6, matrix metalloproteinase 9 (MMP9; Fig. 3B), and α-smooth muscle actin (α-SMA; Fig. 3C). Conversely, TGFβ1, MMP1, and thrombospondin 1 (TSP1), which also have been recognized as markers of an activated, myofibroblast-like phenotype (6, 14, 36–38), were not altered (data not shown), suggesting that LO induce a distinct reprogramming of the fibroblasts, which results in a provascularization phenotype.

LO activate the TF MYC in NAF

TF activation might be an important mechanism underlying the responses of target cells to EVs (39). However, how frequently this happens and whether this phenomenon is specific for a given subpopulation of EVs, or for a given TF, has not yet been investigated. We thus tested if LO treatment perturbed TF activity, with the underlying hypothesis that this could be the mechanism modulating the effects described above. Nuclear extracts of fibroblasts exposed to LO or vehicle were tested for functional binding of TFs to DNA. We employed an activity array for TFs with a known role in somatic cell reprogramming (including EGR1, Nanog, SOX2, ETS, KLF4, MEF2, MYC, Pax6, TCF/LEF). Two independent trials revealed reproducible enhancement of MYC binding to DNA in response to LO (Supplementary Fig. S3B). To further validate this result, we measured MYC activity by examining the stimulation of MYC-dependent transcription. Significant activation of MYC-regulated CDK4 promoter was observed upon treatment with LO, but not with the same amount of Exo (Fig. 3D, $P < 0.05$). This estimation was based on protein concentration (20 μg/mL), normalized to the number of cells. However, we reasoned that the array was composed of very few TFs, and

Figure 2.

Internalization of LO in target cells is functionally important. **A,** WPMY-1 fibroblasts were exposed to PKH26-labeled LO from $LNCaP^{MyrAKT1}$ cells or vehicle for 1 hour. The shift of the red line to the right, which is quantifiable, indicates LO internalization by the target cells, and it is expressed as percentage of cells internalizing LO. **B,** Cells negative and positive for PKH26 were FACS-sorted and imaged by confocal microscopy demonstrating the presence of abundant vesicular structures in the LO size range. Control cells are visible in the bottom left plot. **C,** WPMY-1 cells were incubated with increasing doses of PKH26-labeled LO and then analyzed by FACS. Uptake rates, expressed as RFI, correlate with LO doses. **D,** PKH26-positive WPMY-1 cells were sorted and stained with a HA-FITC antibody against the HA-tag on the MyrAKT1 construct. The two signals colocalize in internalized EVs. **E,** FACS analysis demonstrates variable uptake rate in the indicated cell lines exposed to PKH26-labeled LO. **F,** Treatment of WPMY-1 cells with LO at 4°C inhibits the uptake. **G,** LO uptake by WPMY-1 cells was significantly inhibited by Dyn (20 μmol/L) but not by EIPA (50 μmol/L). As expected, uptake was inhibited at 4°C. **H,** Transient silencing of DNM2 (siDNM2) in WPMY-1 cells resulted in a significant reduction of LO uptake. **I,** HUVEC were seeded on Matrigel-coated wells and exposed to Exo or LO (20 μg/mL). The number of branched tubes was significantly altered by both LO and Exo. **J,** Dyn treatment prevented the LO-induced tube formation. Bar plots show the average of three biological replicates (*, $P < 0.05$; **, $P < 0.02$; ***, $P < 0.002$; and ****, $P < 0.000001$).

Published OnlineFirst February 15, 2017; DOI: 10.1158/0008-5472.CAN-16-2942

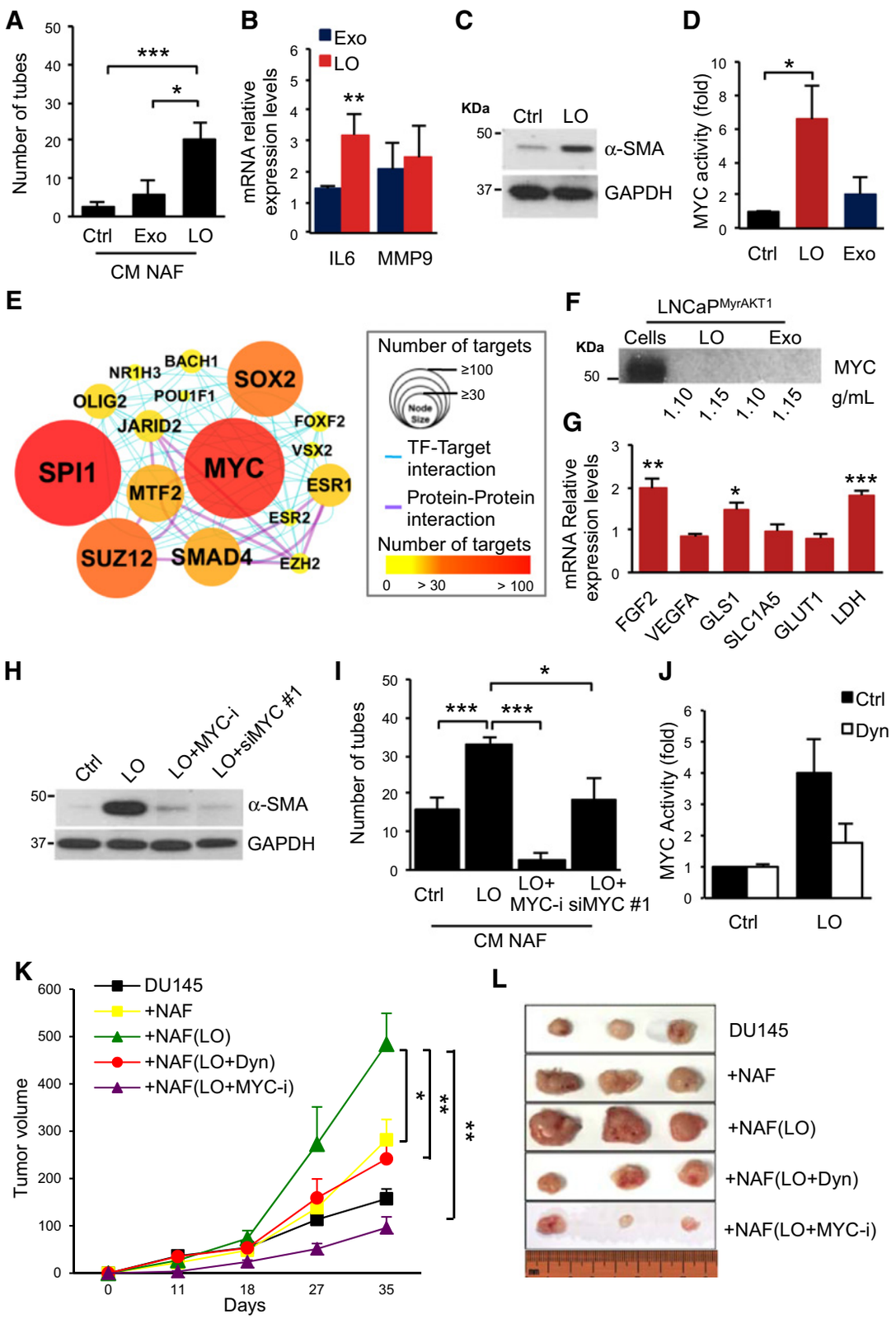

Published OnlineFirst February 15, 2017; DOI: 10.1158/0008-5472.CAN-16-2942

a large-scale approach might be useful to unambiguously define the TF pathways involved in LO-mediated activation. RNA-seq was carried out in NAF exposed to LO or vehicle to obtain an in-depth analysis of the transcriptome of these cells in response to LO. This analysis, performed in biological duplicate, identified 207 differentially expressed genes (DEG; FDR < 0.1, fold change $\geq$ 1.5) in response to LO. MRA was then applied to the DEG set using TF-target interaction information collected from public databases. This allowed us to infer functional interactions between TFs and their target genes following a strategy we previously employed to identify important transcriptional regulators (21). Sixteen of a total of 274 activated TFs emerged as strong putative TFs (empirical test P value < 0.01 and hypergeometric test P value < 0.01). The number of putative TFs that were activated by LO is relatively small (~6%), suggesting that modulation of gene expression is selective. MYC emerged as a highly activated TF in response to LO (Fig. 3E; Supplementary Table S2), confirming our initial results. MYC was not identified in LO, suggesting that LO stimulate MYC activation rather than mediating transfer of the protein (Fig. 3F). Detection of higher levels of MYC in cancer-associated fibroblasts compared with NAF (Supplementary Fig. S3C) supports the concept that this activation might occur naturally in the tumor microenvironment. Furthermore, NAF exposed to LO exhibited increased levels of fibroblast growth factor 2 (FGF2), glutaminase (GLS), and lactate dehydrogenase (LDH), which are known transcriptional targets of MYC (Fig. 3G). Notably, human RNA expression data demonstrated that LDH positively correlates with MYC in prostate cancer tissues with high stromal content (> 70%; Supplementary Fig. S3D). These results support an LO-dependent modulation of MYC activity in fibroblasts.

LO-induced NAF activation is mediated by MYC

The above results prompted us to test whether MYC plays a functional role in LO-mediated fibroblast reprogramming. Both genetic silencing of MYC using MYC inhibition by the low molecular weight compound 10058-F4 (40) and two independent siRNAs (Supplementary Fig. S3E) in NAF were sufficient to block the LO-induced α-SMA increase and the ability of these cells to stimulate branching morphogenesis (Fig. 3H and I; Supplementary Fig. S3F–S3I). The LO-induced MYC activity was blocked by the MYC inhibitor confirming the specific effect of the compound (Supplementary Fig. S3J). A tumor supportive role for stromal MYC was also independently demonstrated by animal experiments in which overexpression of MYC in wild-type mouse primary prostatic fibroblasts induced hyperplasia of the adjacent normal prostatic epithelium in tissue recombinants grafted into the subrenal capsule of syngeneic C57BL/6 mice (Supplementary Fig. S3K). Interestingly, the LO-induced MYC activation was reduced in NAF by blocking LO uptake with Dyn (Fig. 3J), further confirming the effect of this compound on tube branching described above (Fig. 2J). To investigate the contribution of LO–stroma interactions *in vivo*, DU145 cells, alone or recombined with NAF, were injected subcutaneously in nude mice, and tumor growth was measured for up to 35 days. Recombination of tumor cells with NAF led to an approximately 1.5-fold increase of the mean tumor volume compared with the tumor cells alone. Notably, *ex vivo* pretreatment of NAF for 3 days with LO isolated from LNCaP^{MyrAKT1} significantly enhanced tumor growth (~3-fold higher than tumor cells alone). This effect was completely prevented by blocking LO uptake with Dyn and reduced by treatment with the MYC inhibitor (Fig. 3K and L). Treatment with the MYC inhibitor alone also prevented the NAF-supported tumor growth (data not shown). Together, these data provide evidence of an important functional role for MYC in fibroblast reprogramming and modulation of tumor growth mediated by AKT1-loaded LO.

MYC activation in the stroma is dependent on AKT1 kinase activity

Because most of the results described so far were elicited by LO originating from cells expressing a constitutively active AKT1, and because we found high levels of p-AKT1^{Ser473} in LO, we wondered whether this kinase was functionally active in the particles. We first demonstrated that MyrAKT1 can be readily immunoprecipitated in LO (Supplementary Fig. S4A). Then, the AKT1 immunoprecipitation products from the two EV populations, cultured in cell- and serum-free culture conditions for up to 72 hours, were submitted to a AKT1 kinase activity assay, which demonstrated abundant phosphorylation of the AKT1 target glycogen synthase kinase 3α/β (GSK3α/β) in LO, but not in Exo (Fig. 4A). In support of the hypothesis that LO might function as mobile platforms for active kinase, LO induced upregulation of p-AKT1^{Ser473} in NAF (Fig. 4B; Supplementary Fig. S4B). We then tested whether AKT1 activity is necessary for the LO-mediated effects on the stroma. MYC activity (Fig. 4C), α-SMA levels (Fig. 4D), and tube branching (Fig. 4E; Supplementary Fig. S4C and S4D) were reduced in NAF exposed to LO in the presence of the AKT1 inhibitor AZD5363 (41) in comparison with vehicle treatment. The result on tube branching was reproduced with LO derived from an unrelated prostate cancer cell line that endogenously expresses an active AKT1 (Fig. 4E). Collectively, these data suggest that the

Figure 3.

LO treatment of NAF induces a MYC-dependent reprogramming. **A,** HUVEC cells were exposed to CM from NAF, previously incubated with LO and Exo. The CM from NAF pretreated with LO, but not Exo, induced tube formation. **B,** qRT-PCR of NAF exposed to LO or vehicle shows increased levels of IL6 and MMP9 mRNA in response to LO treatment. **C,** Immunoblot experiments demonstrated increased levels of α-SMA in NAF upon 24-hour exposure to LO. **D,** Luciferase activity of MYC-regulated CDK4 promoter significantly increased in NAF exposed to LO but not Exo. **E,** MRA of DEG obtained after RNA-seq in NAF treated with LO or vehicle. MYC is one of the most active TF in NAF in response to LO. TF network illustrating interactions between key TFs and the degree of influence to potential target genes among the DEGs (node size and color, respectively). TFs with a large number of targets (> 105) are represented by big red nodes, whereas TFs with smaller numbers of targets (< 50) are indicated with small yellow nodes. Cyan and purple connectors indicate TF–target and protein–protein interactions, respectively. **F,** Protein lysate from LNCaP^{MyrAKT1} cells and derived LO and Exo were blotted with MYC antibody. **G,** qRT-PCR in NAF, exposed to LO or vehicle, shows increase levels of MYC targets in response to LO. **H,** Immunoblot analysis showing that MYC inhibition, using either the MYC inhibitor 10058F4 (MYC-i; 20 μmol/L) or siRNA specific for MYC (siMYC), prevents LO-dependent induction of α-SMA. **I,** HUVEC cells were exposed to CM from NAF previously incubated with LO with or without MYC inhibition. MYC inhibition (MYC-i, siMYC) induces a reduction of tube formation in response to LO. **J,** Luciferase activity of the MYC-regulated promoter in response to LO is inhibited by Dyn. **K,** DU145 cells were injected subcutaneously into nude mice with or without NAF (ratio 4:1) and the tumor volume (mean ± SE) measured at the indicated intervals (tumors $n \geq 5$ per group). The NAF were either untreated or exposed, *ex vivo*, to LO in the presence or absence of Dyn or MYCi for 72 hours. LO treatment increased significantly the tumor volume, an effect inhibited by both Dyn and MYC-i. **L,** Representative gross photographs of the tumors. Plots shows the average of three biological replicate (*, $P < 0.05$; **, $P < 0.02$; ***, $P < 0.002$).

Published OnlineFirst February 15, 2017; DOI: 10.1158/0008-5472.CAN-16-2942

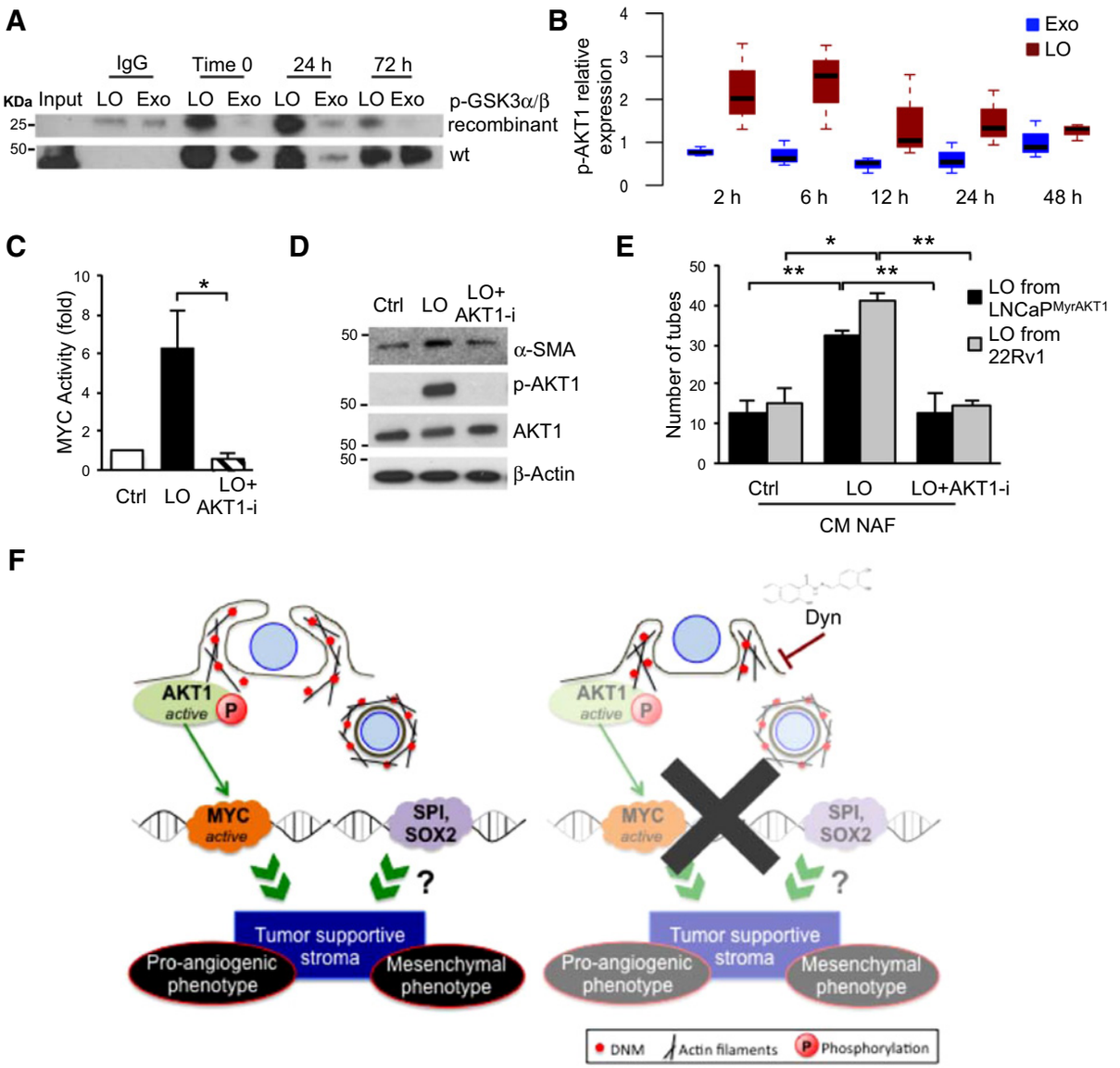

Figure 4.

LO-induced NAF reprogramming is mediated by AKT1 activation. **A,** Protein lysates from LO or Exo were used to immunoprecipitate MyrAKT1 using an HA antibody and IP product subjected to AKT1 kinase activity assay using GSK3α/β-recombinant protein as a substrate. Both the IP product and the input (straight protein lysates) were then blotted with a p-GSK3α/β$^{Ser21/9}$ antibody, which recognizes the wild-type (wt) protein as well as the recombinant protein, demonstrating the presence of active AKT1 in LO but not in Exo. **B,** NAF exposed to LO or Exo for the indicated times were immunoblotted with p-AKT1^{Ser473} and AKT1 antibodies. The box plot shows the average of the p-AKT1^{Ser473} band intensity, normalized over β-actin, from three different experiments. **C,** Luciferase activity of the MYC-regulated promoter in response to LO inhibited by the AKT1 inhibitor AZD5363 (AKT1-i; 1 μmol/L). Bar plot shows the average of three biological replicates (*, $P < 0.05$). **D,** Immunoblot assay showing that AKT1 inhibition prevents LO-dependent induction of α-SMA. **E,** Tube branching in response to LO is reduced by AKT1-i. Bar plots show the average of three biological replicates (*, $P < 0.05$; **, $P < 0.02$). **F,** Our working model suggests that AKT1, which is activated upon LO treatment, can phosphorylate, thus inactivating it, the MYC inhibitor GSK3α/β. Active MYC induces a reprogramming of NAF characterized by upregulation of α-SMA, LDH, and FGF2, and this process can be inhibited by preventing LO internalization.

LO-induced fibroblast reprogramming is dependent on AKT1 kinase activity.

Discussion

In this study, we demonstrate that AKT1 is a LO-resident protein that maintains its activity inside these vesicles and can be detected in LO isolated from plasma of patients with metastatic prostate cancer. This result supports the novel observation that EVs are a heterogeneous category of particles (11, 42). This might be clinically significant because it implies that different EV populations can harbor distinct molecules that can be interrogated as biomarkers.

Although previous studies on Exo have identified TGFβ1 as a key player in modulating the response of the stroma (6, 35), LO

Published OnlineFirst February 15, 2017; DOI: 10.1158/0008-5472.CAN-16-2942

treatment of fibroblasts promotes MYC-dependent reprogramming characterized by upregulation of molecules involved in stroma activation, angiogenesis, and metabolism, and prevented by inhibiting LO internalization and/or AKT1 activity. While the effect of EVs on the endothelium has been previously revealed (3, 4), our study shows an alternative mechanism that alters the endothelium indirectly by activating fibroblasts. This might be an effect not targetable by angiogenesis inhibitors and could be used to develop therapeutic strategies alternative or complementary to antiangiogenesis strategies. LO can condition the fibroblasts promoting their tumor-supportive functions *in vivo*, and this result is abolished not only by MYC inhibition but also by preventing LO uptake with Dyn. A critical feature of LO-mediated reprogramming is therefore the activation of MYC, and we speculate that this might promote fibroblast responses at different levels. LO-mediated MYC activation could be responsible for the acquired ability of the fibroblasts to induce tube formation by regulating its downstream target FGF2 (43). It could also contribute to tumor progression by altering the metabolism of the target fibroblasts as suggested by the observed GLS and LDH upregulation in response to LO, and the significant correlation between MYC and LDH in the tumor stroma *in vivo*. This is important because it could explain, at least in part, the metabolic switch described in tumor-associated fibroblasts (44). Although MYC is a known transcriptional enhancer of genes involved in glycolysis and glutaminolysis often observed in metastatic tumors (45), the demonstration that this might happen in the stroma, and as a response to a discrete EV population that is tumor-specific, is completely novel.

These results strongly point to MYC as one of the master regulators of LO-induced activities in the stroma. Two independent large-scale approaches (TF activity array and RNA-Seq) further suggest that LO might play a more complex function in regulating the response of the fibroblasts to the tumor. We have evidence for additional TFs, with several common targets, whose function is activated by LO. One example is the ETS family member SPI-1 (Fig. 3E), which is known for its role in orchestrating cell fate in hematopoiesis but has been poorly studied in cancer (46) and not at all in the stroma. This TF seems to be highly sensitive to LO regulation, as inferred by the result that it controls most of the DEGs in response to LO. It also shares 125 target genes with MYC (Supplementary Fig. S4E), suggesting that it might cooperate with MYC in regulating gene expression changes in response to LO. A functional array demonstrated that a class of TFs that recognized an ETS binding domain was highly activated in response to LO (Supplementary Fig. S3B). Notably, the ETS TF family has been previously shown to mediate reprogramming of breast cancer–associated fibroblasts in response to PTEN loss (47). Another example is represented by SOX2, which is also robustly activated in response to LO (Fig. 3E; Supplementary Fig. S3B), and has been previously shown to induce properties of mesenchymal stem cells when overexpressed in fibroblasts (48). These considerations led us to a working model in which LO uptake by fibroblasts results in activation of AKT1 and possibly other signaling pathways, which in turn affect transcriptional programs that are regulated by reprogramming factors such as MYC, SPI-1, ETS, and SOX2. These TFs could thus all contribute to reprogram the stroma in favor of a tumor-supportive phenotype (Fig. 4F).

Our observation that inhibition of AKT1 in the fibroblasts abolishes the LO-induced alterations to a degree that is similar to that provoked by inhibition of LO uptake allows us to speculate that preventing phagocytosis of these large vesicles might be a more global strategy to prevent communication between cells and stromal cells than targeting single molecules. To our knowledge, this result has not been previously demonstrated for other EVs. This has important implications, considering that EVs harbor a variety of molecules and blocking the uptake of the whole vesicle instead of inhibiting one or two specific molecules might be a more efficient strategy to prevent dissemination of oncogenic signals (49). This could be combined with current therapies aimed to target tumor cells but not the tumor-supportive environment. In addition, inhibition of EV uptake could block the effect of circulating EVs that are not eliminated with surgery excision or radiation-induced ablation and thus the combined approach might prevent or delay the tumor relapse. However, a deeper understanding of the molecular basis underlying LO phagocytosis is necessary to develop therapeutic strategies aimed to block EV interactions with target cells. For example, it will be important to know whether the activation of AKT1, observed in this study, is the result of endomembrane release of the LO cargo upon fusion of LO membranes with the surrounding endosomes, or if the endogenous protein is recruited and activated by ligand-receptor–induced signaling in response to LO.

In conclusion, this is the first study demonstrating the role of LO in educating the fibroblasts to a tumor-supportive function. We identified a novel AKT1/MYC signaling axis that originates from the tumor and reverberates to the stroma as a specific mediator of LO biological effects. However, the complexity of LO cargo and the resulting molecular effects elicited in target cells suggest that other players contribute to the phenotypic changes elicited by LO. Additional studies will further elucidate the function of LO in the modulation of the tumor microenvironment and identify additional nodes that could be targeted to prevent tumor progression and metastasis.

Disclosure of Potential Conflicts of Interest

N.A. Bhowmick is a researcher at Veterans Administration Greater Los Angeles Healthcare System. No potential conflicts of interest were disclosed by the other authors.

Authors' Contributions

Conception and design: V.R. Minciacchi, D. Di Vizio

Development of methodology: V.R. Minciacchi, C. Spinelli, M. Reis-Sobreiro, L. Cavallini, M. Zandian, P. Chiarugi, E. Cocucci, X. Li, R. Mishra

Acquisition of data (provided animals, acquired and managed patients, provided facilities, etc.): N.A. Bhowmick, E.M. Posadas, P. Chiarugi, G. Viglietto, E. Cocucci

Analysis and interpretation of data (e.g., statistical analysis, biostatistics, computational analysis): S. You, V.R. Minciacchi, R.M. Adam, M.R. Freeman, D. Di Vizio

Writing, review, and/or revision of the manuscript: V.R. Minciacchi, M.R. Freeman, E. Cocucci, D. Di Vizio

Administrative, technical, or material support (i.e., reporting or organizing data, constructing databases): P. Chiarugi, E.M. Posadas

Study supervision: D. Di Vizio

Acknowledgments

We would like to thank first of all our patients and their families for participation in this study. We are grateful to Drs. Chia-Yi Chu and Wen-Chin Huang for their technical support for the animal experiment, to Izon Science (Subhash Kalluri) for the TRPS, to Drs. Andries Zijlstra, Francesca Demichelis,

and Amina Zoubedi for constructive comments, and to Dr. Dennis Hazelett for using his pipeline for normalization of the RNA-seq data.

Grant Support

This study was supported by grants from the NIH (NIH UCLA SPORE in Prostate Cancer award P50 CA092131 to D. Di Vizio); Avon Breast Cancer Foundation Fund 02-2013-043 to D. Di Vizio; the Martz Translational Breast Cancer Research Fund to M.R. Freeman and D. Di Vizio; Department of Defense PC150836 to D. Di Vizio; the Steven Spielberg Discovery Fund in Prostate Cancer Research to M.R. Freeman and D. Di Vizio; and The Ohio State University Comprehensive Cancer Center (P30-CA016058) and an intramural fund (IRP46050-502339) to E. Cocucci.

The costs of publication of this article were defrayed in part by the payment of page charges. This article must therefore be hereby marked *advertisement* in accordance with 18 U.S.C. Section 1734 solely to indicate this fact.

Received November 1, 2016; revised December 12, 2016; accepted February 2, 2017; published OnlineFirst February 15, 2017.

References

1. Barron DA, Rowley DR. The reactive stroma microenvironment and prostate cancer progression. Endocr Relat Cancer 2012;19:R187–204.
2. Tripathi M, Billet S, Bhowmick NA. Understanding the role of stromal fibroblasts in cancer progression. Cell Adh Migr 2012;6:231–5.
3. Al-Nedawi K, Meehan B, Micallef J, Lhotak V, May L, Guha A, et al. Intercellular transfer of the oncogenic receptor EGFRvIII by microvesicles derived from tumour cells. Nat Cell Biol 2008;10:619–24.
4. Minciacchi VR, Freeman MR, Di Vizio D. Extracellular vesicles in cancer: Exosomes, microvesicles and the emerging role of large oncosomes. Semin Cell Dev Biol 2015;40:41–51.
5. Peinado H, Aleckovic M, Lavotshkin S, Matei I, Costa-Silva B, Moreno-Bueno G, et al. Melanoma exosomes educate bone marrow progenitor cells toward a pro-metastatic phenotype through MET. Nat Med 2012;18: 883–91.
6. Webber JP, Spary LK, Sanders AJ, Chowdhury R, Jiang WG, Steadman R, et al. Differentiation of tumour-promoting stromal myofibroblasts by cancer exosomes. Oncogene 2015;34:290–302.
7. Di Vizio D, Kim J, Hager MH, Morello M, Yang W, Lafargue CJ, et al. Oncosome formation in prostate cancer: association with a region of frequent chromosomal deletion in metastatic disease. Cancer Res 2009; 69:5601–9.
8. Meehan B, Rak J, Di Vizio D. Oncosomes - large and small: What are they, where they came from? J Extracell Vesicles 2016;5:33109.
9. Hager MH, Morley S, Bielenberg DR, Gao S, Morello M, Holcomb IN, et al. DIAPH3 governs the cellular transition to the amoeboid tumour phenotype. EMBO Mol Med 2012;4:743–60.
10. Di Vizio D, Morello M, Dudley AC, Schow PW, Adam RM, Morley S, et al. Large oncosomes in human prostate cancer tissues and in the circulation of mice with metastatic disease. Am J Pathol 2012;181:1573–84.
11. Minciacchi VR, You S, Spinelli C, Morley S, Zandian M, Aspuria PJ, et al. Large oncosomes contain distinct protein cargo and represent a separate functional class of tumor-derived extracellular vesicles. Oncotarget 2015; 6:11327–41.
12. Morello M, Minciacchi VR, de Candia P, Yang J, Posadas E, Kim H, et al. Large oncosomes mediate intercellular transfer of functional microRNA. Cell Cycle 2013;12:3526–36.
13. Adam RM, Mukhopadhyay NK, Kim J, Di Vizio D, Cinar B, Boucher K, et al. Cholesterol sensitivity of endogenous and myristoylated Akt. Cancer Res 2007;67:6238–46.
14. Giannoni E, Bianchini F, Masieri L, Serni S, Torre E, Calorini L, et al. Reciprocal activation of prostate cancer cells and cancer-associated fibroblasts stimulates epithelial-mesenchymal transition and cancer stemness. Cancer Res 2010;70:6945–56.
15. Osteikoetxea X, Balogh A, Szabo-Taylor K, Nemeth A, Szabo TG, Paloczi K, et al. Improved characterization of EV preparations based on protein to lipid ratio and lipid properties. PLoS One 2015;10:e0121184.
16. Cocucci E, Gaudin R, Kirchhausen T. Dynamin recruitment and membrane scission at the neck of a clathrin-coated pit. Mol Biol Cell 2014;25: 3595–609.
17. Taddei ML, Cavallini L, Comito G, Giannoni E, Folini M, Marini A, et al. Senescent stroma promotes prostate cancer progression: The role of miR-210. Mol Oncol 2014;8:1729–46.
18. Hermeking H, Rago C, Schuhmacher M, Li Q, Barrett JF, Obaya AJ, et al. Identification of CDK4 as a target of c-MYC. Proc Natl Acad Sci U S A 2000;97:2229–34.
19. Langmead B, Trapnell C, Pop M, Salzberg SL. Ultrafast and memory-efficient alignment of short DNA sequences to the human genome. Genome Biol 2009;10:R25.
20. Li B, Dewey CN. RSEM: Accurate transcript quantification from RNA-Seq data with or without a reference genome. BMC Bioinformatics 2011;12:323.
21. Yang W, Ramachandran A, You S, Jeong H, Morley S, Mulone MD, et al. Integration of proteomic and transcriptomic profiles identifies a novel PDGF-MYC network in human smooth muscle cells. Cell Commun Signal 2014;12:44.
22. Cheng N, Bhowmick NA, Chytil A, Gorksa AE, Brown KA, Muraoka R, et al. Loss of TGF-beta type II receptor in fibroblasts promotes mammary carcinoma growth and invasion through upregulation of TGF-alpha-, MSP- and HGF-mediated signaling networks. Oncogene 2005;24:5053–68.
23. Di Vizio D, Demichelis F, Simonetti S, Pettinato G, Terracciano L, Tornillo L, et al. Skp2 expression is associated with high risk and elevated Ki67 expression in gastrointestinal stromal tumours. BMC Cancer 2008;8:134.
24. van der Mijn JC, Sol N, Mellema W, Jimenez CR, Piersma SR, Dekker H, et al. Analysis of AKT and ERK1/2 protein kinases in extracellular vesicles isolated from blood of patients with cancer. J Extracell Vesicles 2014;3:25657.
25. Abels ER, Breakefield XO. Introduction to Extracellular vesicles: Biogenesis, RNA cargo selection, content, release, and uptake. Cell Mol Neurobiol 2016;36:301–12.
26. Svensson KJ, Christianson HC, Wittrup A, Bourseau-Guilmain E, Lindqvist E, Svensson LM, et al. Exosome uptake depends on ERK1/2-heat shock protein 27 signaling and lipid Raft-mediated endocytosis negatively regulated by caveolin-1. J Biol Chem 2013;288:17713–24.
27. Araki N, Johnson MT, Swanson JA. A role for phosphoinositide 3-kinase in the completion of macropinocytosis and phagocytosis by macrophages. J Cell Biol 1996;135:1249–60.
28. Swanson JA. Shaping cups into phagosomes and macropinosomes. Nat Rev Mol Cell Biol 2008;9:639–49.
29. Falcone S, Cocucci E, Podini P, Kirchhausen T, Clementi E, Meldolesi J. Macropinocytosis: Regulated coordination of endocytic and exocytic membrane traffic events. J Cell Sci 2006;119:4758–69.
30. Macia E, Ehrlich M, Massol R, Boucrot E, Brunner C, Kirchhausen T. Dynasore, a cell-permeable inhibitor of dynamin. Dev Cell 2006;10: 839–50.
31. Kinchen JM, Doukoumetzidis K, Almendinger J, Stergiou L, Tosello-Trampont A, Sifri CD, et al. A pathway for phagosome maturation during engulfment of apoptotic cells. Nat Cell Biol 2008;10:556–66.
32. Kinchen JM, Ravichandran KS. Phagosome maturation: Going through the acid test. Nat Rev Mol Cell Biol 2008;9:781–95.
33. Commisso C, Davidson SM, Soydaner-Azeloglu RG, Parker SJ, Kamphorst JJ, Hackett S, et al. Macropinocytosis of protein is an amino acid supply route in Ras-transformed cells. Nature 2013;497:633–7.
34. Kosaka N, Iguchi H, Yoshioka Y, Takeshita F, Matsuki Y, Ochiya T. Secretory mechanisms and intercellular transfer of microRNAs in living cells. J Biol Chem 2010;285:17442–52.
35. Webber J, Steadman R, Mason MD, Tabi Z, Clayton A. Cancer exosomes trigger fibroblast to myofibroblast differentiation. Cancer Res 2010;70: 9621–30.
36. Orimo A, Gupta PB, Sgroi DC, Arenzana-Seisdedos F, Delaunay T, Naeem R, et al. Stromal fibroblasts present in invasive human breast carcinomas promote tumor growth and angiogenesis through elevated SDF-1/CXCL12 secretion. Cell 2005;121:335–48.
37. Kalluri R, Zeisberg M. Fibroblasts in cancer. Nat Rev Cancer 2006;6: 392–401.
38. Serini G, Gabbiani G. Mechanisms of myofibroblast activity and phenotypic modulation. Exp Cell Res 1999;250:273–83.

39. Cossetti C, Iraci N, Mercer TR, Leonardi T, Alpi E, Drago D, et al. Extracellular vesicles from neural stem cells transfer IFN-gamma via Ifngr1 to activate Stat1 signaling in target cells. Mol Cell 2014;56: 193–204.
40. Yin X, Giap C, Lazo JS, Prochownik EV. Low molecular weight inhibitors of Myc-Max interaction and function. Oncogene 2003;22:6151–9.
41. Lamoureux F, Thomas C, Crafter C, Kumano M, Zhang F, Davies BR, et al. Blocked autophagy using lysosomotropic agents sensitizes resistant prostate tumor cells to the novel Akt inhibitor AZD5363. Clin Cancer Res 2013;19:833–44.
42. Kowal J, Arras G, Colombo M, Jouve M, Morath JP, Primdal-Bengtson B, et al. Proteomic comparison defines novel markers to characterize heterogeneous populations of extracellular vesicle subtypes. Proc Natl Acad Sci U S A 2016;113:E968–77.
43. Xue G, Yan HL, Zhang Y, Hao LQ, Zhu XT, Mei Q, et al. c-Myc-mediated repression of miR-15–16 in hypoxia is induced by increased HIF-2alpha and promotes tumor angiogenesis and metastasis by upregulating FGF2. Oncogene 2015;34:1393–406.
44. Pavlides S, Whitaker-Menezes D, Castello-Cros R, Flomenberg N, Witkiewicz AK, Frank PG, et al. The reverse Warburg effect: Aerobic glycolysis in cancer associated fibroblasts and the tumor stroma. Cell Cycle 2009; 8:3984–4001.
45. Dang CV. MYC on the path to cancer. Cell 2012;149:22–35.
46. Yu M, Al-Dallal S, Al-Haj L, Panjwani S, McCartney AS, Edwards SM, et al. Transcriptional regulation of the proto-oncogene Zfp521 by SPI1 (PU.1) and HOXC13. Genesis 2016;54:519–33.
47. Bronisz A, Godlewski J, Wallace JA, Merchant AS, Nowicki MO, Mathsyaraja H, et al. Reprogramming of the tumour microenvironment by stromal PTEN-regulated miR-320. Nat Cell Biol 2011;14:159–67.
48. Szabo P, Kolar M, Dvorankova B, Lacina L, Stork J, Vlcek C, et al. Mouse 3T3 fibroblasts under the influence of fibroblasts isolated from stroma of human basal cell carcinoma acquire properties of multipotent stem cells. Biol Cell 2011;103:233–48.
49. Sung BH, Ketova T, Hoshino D, Zijlstra A, Weaver AM. Directional cell movement through tissues is controlled by exosome secretion. Nat Commun 2015;6:7164.

Cancer Research

Correction: MYC Mediates Large Oncosome-Induced Fibroblast Reprogramming in Prostate Cancer

In this article (Cancer Res 2017;77:2306–17), which appeared in the May 1, 2017, issue of *Cancer Research* (1), the Authors' Contributions section was incorrect due to publisher error; the section should appear as follows:

Conception and design: V.R. Minciacchi, D. Di Vizio

Development of methodology: V.R. Minciacchi, C. Spinelli, M. Reis-Sobreiro, L. Cavallini, M. Zandian, P. Chiarugi, E. Cocucci, X. Li, R. Mishra

Acquisition of data (provided animals, acquired and managed patients, provided facilities, etc.): N.A. Bhowmick, E.M. Posadas, P. Chiarugi, G. Viglietto, E. Cocucci

Analysis and interpretation of data (e.g., statistical analysis, biostatistics computational analysis): S. You, V.R. Minciacchi, R.M. Adam, M.R. Freeman, D. Di Vizio

Writing, review, and/or revision of the manuscript: V.R. Minciacchi, M.R. Freeman, E. Cocucci, D. Di Vizio

Administrative, technical, or material support (i.e., reporting or organizing data, constructing databases): P. Chiarugi, E.M. Posadas

Study supervision: D. Di Vizio

The online version of the article has been corrected and no longer matches the print. The publisher regrets this error.

Reference

1. Minciacchi VR, Spinelli C, Reis-Sobreiro M, Cavallini L, You S, Zandian M, et al. MYC mediates large oncosome-induced fibroblast reprogramming in prostate cancer. Cancer Res 2017;77:2306–17.

Published online July 15, 2017.
doi: 10.1158/0008-5472.CAN-17-1493

Published OnlineFirst February 15, 2017; DOI: 10.1158/0008-5472.CAN-16-2942

Cancer Research
The Journal of Cancer Research (1916–1930) | The American Journal of Cancer (1931–1940)

AACR American Association for Cancer Research

MYC Mediates Large Oncosome-Induced Fibroblast Reprogramming in Prostate Cancer

Valentina R. Minciacchi, Cristiana Spinelli, Mariana Reis-Sobreiro, et al.

Cancer Res 2017;77:2306-2317. Published OnlineFirst February 15, 2017.